Identifying a role for Ciz1 in the DNA damage response

Katherine Roper

Thesis submitted for the degree of Ph.D.

The University of York

Department of Biology

March 2011

ABSTRACT

In proliferating cells, cell cycle arrest and DNA repair are induced upon detection of DNA damage. The DNA damage response (DDR) to double strand DNA breaks is mediated by phosphatidylinositol 3-kinase-like protein kinases (PIKKs), which propagate DDR signalling by phosphorylating SQ/TQ motifs in substrate proteins. Ciz1 is a vertebrate protein previously shown to stimulate DNA replication initiation and facilitate cyclin exchange at pre-replication complexes. Ciz1 contains several SQ/TQ motif clusters, suggesting it is a PIKK substrate. This thesis investigates the potential role of Ciz1 in the DDR.

A cell free system cell free system previously used to study DNA replication initiation was adapted to permit study of events resulting from etoposide-induced DNA damage. The system was characterised, and its potential as a screening tool to assess inhibitors of the DDR demonstrated, before being used to confirm PIKK-dependent phosphorylation of SQ/TQ motifs in both full length Ciz1 and a C-terminal domain fragment, Ciz1-C274. This phosphorylation is inhibited by both wortmannin and LY294002, implicating DNA-PK as the responsible kinase. More traditional methods including immunofluorescence and RT-PCR were used to characterise the effects of DDR signalling upon endogenous and overexpressed Ciz1. The resulting data show that Ciz1 does not localise to foci of phosphorylated histone H2AX, unlike many known DDR signalling proteins. However etoposide treatment affected levels of C-terminal mRNA in intact cells, increasing transcription of exon 16 in WI38 cells, but decreasing overall mRNA levels in a cancer cell line.

Instead the potential of Ciz1 to act as a modulator of DNA replication initiation through its established role in pre-replication complex assembly is discussed, and three models by which it may act are identified. I hypothesise that phosphorylation of Ciz1 stabilises cyclin E upon the pre-replication complex, preventing the CDK2-cyclin A complex from forming, and preventing origin licensing.

CONTENTS

LIST OF FIGURES

CHAPTER 1

CHAPTER 3

CHAPTER 4

CHAPTER 5

CHAPTER 6

LIST OF TABLES

CHAPTER 1

CHAPTER 2

CHAPTER 3

CHAPTER 4

CHAPTER 5

ACKNOWLEDGEMENTS

I would like to thank my supervisor, Dawn Coverley, for taking me into her lab five years ago, fresh from graduation, and not only hiring me again, but also offering me the opportunity to study for a PhD with her. I would also like to express my gratitude to Nikki Copeland for answering numerous questions and providing a wealth of technical advice, and to all the members of the Coverley lab, past and present, who have provided support and made it a joy to work here. I am told by Gillian Higgins that I should include a famous quote in this section - after much research, I feel the only appropriate words are those of the man who inspired me to study biology in the first place:

"My scientific studies have afforded me great gratification; and I am convinced that it will not be long before the whole world acknowledges the results of my work."
Gregor Mendel

I would like to dedicate this thesis to my parents for their support and faith in me throughout my time at university, and to my friends Victor, Veronica, Adam and Christian whose continued attempts to distract me during the course of researching and writing this probably kept me sane.

DECLARATION

All the research in this thesis is my own with the following exceptions:

GST- and GFP-tagged ECiz1, N442 and C274 constructs used in Chapter 4 were originally designed and created by Dr Justin Ainscough

G1 nuclei used in Chapters 3 and 5 were provided by Dr Dawn Coverley

Real time PCR primers and probes used in Chapter 5 were designed by Dr Heather Sercombe

Purified ECiz1 protein used in Chapter 5 was provided by Dr Dawn Coverley and Dr Nikki Copeland

Chapter 1

GENERAL INTRODUCTION

1.1 Introduction to the DNA damage response (DDR)

1.1.1 The cell cycle

In eukaryotes the majority of cells have exited the cell cycle, having reached their end fate from which they can fulfil their function. However for new tissues to grow, or to replace cells that have died, DNA replication must occur. The source of these new cells is normally either a stock of stem cells, or from progenitor cells that lie dormant within tissues and are induced to proliferate by extracellular signals such as hormones and growth factors (Coller, Sang et al. 2006). These restrictions on cellular proliferation limit the potential for DNA replication to a small proportion of the body's cells, allowing control of development and repair of tissues, and guarding against the uncontrolled growth seen in diseases such as cancer.

In order for a cell to duplicate itself, it must go through a series of carefully orchestrated events known as the cell cycle. These events are divided into two phases during which genomic DNA is first replicated and then distributed between the two daughter cells, with two intervening periods during which the cell both prepares itself for the next phase and resolves any problems arising during the previous phase. These phases are known as the first gap (G1) phase, synthesis (S) phase, second gap (G2) phase and mitosis (M) phase (Figure 1.1).

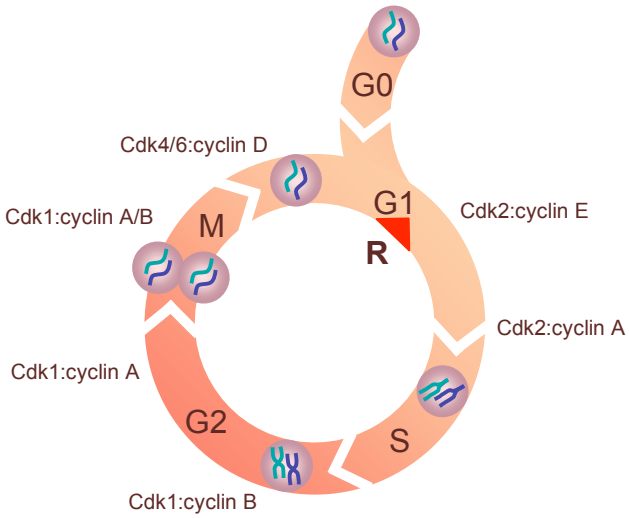

Figure 1.1 Diagram of cell cycle progression showing active Cdk:cyclin complexes driving transitions between phases

Once a certain point in the cell's preparation for division is reached, known as the restriction point (R), the cell no longer relies on external direction. From this point on the cell cycle is regulated by the cyclin dependent kinases (CDKs) and the cyclins. The CDKs are a family of serine-threonine kinases that are expressed throughout the cell cycle, but which only achieve an active conformation when bound to a cyclin binding partner. As cyclin levels fluctuate throughout the cell cycle this allows temporal control of events, with different CDK:cyclin complexes triggering different phases of the cell cycle (Figure 1.1) (Murray 2004).

1.1.2 Accurate replication of DNA and repair of damage is vital to maintain integrity of the genome

A key requirement for cellular proliferation is faithful maintenance of the genome - a process requiring both accurate replication of DNA during S phase, and repair of DNA damage that arises throughout the cell cycle. DNA damage arises constantly within the genome, due to both environmental factors, and as a consequence of cellular processes such as respiration and ATP hydrolysis. In differentiated cells, DNA repair takes place through a set of well-characterised mechanisms and is relatively straightforward, maintaining the stability of RNA and protein production. However in proliferating cells not only is there the need to repair damage before it can be passed on to daughter cells, but conflicting uses of the genome have the potential to interfere with or be affected by DNA repair. In such an instance the ability to halt the cell cycle is invaluable, and the signalling pathways used to do so are commonly called cell cycle checkpoints (Hartwell and Weinert 1989). Cell cycle checkpoints serve a number of other purposes in addition to DNA repair, with a classic example being the mitotic spindle checkpoint. During the spindle checkpoint, the Mad and Bub protein families delay the onset of anaphase upon detection of sister chromatids incorrectly attached to the microtubules linking them to the spindle poles, allowing defects to be resolved (Musacchio and Hardwick 2002; Musacchio and Salmon 2007). In the event of DNA damage, the chief purpose of cell cycle checkpoints is to halt DNA replication until repair has occurred, or to allow initiation of pathways that cause the cell to permanently cease cell division, such as senescence or programmed cell death.

Disease	Gene	Cancer predispositon
Ataxia-telangiectasia	ATM	Leukaemia, lymphoma
Nijmegen breakage syndrome	NBS1	Leukaemia, lymphoma
A-T-like disorder	Mre11	Leukaemia, lymphoma
Fanconi anaemia	Brca2, FanCA, B, C, D1, D2, E, F, G, I, J, L, M & N	Acute myelogenous leukaemias
Familial breast, ovarian carcinoma syndrome	Brca1, Brca2	Breast, ovarian & other cancers
Li-Fraumeni syndrome	p53 Chk2	Sarcomas, leukaemia, brain, adrenal and other tumours

Table 1.1: DDR genes and associated congenital diseases and cancer susceptibilities resulting from mutations (adapted from Kastan and Bartek 2004)

1.1.3 Deregulation of damage detection and repair signalling is necessary for tumourigenesis

In the event that cell cycle checkpoints and DNA repair mechanisms do not function correctly, build up of DNA damage in proliferating cells not only leads to developmental abnormalities, but is also a major contributing factor to carcinogenesis.

Genes which increase susceptibility to cancer when mutated are divided into two classes – oncogenes, which when active promote tumour growth, and tumour suppressor genes, which safeguard against tumour growth when fully functional, and when inactivated permit the proliferation of cancerous cells. The genes involved in DNA damage detection and repair are classic examples of tumour suppressors, with congenital mutations often causing predisposition to the development of cancers, and are among the most commonly altered in tumor cells (Kastan and Bartek 2004). Selective pressure favours their mutation in these rapidly replicating cells, promoting tumorigenesis by allowing further deterioration of the genome (Gorgoulis, Vassiliou et al. 2005). A summary of diseases caused by mutations in DDR genes and their associated cancer susceptibilities is shown in Table 1.1.

There are three main cell cycle checkpoints at which DNA damage can be detected and repaired: the G2/M checkpoint blocking entry to M phase, the G1/S checkpoint blocking entry to S phase and the intra-S phase checkpoint which inhibits origin firing during S phase. These three checkpoints are shown in Figure 1.2. One of the key proteins involved in these proteins is one of the most commonly mutated DNA damage response checkpoint genes, p53, a transcription factor which is lost or altered in 50-55% of all human cancers (Hollstein, Rice et al. 1994). p53 activation in response to stresses

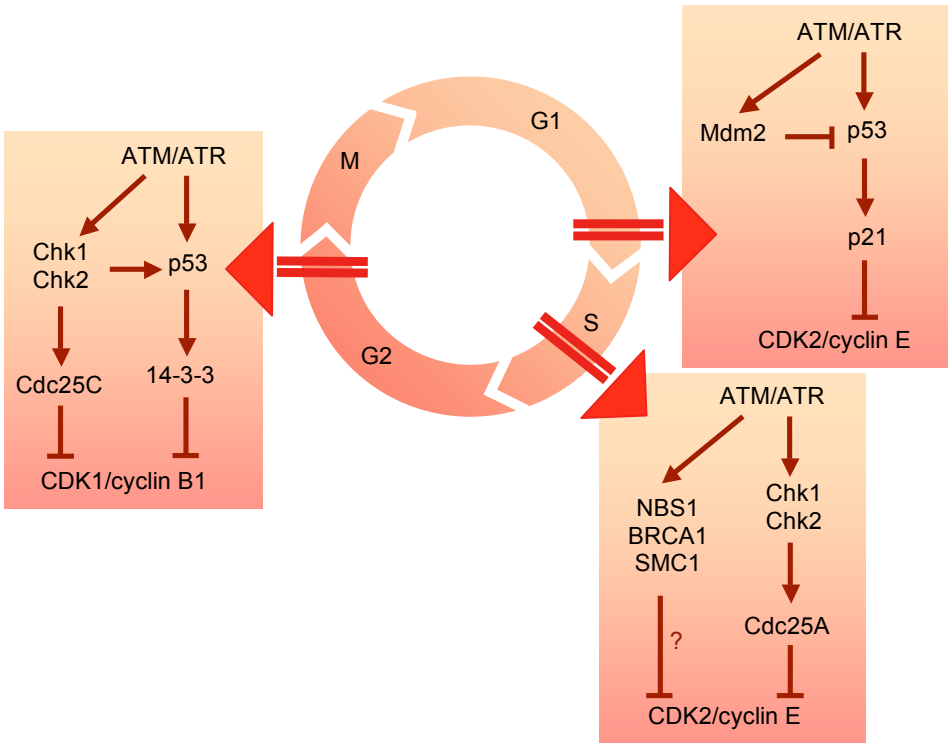

Figure 1.2 Checkpoints halt the cell cycle upon detection of damage

Diagram of cell cycle progression, showing simplified G2/M, G1/S, and intra-S checkpoint pathways following activation of ataxia telangiectasia mutated (ATM) and ATM and Rad3-related (ATR) by double strand breaks or single stranded DNA respectively. Adapted from RND systems DNA damage response mini review.

http://www.rndsystems.com/mini_review_detail_objectname_MR03_DNADamageResponse.aspx

G2/M checkpoint: phosphatidylinositol 3-kinase-like protein kinase (PIKK) mediated activation of checkpoint kinase 1 (Chk1) and checkpoint kinase 2 (Chk2) causes them to phosphorylate cell division cycle 25 protein isoform C (Cdc25C), which binds to p53-activated 14-3-3 protein. The Cdc25C/14-3-3 complex is then sequestered in the cytoplasm, where Cdc25C is unable to activate the cyclin-dependent kinase (CDK1)/cyclin B1 complex, thus preventing the cell from entering mitosis.

G1/S checkpoint: Following activation of the PIKKs, the interaction of mini chromosome maintenance protein 2 (Mdm2) and p53, which normally results in nuclear export of p53 followed by its degradation, is blocked by phosphorylation of both proteins. The resulting accumulation of p53 in the nucleus causes up-regulation of p21, suppressing CDK2/cyclin E activity and preventing entry to S phase.

Intra-S checkpoint: PIKK-mediated activation of Chk1 and Chk2 causes them to phosphorylate cell division cycle 25 protein isoform A (Cdc25A), targeting it for degradation. Cdc25A would normally dephosphorylate CDK2/cyclin E, but in its absence this cannot occur and the complex is not activated, preventing further firing of origins. Additionally phosphorylation of NBS1, BRCA1 and SMC1 by ATM is believed to contribute to delayed origin firing, although the precise mechanisms are as yet unknown.

such as DNA damage and hypoxia commonly leads to senescence or apoptosis of the cell, preventing carcinogenesis (Vousden and Lu 2002). p53 is vital for induction of the G1/S checkpoint, and also contributes to activation of the G2/M barrier (Agarwal, Agarwal et al. 1995). While inactivation of the p53 pathway disables the G1/S checkpoint and lowers the likelihood of apoptosis, it also leaves them more dependent on the intra-S phase checkpoint for repair of lesions.

1.1.4 Knowledge of the DDR can be used to devise targeted therapies against cancer

The lack of specificity of conventional cancer treatments means that while they are often effective at killing tumour cells, they also have many toxic effects on the rest of the body. This "collateral damage" is responsible for the characteristic symptoms of chemotherapy - loss of hair and depressed immune system due to the death of rapidly proliferating cells such as hair follicles and bone marrow progenitor cells - and can result in generation of secondary tumours later in life. There are a multitude of changes required for cancerous cells to arise, which were famously categorised by Hanahan and Weinberg in 2001 as the "hallmarks" of cancer, and updated in 2011 to reflect recent advances in understanding of the disease (Hanahan and Weinberg 2000; Hanahan and Weinberg 2011). These are self-sufficiency in growth signals, insensitivity to anti-growth signals, tissue invasion and metastasis, limitless replicative potential, sustained angiogenesis, evasion of apoptosis, reprogramming of energy metabolism and evasion of immune destruction.

An understanding of the genetic modifications driving and sustaining these changes is vital for the development of more focused treatments, which can exploit these differences to specifically identify and target tumour cells. Such treatments are commonly referred to as targeted therapies, and first arose in the 1970's with the development of tamoxifen, an antioestrogenic molecule effective against breast cancers. As previously described, inactivation of p53 permits an escape from the threat of apoptosis in many human cancers, but leaves them reliant on alternate pathways to detect and repair the lethal DNA damage induced by chemotherapy and radiotherapy. If these pathways can be untangled targeted therapies can be devised to knock them out, leaving p53-deficient cells vulnerable to conventional therapies at lower doses, and patients with a decreased chance of developing secondary tumours.

1.1.5 The p53 and DNA damage response pathways are responsible for repair of double strand breaks

There are several well characterised types of DNA damage, which can be divided into three main categories:

- DNA base modifications - this category encompasses damage to nucleic acid base structure induced by oxidation, alkylation and hydrolysis, chemically induced adduct formation, UV induced generation of pyrimidine dimers and creation of mismatched bases by DNA replication error. Alkylation of DNA can occur either as a result of external exposure to alkylating agents such as methyl methanesulfonate and N-methyl-N'-nitro-N-nitrosoguanidine, or via exposure to compounds such as S-adenosylmethionine which arise as a result of biological processes. Presence of alkylated bases can lead to misincorporation during DNA replication, causing conversion of pyrimidines to purines. Repair of alkylative DNA damage is carried out either directly by alkyltransferase or dioxygenase enzymes, or by base excision repair (BER) or, more rarely, nucleic acid excision repair (NER) (Ura and Hayes 2002; Eker, Quayle et al. 2009). Oxidative damage to DNA arises due to exposure to exogenous factors such as ionising radiation, ultraviolet light (UV) and oxidising chemicals (Kryston, Georgiev et al.). Endogenous reactive oxygen species are also generated by mitochondria, peroxisomes and inflammatory cell activation as a by-product of biological processes (Klaunig, Xu et al. 1998). Repair of oxidative DNA damage is mainly carried out by BER. DNA adducts occur as a result of exposure to polycyclic aromatic hydrocarbons such as benzo[a]pyrene. Once within the body, polycyclic aromatic hydrocarbons undergo metabolic activation by cytochrome P450-dependent oxidation forming highly reactive intermediates that covalently bind to DNA, forming adducts (Barkley, Ohmori et al. 2007). A second class of adduct, the 6-4-photoproduct, can also be formed as a result of exposure to UV light (Mitchell and Nairn 1989). Replication of DNA containing adducts is prone to errors and consequently results in mutations. Repair of adducts is carried out by BER and NER.

- Crosslinking - interstrand crosslinks (ICLs) occur when the two strands of the DNA double helix are covalently linked to an intermediate chemical. ICLs are particularly cytotoxic, disrupting transcription and replication on both strands,

and as a complex form of damage, their repair involves genes from the NER, homologous recombination (HR) and Fanconi anemia (FA) pathways (McCabe, Olson et al. 2009).

- DNA backbone damage - this category includes generation of abasic sites, and single and double strand breaks. Abasic sites are commonly created by spontaneous hydrolysis of the N-glycosilic bond, and can also arise as a product of repair of damaged or erroneous bases. They can block DNA transcription and replication, and are potentially mutagenic. They are normally repaired using the BER pathway (Boiteux and Guillet 2004). Single strand breaks (SSB) and double strand breaks (DSB) can arise as a consequence of errors during replication, or as a result of ionising radiation exposure. Some chemicals are also capable of interfering with replication fork progression, stalling active forks and inducing DSB formation. Double strand breaks are severely cytotoxic, presenting a barrier to DNA transcription and replication and, as both strands are severed, permit physical movement of the double helix that can lead to excision or duplication of entire chunks of the chromosome if wrongly rejoined. DSB can be repaired via non-homologous end joining (NHEJ), microhomology-mediated end joining or by HR, depending on the stage of the cell cycle during which they occur (Shrivastav, De Haro et al. 2008; Yun and Hiom 2009).

Much of the research carried out on the DNA damage response to date has spanned a variety of model organisms, including yeasts, *Xenopus*, mice and humans. While there are similarities between the yeast and mammalian DDR signalling, with conservation of key players like the ATM-Chk2 pathway, there are also a number of unique proteins which play a major role in the higher eukaryotic DDR for which no yeast homolog exists, such as p53 (Carney, Maser et al. 1998; Matsuoka, Huang et al. 1998). In seeking to understand the pathways underlying human diseases, these proteins need to be taken into account, and this thesis will therefore concentrate on, and refer to models for the mammalian response to DNA damage.

Furthermore, while the varying pathways of DNA damage repair are very interesting and present a large field of study, this thesis will focus on the processes that initially detect damage and induce a cellular response. As different types and causes of damage trigger different (albeit frequently overlapping) pathways, I will concentrate on one

specific type of damage and investigate the pathways by which one of the most severe forms of damage, double strand breaks, are detected.

1.1.5.1 DSB detection and repair is mediated by multiple checkpoint pathways relying on shared initial signalling events

While the DSB-response pathways shown in Figures 1.2 vary between checkpoints, they all rely upon one critical initial step to trigger their signalling cascades - activation of the phosphatidylinositol 3-kinase-like protein kinases (PIKKs), ataxia telangiectasia mutated (ATM), ATM and Rad3-related (ATR) and DNA-dependent protein kinase (DNA-PK). ATM primarily responds to direct induction of double strand breaks, while ATR tends to mediate responses to arrest of DNA replication forks, and creation of regions of single stranded DNA (ssDNA), which can then go on to form DSBs (Abraham 2001). Studies show that ATM is the dominant PIKK mediating DSB

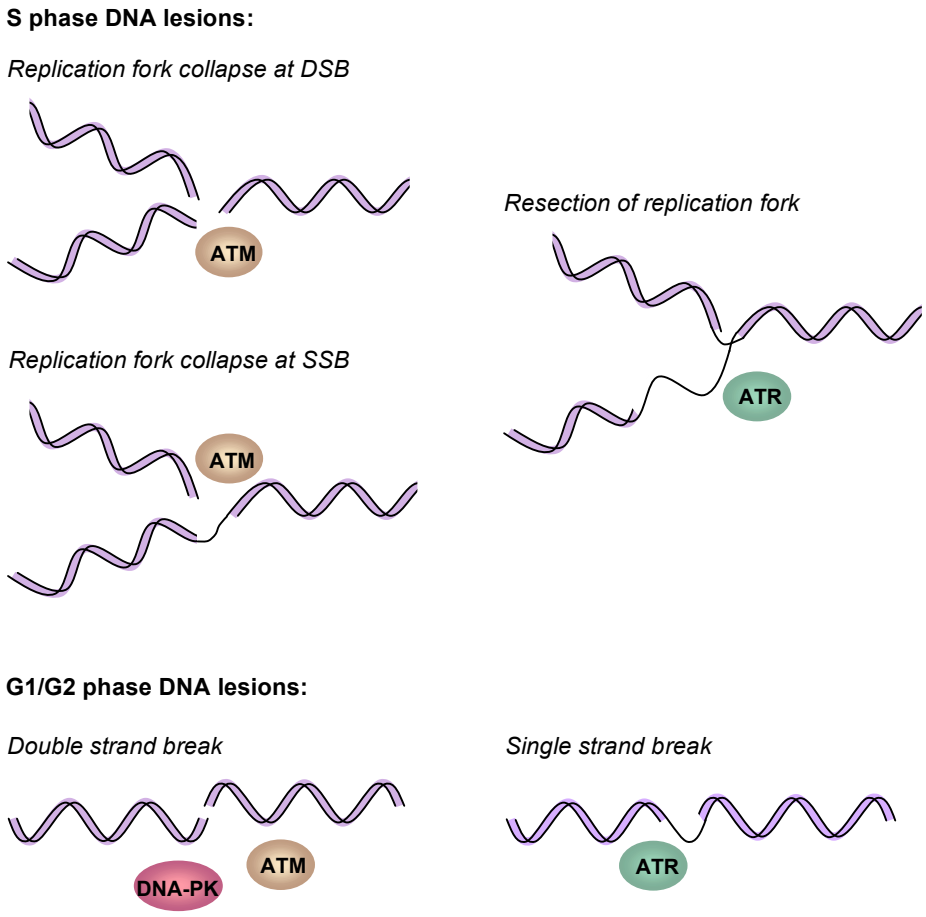

Figure 1.3 Diagrams of common DNA lesions indicating cell cycle phase during which structures are likely to arise, and attendant PIKK

Presence of undetected double or single strand breaks during G1 phase can lead to replication fork collapse once DNA replication begins. Adapted from Branzei *et al*

detection, but that DNA-PK also contributes to the response. DNA-PK plays only a small role in early signal propagation, and instead appears to mainly be involved in phosphorylation of E2F-1, a transcription factor controlling the transition from G1 to S phase, and in repair of DSBs by non-homologous end joining (Watanabe, Shinohara et al. 2003; Stiff, O'Driscoll et al. 2004; Dobbs, Tainer et al. 2010). A summary of common PIKK-mediated DNA lesions is shown in Figure 1.3 (Branzei and Foiani 2008).

1.1.5.2 ATM recruits DDR signalling factors to phosphorylated histone H2AX

In mammals, activation of ATM occurs within a minute of DSB formation (Andegeko, Moyal et al. 2001), and is facilitated by the recruitment of the Mre11-Rad50-NBS1 (MRN) complex to the lesion (Lee and Paull 2005; Paull and Lee 2005). Upon recruitment to the site of the DSB, ATM is autophosphorylated (Berkovich, Monnat et al. 2007) and in turn phosphorylates histone H2AX. Mediator of DNA damage checkpoint protein 1 (MDC1) binds to phosphorylated H2AX (γH2AX), and acts as a platform to which proteins independently recruited to the damaged site attach, allowing ATM to further phosphorylate neighbouring H2AX (Figure 1.4a) (Lou, Chini et al. 2003; Peng and Chen 2005). These foci act as a centre for damage signalling and repair proteins, and their rapid formation and subsequent spread across megabase-sized regions of chromatin makes γH2AX a commonly used molecular marker of the DDR. Additionally ATM directly phosphorylates the effector protein Chk2 (Ahn, Li et al. 2002).

1.1.5.3 ATM also activates ATR signalling following DNA damage

ATM also phosphorylates CtIP, leading to its recruitment to the break site (You and Bailis 2010). CtIP facilitates resectioning of DNA around the break to generate short single-stranded regions to which replication protein A (RPA) binds (You, Shi et al. 2009). The presence of RPA stimulates binding of ATR interacting protein (ATRIP) to ssDNA, which exists as a stable complex with ATR in human cells, allowing formation of an ATR-ATRIP-ssDNA complex and stimulating phosphorylation of ATR (Figure 1.4b) (Cortez, Guntuku et al. 2001; Zou and Elledge 2003). ATR goes on to phosphorylate Chk1, while phosphorylated CtIP signals the expression of cell cycle inhibitor genes including p21 and GADD45 (Li, Ting et al. 2000; Zou and Elledge 2003). CtIP also regulates which repair method is used for double strand breaks - during

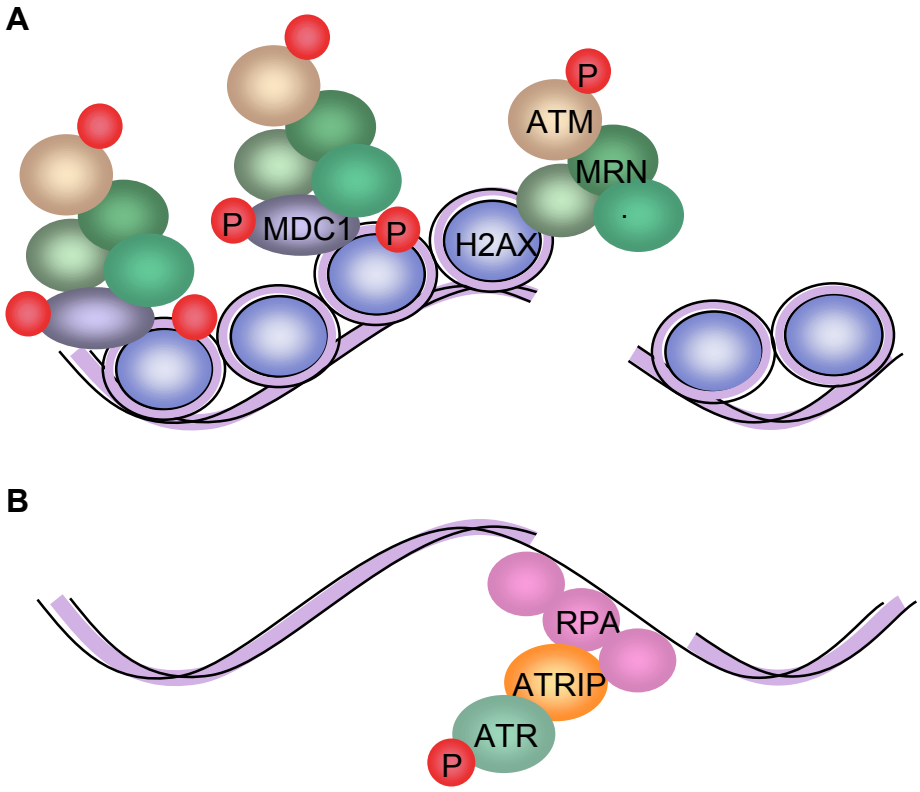

Figure 1.4 Early stages of ATM and ATR-mediated DNA damage detection

a) Schematic of propagation of H2AX phosphorylation by ATM in response to DSB formation. The MRN complex is recruited to the site of the double strand break, allowing recruitment and autophosphorylation of ATM. Phosphorylation of nearby H2AX by ATM recruits MDC1, which acts as a tether for proteins recruited by ATM and the MRN complex, allowing foci of damage signalling and repair proteins to spread across the surrounding chromatin.

b) Schematic of recruitment of ATR to ssDNA. Exposed ssDNA is coated by RPA, to which ATRIP and ATR bind, activating ATR and allowing recruitment of damage signalling and repair proteins.

the S and G2 phases, HR is favoured, due to a lower rate of error, but following mitosis, changes in chromatin structure necessitate a switch to non-homologous end-joining or microhomology-mediated end-joining. RPA-dependent recruitment of ATR to ssDNA is also required for ATR's involvement in ATM-independent detection and repair of other forms of DNA lesions (Zou and Elledge 2003).

1.1.5.4 Following initial detection of damage, signal propagation is controlled by the mediator and effector proteins

Despite their similar names the effector proteins, Chk1 and Chk2, share few structural features and are not closely related in sequence, but they are both serine-threonine kinases that relay the DDR signalling cascade initiated by the PIKKs (Bartek and Lukas 2003). Chk1 mainly interacts with ATR, whereas Chk2 is activated chiefly by ATM.

Despite their specificity to individual PIKKs, many of the substrates of Chk1 and Chk2 are shared, allowing similar checkpoint pathways to be activated in response to single and double strand breaks, despite varying requirements for repair pathways. In addition, the Chk proteins are soluble and remain present throughout the nucleus rather than localising solely to sites of damage, allowing propagation of signalling throughout the nucleus (Bartek and Lukas 2003; Lukas, Falck et al. 2003; Bekker-Jensen, Lukas et al. 2006). Between them the Chks affect processes as diverse as damage-induced transcription, DNA repair, cell cycle arrest, apoptosis and chromatin remodelling via proteins including CDC25, p53, the tousled-like kinases, Pml, breast cancer 1 (Brca1) and E2F1 (Shieh, Ahn et al. 2000; Yang, Kuo et al. 2002; Groth, Lukas et al. 2003; Stevens, Smith et al. 2003; Karlsson-Rosenthal and Millar 2006; Zhuang, Zhang et al. 2006).

Throughout the DNA damage response, the signalling initiated by the PIKKs and Chks is mediated by checkpoint mediator proteins. While the effectors are dispersed throughout the nucleus, mediators act locally to DNA lesions, regulating PIKK activity and interactions and contributing to recruitment and assembly of protein complexes in the chromatin regions adjacent to sites of damage. The foci of damage signalling and repair proteins that are orchestrated by these mediators are commonly known as ionising radiation induced foci (IRIF), and co-localise with phosphorylated H2AX. MDC1 and the MRN complex, which facilitate and propagate phosphorylation of H2AX by ATM, are mediators, as are proteins such as Brca1, 53BP1, Brit1 and claspin (Harper and Elledge 2007). A common feature of mediator proteins is the presence of multiple Brca1 C-terminal (BRCT) domains in their C-terminal region (Huyton, Bates et al. 2000; Shang, Bodero et al. 2003; Lin, Liang et al. 2010; Watts and Brissett 2010). The BRCT domain has been shown to act as a phospho-protein binding domain, potentially facilitating interaction of the checkpoint mediators with other proteins phosphorylated by ATM, ATR, Chk1 and Chk2 (Yu, Chini et al. 2003). Mediators are frequently tumour suppressors or oncogenes, and their loss or mutation contributes to carcinogenesis (Kastan and Bartek 2004; Harper and Elledge 2007; Lowndes 2010).

1.2 The Ciz1 protein

$P21^{Cip1/Waf1}$-interacting zinc finger protein 1 (Ciz1) is a member of the matrin family of nuclear proteins. Ciz1 was first characterised in 1999 through its interactions with the p21/CDK2 complex (Mitsui, Matsumoto et al. 1999), then independently isolated and

characterised as NP94 in 2003 (Warder and Keherly 2003). This study found expression within a variety of tissue types and demonstrated colocalisation with DNA, identifying a weak consensus DNA-binding sequence for Ciz1. Ciz1 was also independently identified as a cyclin A-responsive protein involved in the promotion of mammalian DNA replication (Coverley, Marr et al. 2005). Ciz1 homologues have been found in vertebrates such as mouse, chimpanzees, rats and pufferfish, but not in lower eukaryotes (Coverley, Marr et al. 2005). Over the past decade understanding of Ciz1's function has been greatly improved, largely (but not exclusively) through the work of the Coverley laboratory at the University of York.

1.2.1 Ciz1 promotes DNA replication initiation

The most extensively characterized role identified for Ciz1 is in cell cycle progression, specifically control of DNA replication initiation.

1.2.1.1 Faithful replication of DNA requires spatial and temporal control of origins

Unlike bacteria, which use a single origin from which to replicate the entire genome, the size of the eukaryotic genome and the complexity of its replication machinery necessitate use of multiple origins of replication. The mammalian genome therefore possesses between 30,000-50,000 origins per cell cycle, not all of which are active concurrently (Huberman and Riggs 1966). To further complicate matters, an excess of replication origins exists with only a subset of the full number being used during each cell cycle (Li, Bogan et al. 2000). In order for replication to take place, the cell must choose both which origins are to be used and in which order they are to be activated. The different types of replication origin and the factors surrounding their selection are reviewed by Méchali (Mechali 2011), but the process can be summarised as involving two key checkpoints. Firstly the origin decision point, during which the origins to be used are selected, and secondly the timing decision point, during which origins are divided into early-, mid- and late-S phase firing (Wu and Gilbert 1997; Dimitrova and Gilbert 1999; Li, Chen et al. 2001).

1.2.1.2 Origin-licensing is controlled by CDK2:cyclin E

Once origins are selected, they are licensed by the assembly of pre-replication complexes (pre-RC) containing the basic structure necessary for unwinding of DNA and loading of DNA polymerases (Blow and Hodgson 2002). These pre-replication

complexes are targeted to the site of origins by the origin replication complex (ORC) a six protein complex which binds to DNA at the sites of origins (Bell and Stillman 1992). ORC then recruits Cdc6, and together ORC and Cdc6 promote loading of a complex made up of MCM2-7, a helicase, and Cdt1 onto the DNA (Tsakraklides and Bell 2010). At this point the pre-replication complex is fully assembled, and the origin is referred to as "licensed", but it is not yet activated for replication. Dividing licensing and activation of origins into two temporally distinct phases allows the cell to prevent rereplication, as pre-replication complexes are disassembled following DNA replication, preventing further initiation at the fired origin (Arias and Walter 2007). Origin licensing is regulated by the Cdk2:cyclin E complex, which promotes loading of MCM2-7 onto the pre-replication complex and protectively phosphorylates Cdc6, preventing its degradation by licensing inhibitors (Furstenthal, Kaiser et al. 2001; Coverley, Laman et al. 2002; Geng, Yu et al. 2003; Mailand and Diffley 2005).

1.2.1.3 Origin firing is controlled by CDK2:cyclin A and DDK

Activation of origins is carried out by recruitment of proteins that activate MCM2-7, allowing unwinding of DNA to commence (Takeda and Dutta 2005). The first stage of this is the recruitment of MCM10 to the complex, and phosphorylation of MCM2-7 by Dbf4-dependent kinase (DDK), both of which promote loading of Cdc45 (Gregan, Lindner et al. 2003; Sheu and Stillman 2006). The other key set of proteins in activation of the pre-replication complex are the GINS complex, a ring-like structure which may coordinate DNA polymerases at the replication fork (Hubscher, Maga et al. 2002; De Falco, Ferrari et al. 2007). Origin firing is also controlled by a second kinase, the Cdk2:cyclin A complex. The precise targets of Cdk2:cyclin A are as yet undefined, but the complex has repeatedly been shown to be necessary for origin firing (Coverley, Laman et al. 2002; Katsuno, Suzuki et al. 2009; Nakanishi, Katsuno et al. 2010).

1.2.1.4 Ciz1 stimulates initiation of DNA synthesis both in vitro and in intact cells

Ciz1's role in initiation has been explored using a cell free system permitting quantification of the number of nuclei initiating DNA replication. Cell free DNA replication systems were originally developed using viral control elements (Stillman 1989) and later, activated Xenopus egg cells (Murray and Kirschner 1989). These systems allowed study of enzymatic and regulatory features of replication, but because of the nature of their components, did not permit study of the structural organisation or

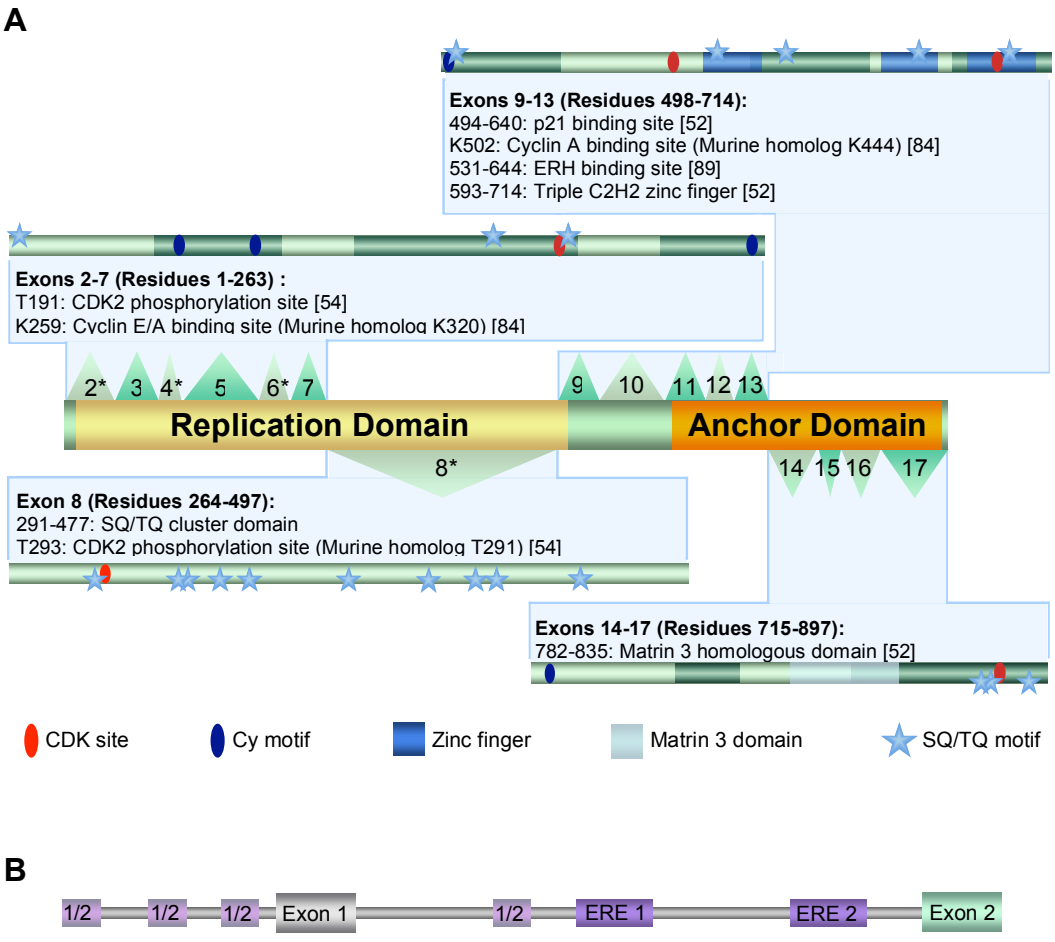

Figure 1.5 Maps of human Ciz1

a) Full schematic of translated exons, showing SQ/TQ motifs and functional domains as defined by a range of published and unpublished studies into Ciz1. Amino acid positions of characterised features of Ciz1 are given, along with references. Exon numbers marked with an asterisk indicate observation of alternate splicing or exon skipping in diseased tissue or tumour-derived cell lines. The replication and anchor domains displayed have been shown to undergo uncoupled transcription during cellular differentiation and tumourigenesis.

b) Schematic of untranslated region preceding exon 2, showing location of partial (1/2) and full estrogen response elements (ERE). Exon 1 appears to be an untranslated region with the first translational start site in exon 2. Adapted from Den Hollander and Kumar, 2006.

regulatory events specific to the somatic cell cycle in differentiated cells. The system used by the Coverley laboratory to study initiation is instead derived from mammalian cells, allowing the combination of cytosolic extracts with isolated nuclei, which are then incubated with fluorescently labelled nucleotides. The mixture can then be examined by microscopy to determine the number of nuclei that have incorporated labelled nucleotides, allowing study of the initiation of DNA replication in G1 phase, and of replication elongation in S phase nuclei (Krude, Jackman et al. 1997; Coverley, Laman et al. 2002; Coverley, Marr et al. 2005).

Addition of purified Ciz1 to this system demonstrated that Ciz1 increases the number of nuclei that undergo initiation, while transfection of a Ciz1 overexpression vector into cell lines in culture stimulated the number of cells that incorporate bromodeoxyuridine (BrdU) (Coverley, Marr et al. 2005). Stimulation of *in vitro* DNA synthesis has only previously been observed with proteins known to be involved in DNA replication (Coverley, Laman et al. 2002). Mutation of the CDK phosphorylation site T191 (Figure 1.5a) in ECiz1 (an embryonic splice variant of Ciz1) increased the range of concentrations at which initiation was stimulated in this cell free system (Coverley, Marr et al. 2005), suggesting that its function is regulated by the cell cycle machinery. In addition to its capacity to stimulate initiation *in vitro*, endogenous Ciz1 forms nuclear foci during S phase (Coverley, Marr et al. 2005) which partially co-localise with proliferating cell nuclear antigen (PCNA), a cofactor of DNA polymerase δ (Moldovan, Pfander et al. 2007), and with early sites of DNA synthesis (Ainscough, Rahman et al. 2007).

1.2.2 Dissection of the role of Ciz1 in initiation

Closer investigation of this stimulation of DNA replication initiation has shown that Ciz1 is necessary for cell cycle progression, with siRNA depletion of Ciz1 from cells inhibiting their entry to S phase (den Hollander and Kumar 2006). However pre-RC assembly on to chromatin is unaffected, with MCM3 recruitment to detergent-resistant nuclear structures increasing when Ciz1 is depleted (Coverley, Marr et al. 2005). This suggests that pre-replication complexes persist for a longer period in the absence of Ciz1, placing its function in between pre-RC assembly and conversion to active replication complexes. It was also shown that only soluble Ciz1 was affected by siRNA depletion, implying that newly synthesized Ciz1 is needed for DNA replication initiation and cell cycle progression to take place (Coverley, Marr et al. 2005).

Insoluble, nuclear matrix-associated Ciz1 remained unaffected, suggesting that this fraction may persist from previous cell cycles.

1.2.2.1 Ciz1 interacts with cyclins A and E

Ciz1 contains five Cy-motifs, domains with which the cyclin family of proteins are known to interact (Figure 1.5a) (Wohlschlegel, Dwyer et al. 2001). As cyclins E and A have major roles in the transition between G1 and S phase, with CDK2 swapping binding partners from cyclin E to cyclin A, these Cy-motifs seemed a potential candidate to explain Ciz1's role in initiation, and have been scrutinised in detail (Coverley, Laman et al. 2002; Woo and Poon 2003). Recent data shows that Ciz1 interacts with both cyclins, and that cyclin A displaces Ciz1-bound cyclin E *in vitro* (Copeland, Sercombe et al. 2010). A model for Ciz1's interactions with the cyclins has been suggested, proposing that Ciz1 supports the sequential accumulation of cyclins E and A at the pre-replication complex during its assembly and activation. This model is given further weight by the fact that levels of Cdk2 activity are also reduced in breast cancer cells when Ciz1 is depleted (den Hollander and Kumar 2006).

1.2.2.2 The C-terminal domain of Ciz1 does not stimulate DNA synthesis, but acts as a nuclear matrix anchor

The model of Ciz1 as a platform for cyclin exchange during origin licensing and assembly also incorporates the possibility that Ciz1 spatially regulates cyclin A. Experiments using truncated forms of Ciz1 have shown that the C-terminal domain of Ciz1 is not required for stimulation of DNA replication, but that in its absence Ciz1 does not form nuclear foci. This region is required for recruitment of Ciz1 to insoluble DNase 1 resistant foci within the nucleus during S phase (Ainscough, Rahman et al. 2007). DNase I resistant non-chromatin protein/RNA structures are commonly known as the nuclear matrix, and are known to be enriched with replication origins during G1 phase (Djeliova, Russev et al. 2001). As such, Ciz1 can be divided into two main domains – an N-terminal replication domain (RD) which promotes initiation via interaction with cyclins, and a C-terminal anchor domain (AD) responsible for correct localisation of Ciz1 within the nucleus (Figure 1.5a) – and it is believed that these two regions cooperate to ensure correct targeting of cyclin A to the nuclear matrix during pre-RC activation.

1.2.3 Several proteins that interact with p21 have been linked with Ciz1

p21 is known to be vital for the arrest of the cell cycle as part of the DDR (Roninson 2002), and Ciz1 was originally identified by virtue of its interaction with the protein (Mitsui, Matsumoto et al. 1999). It is known that Ciz1's role in DNA replication is not dependent on p21, as Ciz1 overexpression stimulates synthesis of DNA even in p21 null cells (Coverley, Marr et al. 2005). This shows that Ciz1 does not promote DNA replication by sequestration of p21, and suggests that the interaction of the two proteins could play another role in the cell. Recent research has fuelled speculation over which mechanisms and functions this interaction could influence.

1.2.3.1 Ciz1 interacts with dynein light chain 1

The N-terminal region of Ciz1 binds dynein light chain 1 (DLC1) (den Hollander and Kumar 2006), an estrogen-regulated component of the cytoplasmic dynein motor involved in organelle transport within the cytoplasm (Hirokawa, Noda et al. 1998). DLC1 has been implicated in breast cancer tumourigenesis (Vadlamudi, Bagheri-Yarmand et al. 2004) and overexpression is known to promote the G1-S phase transition by promoting Cdk2 kinase activity. This is stimulated by targeting of p21 to the nuclear compartment by DLC1, and does not occur when the Ciz1 binding domain of DLC1 is deleted (den Hollander and Kumar 2006). A model has been suggested in which DLC1 transports Ciz1 to the nucleus, where Ciz1 binds p21 and Cdk2. Ciz1 and DLC1 together target p21 to the cytoplasm, leading to increased Cdk2 activity. While this is supported by observations that overexpression of both p21 and Ciz1 induced cytoplasmic localisation of p21 (Mitsui, Matsumoto et al. 1999), it should be noted that these conclusions are drawn solely from protein overexpression in cancer cell lines, in which the DNA replication and repair processes are damaged. Thus the observations may not reflect the pathways used in healthy cells. Furthermore as Ciz1 has already been shown to promote entry to S phase in p21 null cells (Coverley, Marr et al. 2005), it seems unlikely that the trimer formed between DLC1, Ciz1 and p21 and any subsequent changes in localisation of proteins are involved in pre-RC assembly and stimulation of CDK2 activity.

1.2.3.2 Ciz1 interacts with human enhancer of rudimentary

Ciz1 also interacts with human enhancer of rudimentary (ERH) (Lukasik, Uniewicz et al. 2008). Increased levels of ERH mRNA observed in more rapidly proliferating

mammalian cell lines, and observed *in vitro* phosphorylation of Drosophila ERH by casein kinase II suggest that ERH may be involved in cell cycle progression (Gelsthorpe, Pulumati et al. 1997). ERH may be regulated by casein kinase II, a protein kinase targeting many transcription factors and regulators involved in the cell cycle. The ERH and p21 binding sites in Ciz1 are known to overlap (Figure 1.5a), raising the possibility that ERH binding could block p21 interaction with Ciz1 or vice versa.

1.2.4 Ciz1 may be involved in the DNA damage response

Bioinformatic analysis has revealed a number of SQ/TQ motifs present in Ciz1's amino acid sequence. These SQ/TQ motifs are simple two amino acid sequences made up of either a serine or a threonine residue followed by a glutamine residue, and are commonly phosphorylated by the PIKKs (Kim, Lim et al. 1999; O'Neill, Dwyer et al. 2000). SQ/TQ motifs are often found in clusters and their presence is thought to be indicative of DNA damage response proteins (Traven and Heierhorst 2005). Their function as phosphorylation sites for ATM, ATR and DNA-PK was originally discovered in the DDR effector and tumour suppressor BRCA1, which contains 20 motifs across its 1863 amino acids (Cortez, Wang et al. 1999). In comparison human Ciz1 contains 21 S/TQ motifs (Figure 1.5a), grouped in 3 main clusters across 898 amino acids. This high incidence of potential phosphorylation sites raises the possibility that Ciz1 could be a substrate of ATM or ATR. If so, like many other genes involved in cell cycle control it may play a role in maintenance of the genome in addition to its role in promoting DNA synthesis.

As mentioned in section 1.1.3, genes involved in the DNA damage response are frequently lost or mutated during carcinogenesis, and their disruption contributes to further deterioration of the genome. In recent years a number of observations have been made implicating Ciz1 as a player in tumour development, which are summarised below.

1.2.4.1 Isoforms of Ciz1 are prevalent in diseased cells

A survey of Ciz1 EST sequences found alternative splicing in approximately 11% of transcripts available on unigene in 2006, with spliced sites including exons 2, 4, 6 and 8 (Rahman, Ainscough et al. 2007). Transcripts were derived from both healthy and diseased cells, with diseased samples displaying an increased frequency of alternate

splicing, and preferential skipping of exons 2, 4 and 6. Focused analysis of exon 4 has been undertaken in the Coverley lab (Rahman, Ainscough et al. 2007) and has shown that exon 4 is involved in Ciz1 nuclear foci formation, and that it is commonly mispliced in Ewing's sarcoma family tumour cell lines as a direct consequence of mutation of intronic splicing regulators. Exon 4 deleted transcripts are also observed in non-diseased samples, particularly mouse embryonic stages, therefore exon 4 skipping could play a physiological role in normal cells, possibly during early developmental stages (Rahman, Ainscough et al. 2007). Differences in expression of the replication and anchor domains of Ciz1 have also been found in tumours. Transcription of exons in the C-terminus exceeded levels of N-terminal exon mRNA in a range of stage I through to III tumours, followed by an excess of the N-terminal replication domain once metastasis occurred (Sercombe *et al*, submitted).

A Ciz1 splice variant lacking an eight amino acid sequence from exon 14 has been identified. This b-variant of Ciz1 has an altered sub-nuclear distribution (Higgins, Roper et al, submitted). B-variant is limited to tumour cells, and has so far been detected in neuroendocrine tumours, small cell lung cancers, non-small cell lung cancers, thyroid cancers and lymphomas. The b-variant protein is sufficiently stable that its exclusive expression by tumours is being exploited to develop a blood test with the goal of detecting early stage lung cancers. In initial tests b-variant was detected in as little as one microlitre of plasma in 37 out of 40 small cell and non-small cell lung cancer patients (Higgins *et al*, submitted).

Lastly, a Ciz1 splice variant lacking exon 8 has also been found to be upregulated in a study of RNA isolated from the hippocampal region of brains of patients suffering from Alzheimer disease. While total Ciz1 showed no change in transcription compared to healthy tissue, expression of this exon 8 variant is increased 2.5-fold in the Alzheimer's samples (Dahmcke, Buchmann-Moller et al. 2008). Recent years have seen speculation that dysregulation of the DNA damage response may contribute to neurodegenerative diseases such as Alzheimer's, with BRCA1 known to be upregulated in neurofibrillary tangles, one of the classic lesion types symptomatic of the disease (Evans, Raina et al. 2007; Staropoli 2008). Upregulation of this Ciz1 isoform could therefore potentially be representative of a similar loss of DDR function to that seen in tumours and tumour-derived cell lines.

1.2.4.2 Matrix binding of Ciz1 is impaired in tumour-derived cell lines

As previously described, the C-terminal region of Ciz1 mediates binding of the protein to the nuclear matrix (Ainscough, Rahman et al. 2007). Further study of Ciz1's matrix binding properties also shows that it does not bind to the nuclear matrix in a range of tumour-derived cell lines. Immunofluorescence and Western blot experiments done in LnCap, SBC5, H727, RT4 and EJ cell lines showed that no Ciz1 was retained in the nucleus following treatment with DNase I, while HeLa-S3 cells showed a diminished level of matrix-bound Ciz1 [Munkley, unpublished]. These results mirror the behaviour of cyclin E in a panel of cancer and normal cell lines (Munkley, Copeland et al. 2010). This lack of matrix-binding may well reflect alternative splicing of Ciz1 in tumour-derived cell lines impairing function of the anchor domain, similar to the changes in sub-nuclear localisation seen with the b-variant (Higgins *et al*, submitted). The correlation with cyclin E recruitment is being investigated, with particular focus on the order in which these two proteins are normally recruited to the nuclear matrix.

1.2.4.3 Ciz1 is implicated in breast cancer

There are two full and one partial estrogen response elements (ERE), to which the estrogen receptor α (ERα) is recruited, present between exons 1 and 2 of the Ciz1 gene and three partial EREs spread across the sequence downstream of exon 1 (Figure 1.5b). A region at the N-terminus of the Ciz1 protein interacts with the DNA-binding domain of ERα and co-localisation of the two proteins has been observed in the nuclear compartment (den Hollander, Rayala et al. 2006). Estrogen treatments of breast cancer cell lines were also shown to stimulate physical interactions between ERα and Ciz1 and to increase levels of Ciz1 mRNA. This increase does not occur in ERα negative cell lines, or in cells pre-treated with transcriptional inhibitors, but may not reflect the full extent of transcription as primers located in a region of exon 8 that is known to be alternatively spliced were used to detect Ciz1 mRNA (den Hollander, Rayala et al. 2006).

Ciz1 overexpression in breast cancer cell lines increased the growth rate over 6 days, and induced tumor formation in estrogen sensitive cells implanted into immunocompromised mice. This increase in cell proliferation was accompanied by increased levels of cyclin D1, an ERα-regulated gene, and could be inhibited by the addition of antiestrogenic agents (den Hollander, Rayala et al. 2006), and is notable for

its contrast with the effects of Ciz1 overexpression in healthy cell lines. In normal cells overexpression of Ciz1 triggers a block in the cell cycle, with an initial stimulation of DNA synthesis followed by an accumulation of cells in S phase [Sercombe, unpublished]. Conversely Ciz1-overexpressing breast cancer cell lines continued to replicate 6 days after transfection (den Hollander, Rayala et al. 2006).

1.3 Aims

This thesis seeks to investigate whether Ciz1 contributes to the response to DNA damage, using both traditional methods, such as immunofluorescence and real time PCR, and by modifying a cell free DNA replication system which has previously been used to study Ciz1's role in DNA replication (Coverley, Marr et al. 2005).

Initially, this thesis aims to adapt an existing cell-free system to permit use of nuclei and cytoplasmic extracts in which DNA damage signalling pathways have been activated. Furthermore it will show how immunofluorescence can be used to detect phosphorylated H2AX as a marker of DNA damage response activation in addition to the system's original function of measuring DNA synthesis. By separating the nuclear and cytoplasmic components of the DDR and studying the effects of combining extracts treated with DNA damaging agents with untreated nuclei and vice versa, it is hoped that a clearer picture of the mechanisms of the DDR and the possible contribution of Ciz1 can be gained. By exposing Ciz1 to damage-activated nuclei and cytosol, I aim to understand how Ciz1 fits in the DDR, to establish whether its SQ/TQ motifs are phosphorylated by the PIKKs, and to identify whether such modification takes place throughout the protein or is limited to certain regions. By tracking phosphorylation of the protein to specific functional domains, models for involvement of Ciz1 in the DDR can first be identified, and then tested with greater depth using more traditional methods.

Chapter 2

MATERIALS AND METHODS

2.1 Protein Analysis

2.1.1 Sodium Dodecyl Sulphate Polyacrylamide Gel Electrophoresis (SDS-PAGE)

Polyacrylamide gels were cast and run using the TTO slab electrophoresis system. Precision Plus All Blue^{TM} protein standards were used. 6.5% resolving polyacrylamide gels were routinely used. An appropriate ratio of distilled water to 30% w/v acrylamide, 0.8% bis-acrylamide (37.5:1) (National Diagnostics) was prepared. Tris-HCl pH8.8 was added to a final volume of 367mM, SDS to 0.1% w/v (Melford), ammonium persulphate (Sigma Aldrich) to 0.7% w/v and TEMED (Sigma Aldrich) to $1.3x10^{-3}$ v/v. 5% stacking gels were routinely used. These were prepared in a similar manner to resolving gels, except that Tris-HCl pH6.8 was added to 125mM in place of Tris-HCl pH8.8 and TEMED to $2x10^{-3}$ v/v.

2.1.2 Sample preparation for SDS-PAGE

Protein extractions were generated by scrape harvesting cells in 4x SDS-PAGE loading buffer (3ml 1M Tris-HCl pH6.8, 6ml 100% glycerol, 1.6g SDS, 680µl β-mercaptoethanol, 0.1% bromophenol blue). Purified protein on GST beads was resuspended in 4x SDS-PAGE loading buffer. Samples were boiled for 5 minutes, vortexed and boiled for a further 10 minutes to ensure complete denaturation.

2.1.3 Western blotting

2.1.3.1 Transfer

A semi-dry blotter (Sigma Aldrich) was used to transfer proteins from polyacrylamide gels onto PROTRAN® nitrocellulose transfer membrane (pore size 0.45µm, Whatman®). The gel and membrane were sandwiched in between 8 pieces of 3mm chromatography paper (Whatman®). All components were pre-soaked in semi-dry blotting buffer (297mM Tris-base, 10mM CAPS, 10% v/v methanol, 0.02% w/v SDS).

Table 2.1 Wash buffers for Western blot

Buffer name	Phosphate (PBS) or Tris (TBS) buffered saline	% TWEEN-20 (v/v)	% Non-fat dried milk (w/v)	BSA
PBS	PBS	0.01%	10%	-
TBS	TBS	0.01%	5%	-
TBS BSA	TBS	0.01%	-	1mg/ml

2.1.3.2 Antibody detection

Western blots were blocked in the appropriate wash buffer with milk or BSA (Table 2.1) prior to addition of primary antibodies (Table 2.2) in the same buffer for a minimum of 30 minutes. Membranes were then washed for 30 minutes in three changes of wash buffer with milk or BSA. Complementary secondary antibodies (Table 2.2) were applied in milk or BSA buffer for at least 30 minutes prior to three 10 minute rinses in wash buffer (without milk or BSA). Proteins were detected using ECL™ Western Blotting Detection Reagents and pre-flashed chemiluminescent Hyperfilm ECL™ (GE Healthcare).

2.2 Cell culture

2.2.1 Cell lines and culture conditions

All media and supplements were obtained from Gibco® (Invitrogen). All cell lines were grown in Dulbecco's modified eagle medium with GLUTAMAX™ (DMEM) supplemented with 10% v/v foetal calf serum and 1x penicillin-streptomycin-glutamate. Cells were cultured in Nunclon™Δ dishes (Nunc™) and maintained at 37°C in a humidified atmosphere of 5% CO_2. For S phase cell synchrony cells were also cultured in roller bottles (Corning®) at 37°C and gassed once every 24 hours with 5% CO_2 balanced air through a 0.20µm syringe filter (Sartorius).

Adherent cells were passaged by washing in Dulbecco's phosphate buffered saline, without calcium, magnesium or phenol red (dPBS) and incubated with 0.05% v/v trypsin-EDTA at 37°C until cells were detached. Trypsin was quenched with supplemented DMEM.

Table 2.2 Antibody details

Antibody	Host/Isotype	Buffer for Western blot	Dilution for Western blot	Dilution for immunofluorescence	Supplier
Actin A-4700	Mouse monoclonal	PBS	1:1000	n/a	Sigma Aldrich
Phospho-ATM ab2888	Rabbit polyclonal	TBS	1:1000	n/a	AbCam
Ciz1 1793	Rabbit polyclonal	PBS	1:1000	1:1000	(Coverley, Mann et al. 2005)
Ciz1 anchor domain TED	Mouse monoclonal	n/a	n/a	1:10	
GST Ab9805	Rabbit polyclonal	PBS	1:1000	n/a	AbCam
γH2AX 05-636	Mouse monoclonal	TBS	1:1000	1:1000	Upstate
γH2AX 07-164	Rabbit polyclonal	n/a	n/a	1:1000	Upstate
MDC1 Ab11169-50	Rabbit polyclonal	n/a	n/a	1:1000	AbCam
p21 05-345	Mouse monoclonal	n/a	n/a	1:1000	Upstate
PCNA P-8825	Mouse monoclonal	n/a	n/a	1:1000	Sigma Aldrich
Phospho-(Ser/Thr) ATM/ATR Substrate 2851S	Rabbit polyclonal	TBS BSA	1:1000	1:1000	Cell Signaling
Anti-mouse IgG peroxidase conjugate	Goat	Same as primary	1:10000	n/a	Sigma Aldrich
Anti-rabbit IgG peroxidase conjugate	Goat	Same as primary	1:10000	n/a	Sigma Aldrich
Anti-rabbit TRITC conjugate	Goat	n/a	n/a	1:100	Sigma Aldrich
Anti-mouse Alexa 568 conjugate	Goat	n/a	n/a	1:1000	Sigma Aldrich
Streptavidin fluorescein		n/a	n/a	1:500	GE Healthcare

2.2.2 Cell synchrony

2.2.2.1 S phase synchrony

HeLa-S3 cells were synchronised in S phase using thymidine (Sigma Aldrich). 2.5mM thymidine was added to DMEM for 24 hours. Cells were harvested for cell free components or subjected to immunofluorescence immediately following the 24 hour incubation

2.2.2.2 G1 phase synchrony

D3T3 cells were grown in 15cm^2 dishes until confluent and released three days later. Cells were released by passaging and re-plating the equivalent of one 15cm^2 plate onto four 15cm^2 plates. Replated cells were grown for 17 hours after release before harvesting preparation of 'replication competent' late G1 phase nuclei (Coverley, Marr et al. 2005).

2.2.3 DDR treatments

2.2.3.1 Double strand break induction

Induction of double strand DNA breaks was carried out by treating cells with etoposide (Sigma Aldrich). Etoposide was made up to a stock concentration of 42.5mM in DMSO (Sigma Aldrich) and stored at -20°C. DMEM was supplemented with 2μM or 20μM etoposide for a period of up to 24 hours.

2.2.3.2 PIKK inhibition

PIKK inhibition within cells was achieved by treatment with wortmannin (Sigma Aldrich). Wortmannin was made up to a stock concentration of 40mM in DMSO and stored at -20°C. DMEM was supplemented with 200μM wortmannin for 2 hours.

2.2.4 Transfection of Ciz1/c-term/n-term

GFP-C3 Ciz1, GFP-C3 Ciz1-C274, GFP-C3 Ciz1-N442 and pmax-GFP (Amaxa) were used for overexpression experiments. Constructs were transfected into cells using *Trans*IT®-3T3 (Mirus) or Amaxa Nucleofector Kit R (Amaxa).

2.2.4.1 Electroporation

NIH3T3 cells were grown on 15cm^2 plates and lifted using 0.05% v/v trypsin. Detached cells were quenched with DMEM and aliquoted into samples containing approximately 2x10^6 cells. Cells were then collected by centrifugation at 200g for 10 minutes, and resuspended in 100µl of Nucleofector^{TM} solution (Amaxa) prewarmed to room temperature. 5µg of construct to be transfected was added to the sample, which was then transferred into an Amaxa certified cuvette. An Amaxa Nucleofector ^{TM} was then used to transfect cells, using program T-30. Following electroporation, 500µl of DMEM pre-warmed to 37°C was added, and cells removed from cuvettes using plastic sterile pipettes (Amaxa). Cells were then plated onto 6 well plates or glass coverslips in 24 well plates.

2.2.4.2 Lipid transfections

NIH3T3 cells were plated onto 6 well plates or glass coverslips in 24 well plates and transfected using the *Trans*IT®-3T3 transfection kit (Mirus Bio Corporation). 3.5µl *Trans*IT®-3T3 transfection reagent was incubated with 100µl Opti-MEM® I reduced serum media (Invitrogen) for 15 minutes at room temperature. 3µl of the purified construct to be transfected was then added and incubated for a further 5 minutes at room temperature. Finally 1.5µl 3T3 Authority reagent was added and incubated for 15 minutes at room temperature before adding to the cells. Transfection was allowed to continue for between 3 and 12 hours before *Trans*IT® reagents were replaced with fresh medium.

2.3 Microscope analysis of cells

2.3.1 Nuclear immunofluorescence

Cells grown on glass coverslips were exposed to 0.05% Triton X-100 in 1xdPBS, and fixed with 4% paraformaldehyde. Cells were washed three times in dPBS before being blocked for 20 minutes in antibody buffer (10 mg/ml BSA, 0.02% SDS, 0.1% Triton X-100 in PBS). Cells were incubated in primary antibody at an appropriate concentration in antibody buffer (Table 2.2) for a minimum of 1 hour at 37°C. Cells were then washed three times in antibody buffer before incubation in a complementary secondary antibody at an appropriate concentration and 1/1000 Hoechst 33258 in antibody buffer for a minimum of 30 minutes. Cells were washed three more times in antibody buffer before

analysis by fluorescent microscopy. Images were captured using Image Lab. fluorescent secondary antibodies Rabbit IgG F-0382 (Sigma) and alexa fluorescin-568 mouse IgG A11031 (Molecular Probes).

2.3.2 Nuclear matrix preparations

Cells grown on glass coverslips were washed three times in dPBS, before a 5 minute incubation at room temperature in cytoskeletal buffer (CSK; 10mM Pipes, pH 6.8, 300mM sucrose, 100mM NaCl, 1mM $MgCl_2$, 1mM EGTA, 1mM DTT, 0.1mM ATP) supplemented with 0.05% Triton X-100. Cells were then washed three times in DNase buffer (20mM Tris-HCl, 50mM NaCl, 2mM $CaCl_2$, 2mM $MgCl_2$, 1mM DTT) before a 30 minute incubation in DNase I (Roche) diluted 1:20 in the buffer provided. Cells were then washed twice in dPBS and fixed with 4% paraformaldehyde (PFA), before processing as described in 2.3.1.

2.4 Gene expression analysis

2.4.1 Total RNA extraction

WI38 and U2OS cells were grown on 6 well plates. 1ml of TRIzol® (Invitrogen) was added to each well and passed through a pipette several times before transfer to a 1.5ml eppendorf. After a 5 minute incubation at room temperature, 200µl chloroform was added and the sample shaken vigorously for 15 seconds, before a further 5 minute incubation. The aqueous phase was then isolated by centrifugation for 15 minutes at 12000g and 4°C, and transferred to a fresh eppendorf. 0.5ml isopropanol was added, and a further 15 minute incubation at room temperature carried out. RNA was then pelleted by centrifugation for 10 minutes at 12000g and 4°C, and the supernatant discarded. The RNA pellet was washed in 1ml of 75% ethanol and vortexed before centrifuging for 5 minutes at 7500g and 4°C. Ethanol was then removed from the pellet, which was allowed to air dry before resuspension in 20µl nuclease-free water at 55°C for 10 minutes. Total RNA was stored at -20°C.

Table 2.3 Primers and probes

Name	Primer or probe	Sequence	5' reporter/ 3' quencher
hCIZ1 EXON6 F	Primer	TGCCTGTGGAAGACAAGTCA	n/a
hCIZ1 EXON 7 R3	Primer	TGCTGGAGTGCGTTTTTCCT	n/a
EX14F	Primer	CGAGGGTGATGAAGAAGAGGA	n/a
EX16R	Primer	CCCCTGAGTTGCTGTGATA	n/a
Hs ActB-F	Primer	GGTCATCACCATTGGCAATG	n/a
Hs ActB-R	Primer	CGTCACACTTCATGATGGAGTTG	n/a
Exon 7 Joe probe	Probe	CCCTGCCCAGAGGACATCGCC	Joe/Blackhole quencher 1
New ex16 probe	Probe	CACGGGCACCAGGAAGTCCA	Fam/Tamra
Hs ActinB	Probe	ATGGAGTCCTGTGGCATCCACGAAACTAC	Fam/Tamra
AQ1FWD	Primer	AGGCCAGCAGCAGCGCCCAGCAGGAGTTCC	n/a
AQ1REV	Primer	GGAACTCCTGCTGGGCGCTGCTGCTGGCCT	n/a
AQ2FWD	Primer	CAACACTCGGCCCAGACCTGCCTGCTGTCC	n/a
AQ2REV	Primer	GGACAGCAGGCAGGTCTGGGCCGAGTGTTG	n/a
AQ3FWD	Primer	ATCCAGCACCGTAGGGCACAGGAGCACAAG	n/a
AQ3REV	Primer	CTTGTGCTCCTGTGCCCTACGGTGCTGGAT	n/a
AQ4FWD	Primer	GTGGAGCACGTGAAGGCCCAGGGACACAAG	n/a
AQ4REV	Primer	CTTGTGTCCCTGGGCCTTCACGTGCTCCAC	n/a
pGEXFor	Primer	GGGCTGGCAAGCCACGTTTGGTG	n/a
pGEXRev	Primer	CCGGGAGCTGCATGTGTCAGAGG	n/a

2.4.2 Reverse transcription

1µg of total RNA in 10µl nuclease-free water was incubated with 1µl 10mM dNTP (dGTP, dATP, dCTP, dTTP; Invitrogen) and 1µl 500µg/ml random primers (Promega). Samples were incubated at 65°C for 10 minutes in a PTC-200 Peltier Thermal Cycler (MJ Research). Reactions were then incubated on ice for 5 minutes. 1x M-MLV 5x reaction buffer, 0.01M DTT and 10U/µl M-MLV reverse transcriptase (Promega) were added to all reactions to give a final volume of 20µl. Reactions were incubated at 42°C for 52 minutes followed by 70°C for 15 minutes. cDNA was stored at -20°C.

2.4.3 Real time PCR

Primers and TaqMan® probes (Sigma Aldrich) for actin and for Ciz1 exons 7 and 16 were kindly supplied by Dr Gillian Higgins (Table 2.3).

Reactions were carried out in MicroAmp™ optical 96-well reaction plates with optical adhesive film (Applied Biosystems) in a total volume of 25µl. 50ng cDNA was incubated in 1x TaqMan® PCR mix, 0.4µM forward primer, 0.4µM reverse primer and 0.4µM probe. Samples were run on the ABI Prism 7000 Sequence Detection system using the relative quantification assay. The standard protocol for 25µl reaction volumes was used (50°C [2 minutes], 95°C [10 minutes], followed by 40 cycles of 95°C [15 seconds], 60°C [1 minute]). The threshold level of fluorescence was detected automatically by the ABI Prism software. The cycle number at which the sample passed the threshold level is the Ct value. To control for variation in sample recovery both exon primer pairs were normalised to the housekeeping gene actin by subtracting the actin Ct value from the exon Ct value for each sample (ΔCt). The zero hour time point sample for exon 7 was selected as a calibrator sample and all other exon 7 and 16 expression values were expressed relative to it.

2.5 DNA manipulation and bacterial transformation

2.5.1 Glycerol stocks

Glycerol stocks or single colonies from agar plates were used to inoculate 6ml LB broth (Merck Biosciences) in 12ml round bottom culture tubes supplemented with 100µg/ml ampicillin. Cultures were grown overnight at 37°C and 200rpm on a shaker. Glycerol stocks were prepared by mixing 0.7ml of bacterial culture with 0.3ml sterile glycerol and stored at -80°C.

2.5.2 Plasmid purification

Overnight bacterial cultures were harvested by centrifugation at 3000g for 12 minutes. Plasmid DNA was purified using the QIAprep® spin mini-prep kit (Qiagen) according to manufacturer's instructions. Purified DNA was stored at -20°C.

2.5.3 Preparation of chemically competent *E. coli*

Chemically competent BL21(pLys) cells were prepared by streaking cells from glycerol stocks onto LB agar with 34µg/ml chloramphenicol and incubating overnight at 37°C. A single colony was used to inoculate 6ml LB broth and cultured overnight as described in 2.7.1. 50ml LB broth was inoculated with 0.5ml overnight culture and allowed to grow at 37°C on a shaker until the OD_{550} reached 0.6. The cells were harvested by 10

minutes centrifugation at 2000g and 4°C, and resuspended in 20ml ice cold buffer (10mM Tris-HCl pH8.0, 50mM $CaCl_2$). Cells were incubated on ice for 20 minutes and then harvested by 10 minutes centrifugation at 2000g and 4°C. The cell pellet was resuspended in 2ml freeze/thaw buffer (10mM Tris-HCl pH8, 100mM $CaCl_2$, 15% v/v glycerol), and stored as 100µl aliquots at -80°C.

2.5.4 Transformations

Competent *E. coli* cells were thawed on ice and incubated with 1-3µl plasmid DNA for 20 minutes on ice. Cells were heat-shocked at 42°C for 45 seconds and incubated on ice for 2 minutes. Cells were resuspended in 300µl S.O.C medium (Invitrogen) and incubated at 37°C on a shaker at 200rpm for 90 minutes. Cells were then plated onto LB agar containing 100µg/ml ampicillin and incubated overnight at 37°C.

2.5.5 Site directed mutagenesis

Sequential ECiz1 alanine substitution mutations of the S/TQ at S411, S435 and T480 were generated so that the three SQ/TQ motifs were changed to AQ. Mutagenesis was performed using the Stratagene QuikChange method, following the manufacturer's instructions, using pGEX-ECiz1 as template, and custom primers synthesized by Sigma Aldrich (Table 2.3).

2.5.5.1 Sequencing

ECiz1 AQ1-3 in pGEX-6P-3 was sequenced using the pGEXFor and pGEXRev primers (Table 2.3). Sequencing was carried out in house by the Technology Facility at the University of York, using the Applied Biosystems 3130.

2.6 Protein expression and purification from bacteria

Full length ECiz1, ECiz1 AQ1-3 (Section 2.5.5), ECiz1 N442 and ECiz1 C274 (Coverley, Marr et al. 2005) were expressed as GST-fusions in pGEX-6P-3 and purified by sonication for use in SQ/TQ phosphorylation assays. All LB broth cultures were supplemented with 100µg/ml ampicillin and 34µg/ml chloramphenicol.

2.6.1 Manual induction of expression

Glycerol stocks were used to inoculate 75ml LB broth cultures which were grown at 37°C overnight on a shaker at 200rpm. Overnight cultures were used to inoculate 750ml cultures of LB broth. Cultures were grown at 20°C on a shaker at 160rpm and induced to express with 100µM isopropyl-β-D-thiogalactopyranoside at OD600 0.6-0.8 and then cultured for a further 20 hours.

Cells were collected by 12 minutes centrifugation at 4500rpm and 4°C in a Sorvall Evolution centrifuge, resuspended in PBS and divided into two or more equal aliquots. Aliquots were spun down for 15 minutes at 3000rpm and 4°C, and the supernatant discarded. Pellets were flash frozen in liquid nitrogen and stored at -80°C.

2.6.2 Autoinduction of expression

Glycerol stocks were used to inoculate 75ml LB broth cultures which were grown at 37°C overnight on a shaker at 200rpm. Overnight cultures were used to inoculate 750ml cultures of autoinducing medium. Autoinducing medium was prepared by supplementing NZY medium (750ml NZY medium [Fisher], 7.5g tryptone, 3.75g yeast extract) with 1mM $MgSO_4$, 50µM Fe, 20µM Ca, 10µM Mn, 10µM Zn, 2µM Co, 2µM Cu, 2µM Ni, 2µM Mo, 2µM Se, 2µM H_3BO_3, 25µM $(NH_4)_2SO_4$, 50µM KH_2PO_4, 50µM Na_2HPO_4 and 360.31mM α-Lactose monohydrate. Cultures were grown at 20°C on a shaker at 200rpm for 24 hours.

Cells were harvested and frozen as described in Section 2.6.1.

2.6.3 Sonication

Pelleted cells were thawed in 12.5ml resuspension buffer (50mM HEPES pH7.8, 135mM NaCl, 3mM EDTA, 1:10000 monothioglycerol, 1mM PMSF, 0.1mg/ml lysozyme, 1 Roche complete protease inhibitor tablet/25ml of buffer). The suspension was sonicated on ice for 3 minutes at 50% power using a Bandelin sonicator (Bandelin, Berlin, Germany). Samples were then cleared through centrifugation for 30 minutes at 20,000rpm and 4°C in a Sorvall Evolution centrifuge.

2.6.4 GST binding

375µl GST beads (GE Healthcare) were resuspended in 25ml HEPES buffered saline (50mM HEPES pH7.8, 135mM NaCl, 3mM EDTA, 1:10000 monothioglycerol) and incubated on a shaker for 1 hour at room temperature. Beads were then collected by centrifugation at 1000rpm for 1 minute. The lysate collected in Section 2.6.3 was added to GST beads, and incubated on a wheel for 1 hour at 4°C. Supernatant was removed by centrifugation for 10 minutes at 1000rpm and 4°C, then beads were resuspended in 5ml wash buffer (50mM HEPES pH7.8, 135mM NaCl, 3mM EDTA, 1:10000 monothioglycerol, 1 Roche complete protease inhibitor tablet/50ml) and transferred to a fresh tube. The original tube was washed with a further 5ml of wash buffer, which was then added to the transferred beads. Beads were then incubated on a wheel for 5 minutes at 4°C, before this centrifugation and resuspension step was repeated a further 5 times.

2.7 Cell free system

2.7.1 Harvesting of S phase nuclei and extracts

HeLa S3 cells in the process of S phase synchrony were treated with etoposide at the indicated concentration for a period of up to 3 hours, to coincide with the final 3 hours of thymidine-induced synchronisation. Cells were harvested from suspension culture by centrifugation for 10 minutes at 1000rpm at 4°C under minimal lighting, washed in ice cold PBS and in ice-cold hypotonic buffer (20mM K-HEPES pH 7.8, 5mM potassium acetate, 0.5mM MgCl, 0.5mM DTT). After centrifugation for 10 minutes at 1500rpm at 4°C cell pellets were resuspended in an equal volume of hypotonic buffer and disrupted using a Dounce Homogeniser. Nuclei were pelleted by centrifugation at 3000rpm for 10 minutes. The supernatant "soluble extract" fraction was removed and immediately frozen as 50µl beads in liquid nitrogen. The pellet fraction containing nuclei was resuspended in an equal volume of hypotonic buffer, snap frozen in 5µl aliquots and stored in liquid nitrogen.

2.7.2 Harvesting of G1 nuclei

Late G1 synchronised D3T3 nuclei on 15cm^2 plates were washed twice in ice cold PBS and once in ice-cold hypotonic buffer, before a ten minute incubation in hypotonic buffer at 4°C. Plates were then drained before scrape harvesting cells at 4°C. Harvested cells were disrupted using a Dounce Homogeniser and nuclei were pelleted by

centrifugation at 3000rpm for 10 minutes. The supernatant "soluble extract" fraction was removed before the pellet fraction containing nuclei was resuspended in an equal volume of hypotonic buffer. Nuclei were snap frozen in 5µl aliquots and stored in liquid nitrogen.

2.7.3 DNA replication elongation assay

Replication elongation assays were carried out in S phase cytosolic extract supplemented with 1:10 premix, 1:50 CPK, and 1:75 $MgCl_2$ (to final concentrations of 40mM K–HEPES pH 7.8; 7mM $MgCl_2$; 3mM ATP; 0.1mM each of GTP, CTP, UTP; 0.1mM each of dATP, dGTP, and dCTP; 0.5mM DTT; 40mM phosphocreatine and 40mM creatine phosphokinase). Nuclei (~$1x10^4$/µl) and supplemented extracts were incubated together for up to 30 minutes at 37°C. Typically, 10µl of extract was combined with 1.5µl nuclei. 1nM biotin-16-dUTP (Roche) was added to reactions either at the start or after 5 minutes, as indicated, and was incorporated into newly synthesised DNA.

To visualise DNA synthesis, cell free reactions were quenched by addition of 50µl 0.2% Triton X-100 in PBS, followed by 50µl 8% PFA, before transfer of nuclei onto polylysine-coated coverslips by centrifugation through a 20% sucrose cushion. Incorporation of biotinylated-nucleotides was detected with streptavidin-FITC (Amersham) diluted 1/500 in antibody buffer for 1 hour at 37°C, before visualisation by fluorescent microscopy. Cells were probed for γH2AX using monoclonal antibody 05-636 (Upstate) diluted 1/2000 in antibody buffer for 1 hour at 37°C. Alexa 568 goat anti-mouse secondary antibody (Molecular Probes) was used diluted 1/1000 in antibody buffer for 1 hour at 37°C. DNA was counterstained by inclusion of 1/1000 Hoechst 33258 in the secondary antibody step. For combined detection of γH2AX and DNA synthesis, nuclei were probed for phosphorylated H2AX as described above, with inclusion of streptavidin-FITC in both primary and secondary antibody steps. Hoechst, Alexa 568 and streptavidin-FITC were visualised using Zeiss filter sets 10, 15 and 2 respectively.

2.7.3.1 Inhibition of PIKKs

To inhibit PIKKs, supplemented cell free extracts were incubated with 200μM wortmannin (Sigma-Aldrich) or 200μM LY294002 (Sigma-Aldrich) for ten minutes at 4°C prior to addition of nuclei.

2.7.3.2 Pre-conditioning of extracts

For "preconditioning" experiments, 20μl supplemented naive extract was incubated for 10 minutes at 37°C with ~$2x10^5$ nuclei. Reactions were then centrifuged at 3000rpm to pellet nuclei and 10μl extract was removed and applied to fresh nuclei.

2.7.3.3 Inhibition of DNA synthesis

To inhibit DNA synthesis, supplemented cell free extracts were incubated with 1mM aphidicolin (Sigma-Aldrich) for ten minutes at 4°C prior to addition of nuclei.

2.7.3.4 Ciz1 titration

To titrate Ciz1 into cell free reactions, supplemented cell free extracts were incubated with purified Ciz1 protein at the indicated concentration for ten minutes at 4°C prior to addition of nuclei.

2.7.4 Initiation assay

Replication elongation assays were carried out in supplemented S phase cytosolic extracts. Nuclei (~$1x10^4$/μl) and supplemented extracts were incubated together for 30 minutes at 37°C. Typically, 10μl of extract was combined with 1μl nuclei. 1nM biotin-16-dUTP (BdUTP; Roche) was added to reactions after 5 minutes. To visualise DNA synthesis, cell free reactions were quenched by addition of 50μl 0.2% Triton X-100 in PBS, followed by 50μl 8% PFA, before transfer of nuclei onto polylysine-coated coverslips by centrifugation through a 20% sucrose cushion. Incorporation of biotinylated-nucleotides was detected with streptavidin-FITC (Amersham) diluted 1/500 in antibody buffer for 1 hour at 37°C, before visualisation by fluorescent microscopy.

Nuclei from late G1 populations that were induced to initiate DNA replication *in vitro* in the presence of S phase extract were scored by eye at 600x magnification. All nuclei

with focal staining were scored as positives regardless of the extent of nucleotide incorporation.

2.7.5 Imaging and quantification

Coverslips were mounted using Vectashield mounting medium (Vector Labs) to prevent fading of fluorescence. Hoechst, FITC (newly synthesized DNA) and Alexa 568 (phosphorylated H2AX) fluorescence were photographed at 600x magnification with an Axiovert microscope fitted with an AxioCam camera (Carl Zeiss Vision, Hallbergmoos, Germany) using a 63/1.40 oil immersion objective and constant exposure parameters (FITC: 700mS; Alexa 568: 50mS). The average fluorescence intensity within the largest rectangular area of individual nuclei was measured using Openlab software (Improvision, Coventry, UK). The mean pixel intensity within the selected areas were collected for 28-110 nuclei per reaction prior to any image manipulation, and displayed in histograms along with standard error of the mean (SEM) calculated using Excel. Probability values were calculated using the "t-test: paired two-sample for means" and "t-test: two sample assuming unequal variances" tools in Excel's data analysis package. Example images shown alongside histograms were adjusted using Adobe Photoshop to increase image intensity for reproduction. In all cases, control and test samples were treated identically.

2.7.6 Protein phosphorylation assays

GST-tagged ECiz1, ECiz1-AQ1-3, ECiz1-N442 and ECiz1-C274 bound to GST-beads were incubated in supplemented S phase cytosolic extracts for 30 minutes at 37ºC, before being removed by centrifugation and washed once with PBS. 4x SDS PAGE loading buffer was then added to denature the protein. Samples were then run on a 6.5% SDS-PAGE gel, transferred to nitro-cellulose paper, and probed for antibodies as described. Western blots were developed using enhanced chemiluminescence and Amersham preflashed chemiluminescence film. Antibodies used were Ciz1 1793, GST and phospho-(Ser/Thr) ATM/ATR substrate 2851S (Cell signalling) (Table 2.2).

Chapter 3

THE CELL FREE SYSTEM AS A TOOL TO STUDY THE DNA DAMAGE RESPONSE

3.1 Introduction

Cell free DNA replication systems were originally developed using viral control elements (Stillman 1989) and later, activated Xenopus egg extracts (Murray and Kirschner 1989). These allowed study of enzymatic and structural features of DNA replication, but did not permit study of the regulatory events of the somatic cell cycle. More suitable for this purpose is a system derived from mammalian cells, that supports the replication initiation process using cytosolic extracts and intact isolated nuclei from synchronised cells (Krude, Jackman et al. 1997; Coverley, Laman et al. 2002). This chapter details the adaptation of a mammalian cell-free DNA replication system for reconstitution and analysis of the DNA damage response (DDR).

3.2 Aims

This chapter aimed to develop a cell-free system as a tool with which to study the DDR. Goals were:

- To identify and optimise conditions for production of isolated nuclei and cell extract from cells undergoing the DDR.

- To combine an existing BdUTP assay with immunofluorescence techniques to allow DNA replication initiation and elongation to be visualised in concert with markers of the DDR.

- To investigate whether different steps of the DDR could be reconstituted *in vitro* at multiple stages of the cell cycle.

- To characterise the properties of isolated nuclei and cytosolic extracts in which DDR signalling had been activated.

- To establish whether the presence of physical DNA damage is necessary for activation of the DDR in nuclei.

3.3 Experimental design

The topoisomerase II inhibitor, etoposide, was used to induce double strand breaks in thymidine-synchronised S phase HeLa cells, generating populations of “damaged

nuclei" and "damage-activated extracts" for cell-free experiments. Eukaryotic topoisomerase II catalyses the conformational and topological changes in DNA necessary for DNA replication, allowing formation of a junction between two sections of doublestranded DNA via the formation of transient double strand break. Etoposide functions by stabilising the topoisomerase II cleavable complex, stalling the replication fork and preventing these temporary breaks from being annealed (Chen and Liu 1994; Li and Liu 2001), and was chosen because it could be easily incorporated into existing methods for harvesting nuclei and extracts, unlike ionising radiation. Etoposide also chiefly induces double strand breaks during the S phase of the cell cycle, which could be a drawback if studying cycling cells, but proved compatible with the thymidine synchronisation used here.

Damaged nuclei and damage-activated extracts were combined with "naive" nuclei and extracts from untreated cells to reconstitute distinct steps in the DDR. After incubation in extract supplemented with nucleotide, cofactors and an energy regenerating system the extent of DNA synthesis and H2AX phosphorylation were monitored in nuclei by fluorescent microscopy. Incorporation of biotinylated nucleotide allowed quantification of the extent of DNA synthesis, while phosphorylated H2AX was detected with a well-characterised phosphorylation sensitive monoclonal antibody.

3.4 Results

3.4.1 Optimisation of harvesting and labelling methods

The cell-free system that was adapted to produce the data in this chapter has previously been used by the Coverley laboratory for both DNA replication initiation and elongation studies. In order to adapt the system to permit study of DDR activation and signalling, a number of developments were required.

3.4.1.1 Suitability of thymidine as a synchronisation method for DDR studies

The cell-free system involves the use of thymidine to synchronise cells in S phase before harvesting nuclei and cytosolic extract. Existing protocols treat cells for 24 hours with thymidine, prior to a 24 hour release and a second 24 hour treatment before harvesting. Thymidine inhibits replication by depleting cellular pools of dCTP, slowing progression of replication forks (Bjursell and Reichard 1973). Recovery of replication forks from this block has been shown to occur by a homologous recombination repair

mediated mechanism (Bolderson, Scorah et al. 2004). This process is dependent on both ATM and ATR, a fact which has not been a concern when using the system solely to measure DNA replication elongation, but which could potentially affect the outcome of studies examining DDR induction.

In order to establish whether thymidine treatment was a suitable method of cell synchronisation for these studies, intact S3 HeLa cells were cultured for 24 hours in either 2.5mM thymidine, 20μM etoposide, or both thymidine and etoposide, before two γH2AX antibodies, a mouse monoclonal and a rabbit polyclonal, were used to visualise phosphorylated H2AX by immunofluorescence. The rabbit polyclonal displayed no difference between treated and control cells, and was not used for further experiments.

Using the mouse monoclonal antibody, cells treated with thymidine displayed an increase in H2AX phosphorylation but levels were distinctly lower than in either the etoposide or etoposide & thymidine-treated populations (Figure 3.1a). Additionally a timecourse was carried out during which total protein was harvested from S3 HeLa cells up to 5 hours after release from a 24 hour treatment with 2.5mM thymidine. Protein was then analysed by Western blot for presence of phosphorylated H2AX. γH2AX could not be seen in thymidine treated samples, but was apparent in a control population treated with 20μM etoposide for 2 hours (Figure 3.1b). Subsequently, a single thymidine release was used for preparation of all nuclei and extracts rather than the double synchronisation recommended by the laboratory protocol.

3.4.1.2 Harvesting of nuclei - effect of increasing roughness of Dounce homogenisation

As part of the harvesting protocol for the cell-free system, cells are swollen using a hypotonic buffer, before being lysed by Dounce homogenisation to separate nuclei from cytosolic extract. To investigate whether the physical stress of homogenisation had the potential to induce DNA lesions, S3 HeLa cells synchronised in S phase were divided into three samples with an increasing number of strokes used to lyse each sample. Immunofluorescence was then used to visualise the base level of H2AX phosphorylation in each population of nuclei.

Nuclei from cells lysed using either ten or twenty strokes displayed equivalent, low levels of H2AX phosphorylation in approximately half the population, while nuclei from cells lysed using thirty strokes showed a distinct increase in both the proportion

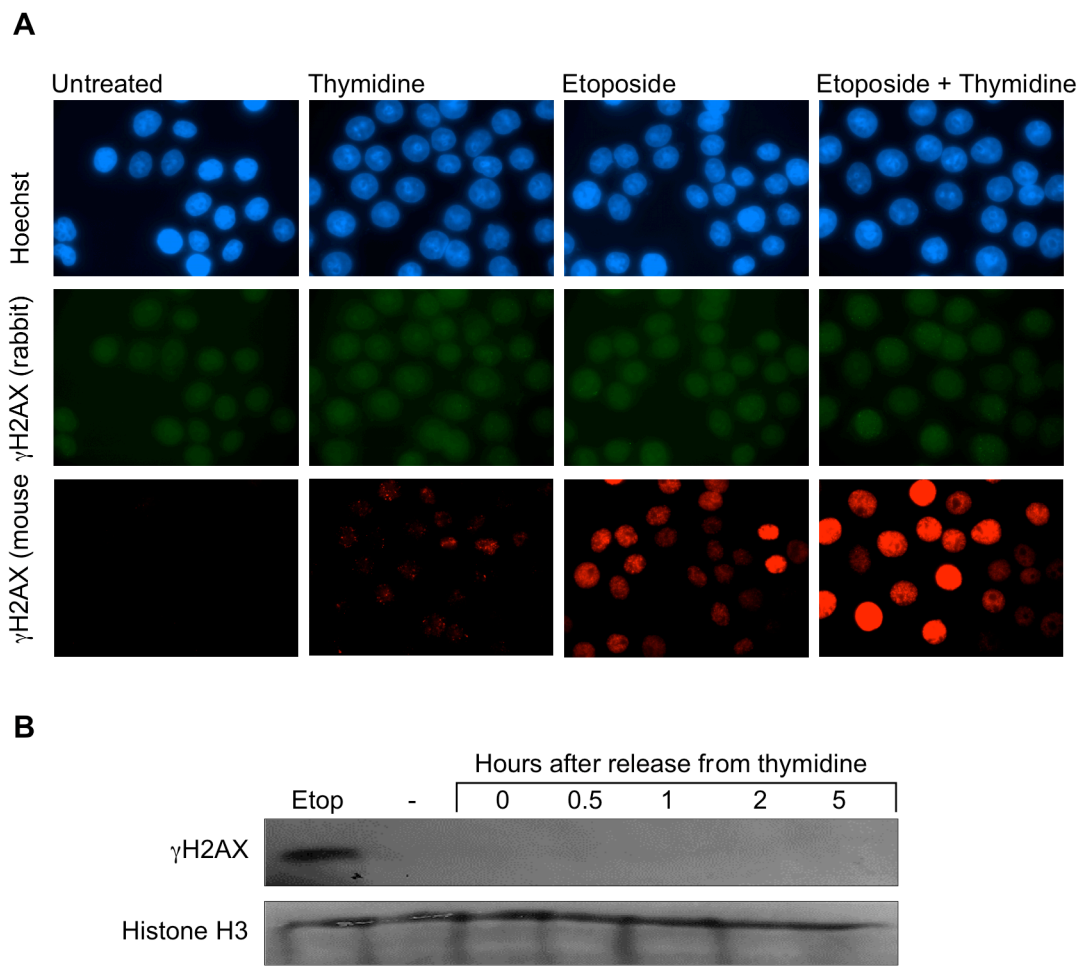

Figure 3.1 H2AX phosphorylation induced by thymidine treatment of HeLa-S3 cells occurs at a lower level than etoposide-induced γH2AX

a) Immunofluorescence images showing phosphorylated H2AX in HeLa-S3 cells treated with thymidine and etoposide. Cells were treated for 24 hours with either 2.5mM thymidine, 20μM etoposide, or both thymidine and etoposide. Cells were washed in 0.5% Triton X-100 for 10 seconds, and then rinsed once in PBS before fixation with PFA. Phosphorylated H2AX was detected using rabbit polyclonal (green) and mouse monoclonal (red) anti-phospho H2AX (Ser139) antibodies and either anti-rabbit FITC conjugated or anti-mouse Alexa 568 conjugated secondary antibodies. Nuclei were counterstained with Hoechst 33258 (blue).

b) Western blot analysis of total γH2AX protein level from HeLa-S3 cells harvested at 0, 0.5, 1, 2 and 5 hours after release from a 24 hour thymidine incubation. Also shown is protein from control populations which received no thymidine treatment, one of which was treated for 2 hours with 20μM etoposide. Protein was harvested by addition of 2x loading buffer directly to cells growing on 10cm plates. Protein was separated by 6.5% SDS-PAGE and detected with mouse monoclonal anti-phospho H2AX antibody. Histone H3 levels are shown as a loading control.

undergoing phosphorylation, and the levels of phosphorylation induced in those nuclei (Figure 3.2). Nuclei were subsequently harvested using ten to fifteen strokes and cytosolic extracts using between twenty and twenty-five strokes, with lysis being visually confirmed by microscopy.

3.4.1.3 Optimisation of BdUTP assay

The initial question asked with this cell free system was whether damaged nuclei incubated in naive cytosolic extract and allowed to undergo DNA synthesis would display a decrease in BdUTP incorporation compared to healthy nuclei in the same conditions. This would serve as a proof of concept to demonstrate that DNA damage signalling was being reconstituted in the system. As expected, a decrease in incorporation of the fluorescently labelled nucleotide biotinylated-UTP (BdUTP) to DNA was observed in the damaged population of nuclei (Figures 3.3a and 3.3b). The question then arose of whether the system could be optimised to increase this differential.

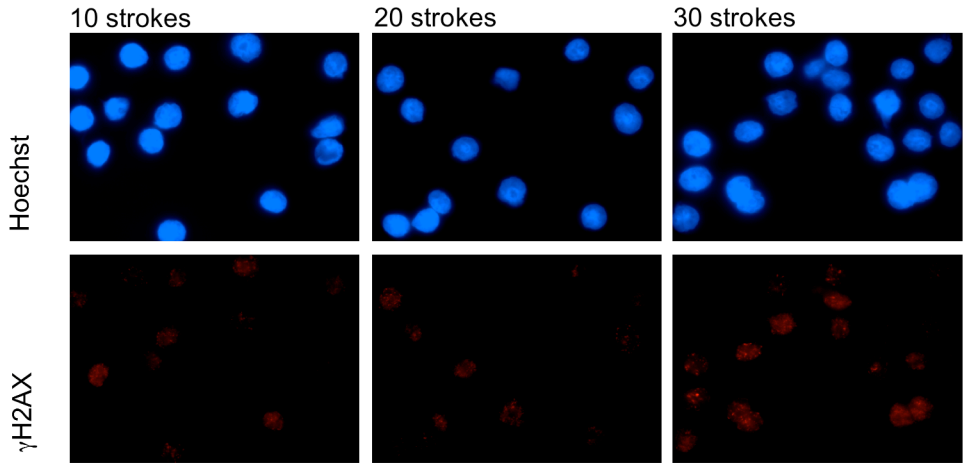

Figure 3.2 Background H2AX phosphorylation increases in S phase HeLa-S3 nuclei as a result of increased physical stress during harvesting

Immunofluorescence images showing phosphorylated H2AX in S phase HeLa-S3 nuclei following harvesting by Dounce homogenisation. Cells were synchronised in S phase for 24 hours with 2.5mM thymidine, before a brief incubation in hypotonic buffer. Cells were then lysed using 10, 20 or 30 strokes in a Dounce homogeniser. Nuclei were collected by centrifugation and flash frozen as 10µl beads in liquid nitrogen. Nuclei were later thawed, rinsed with 0.5% Triton X-100 before fixation with PFA, and then spun onto poly-lysine coated coverslips through a sucrose cushion. Phosphorylated H2AX (red) was detected using mouse monoclonal anti-phospho H2AX (Ser139) antibody, and anti-mouse Alexa 568 conjugated secondary antibody. Nuclei were counterstained with Hoechst 33258 (blue).

Figure 3.3 Damaged nuclei recapitulate the DNA damage response in a cell-free environment

a) Images of sites of DNA replication in naïve and damaged S phase HeLa-S3 nuclei incubated in naïve S phase HeLa-S3 extract and supplemented with BdUTP at either the start of the reaction or after 5 minutes. Reactions were processed as described in the methods (Section 2.7). BdUTP incorporation was visualised using streptavidin-fluorescein (green) and fluorescent microscopy. Nuclei were counterstained with Hoechst 33258 (blue).

b) Quantification of BdUTP incorporated into nuclear DNA in cell-free reactions in which naïve (light blue) or damaged (dark blue) nuclei are incubated with naïve extract, and BdUTP is added at either the start of the reaction or after 5 minutes. Histogram shows average fluorescent intensity with standard error of the mean and is representative data from one of two experiments. Asterisks represent the p-value found by t-test assuming unequal variances: ✳ = $0.05>p>0.01$; ✳✳ = $0.01>p>0.001$; ✳✳✳ $p<0.001$. n = number of nuclei quantified per sample.

c) Fluorescent images of sites of DNA replication and phosphorylated H2AX in naïve and damaged S phase HeLa-S3 nuclei incubated in naïve S phase HeLa-S3 extract. Reactions were processed as described in the methods (Section 2.7). BdUTP incorporation was visualised using streptavidin-fluorescein (green) and H2AX phosphorylation with mouse monoclonal anti-phospho H2AX (Ser139) antibody, and anti-mouse Alexa 568 conjugated secondary antibody. Nuclei were counterstained with Hoechst 33258 (blue).

d) Quantification of BdUTP incorporated into nuclear DNA (blue) and H2AX phosphorylation (red) in cell-free reactions in which naïve and damaged nuclei are incubated in naïve extract. Histogram shows average fluorescent intensity with standard error of the mean and is representative data from one of five experiments. Asterisks represent the p-value found by t-test assuming unequal variances: ✳ = $0.05>p>0.01$; ✳✳ = $0.01>p>0.001$; ✳✳✳ $p<0.001$. n = number of nuclei quantified per sample.

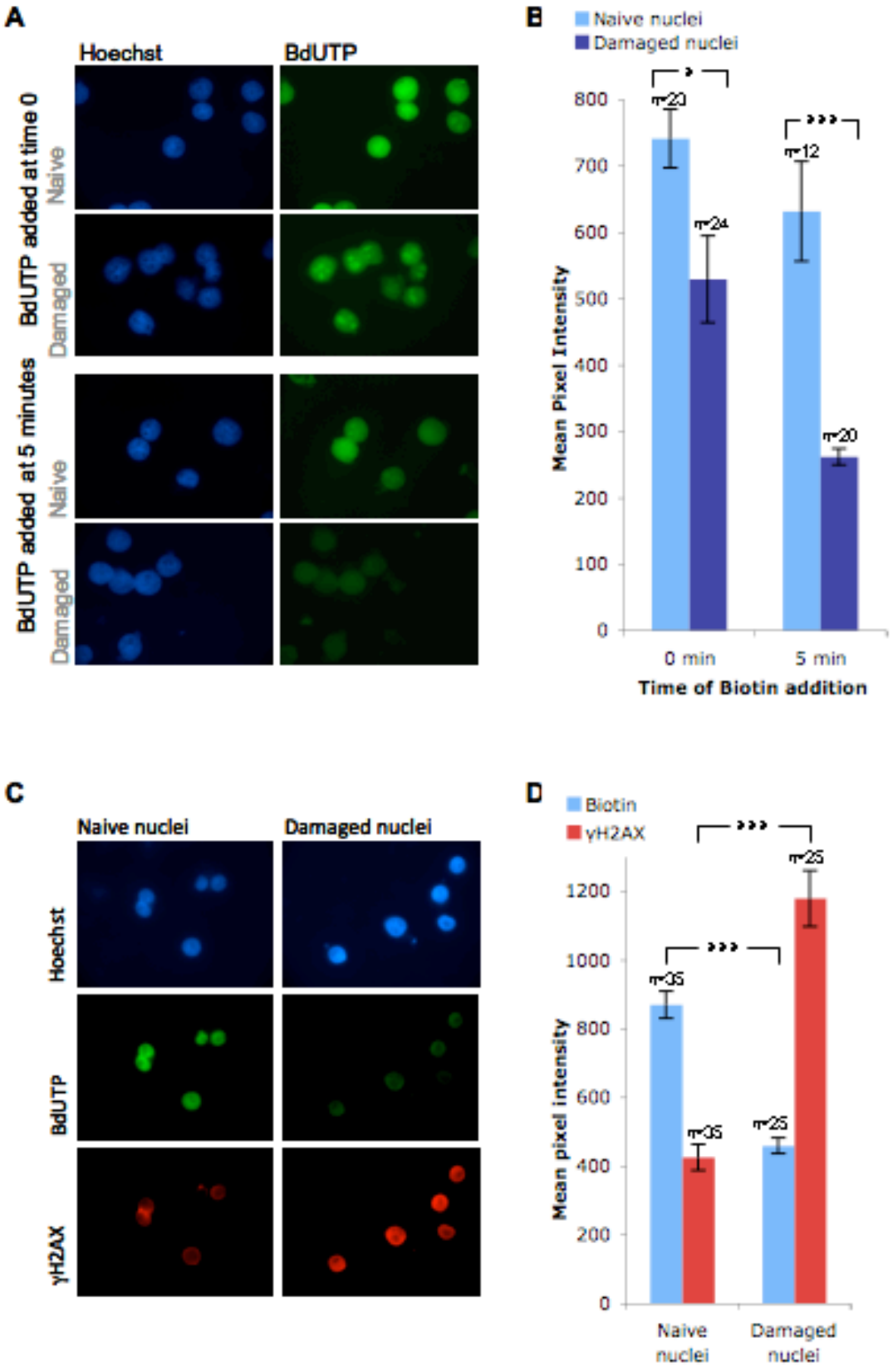
A
Hoechst
BdUTP
BdUTP added at time 0
Naive
Damaged
BdUTP added at 5 minutes
Naive
Damaged
B
Naive nuclei
Damaged nuclei
Mean Pixel Intensity
800
700
600
500
400
300
200
100
0
n=20
n=24
n=12
n=20
0 min
5 min
Time of Biotin addition
C
Naive nuclei
Damaged nuclei
Hoechst
BdUTP
γH2AX
D
Biotin
γH2AX
Mean pixel intensity
1200
1000
800
600
400
200
0
n=35
n=35
n=25
n=25
Naive nuclei
Damaged nuclei

The presence of double strand breaks provides a physical barrier to DNA replication elongation *in vivo*, in addition to halting the cell cycle via the DDR. Using template nuclei that have been severely damaged and contain many double strand breaks, this might be expected to be a major source of replication fork restraint. In order to maximise detection of the effect of this damage on DNA synthesis *in vitro*, the effect of delaying addition of BdUTP to cell free reactions, allowing active replication forks to encounter damaged sites before labelling commenced, was investigated.

Naive and damaged nuclei were either incubated in naive extract supplemented with BdUTP for 30 minutes, or allowed a 5 minute preincubation in naive extract prior to addition of BdUTP, followed by a 25 minute incubation. In both instances BdUTP incorporation was lower in damaged nuclei compared to naive nuclei, but the difference was significantly more marked in reactions that had received the preincubation (Figures 3.3a and 3.3b). A 5 minute preincubation has since been used in all cell-free experiments.

3.4.1.4 Simultaneous detection of both phosphorylated H2AX and BdUTP incorporation

Having confirmed that the DDR could be reconstituted *in vitro*, the next step was to add a second marker into the system, allowing direct visualisation of DDR signalling, rather than relying solely on the indirect measure of damage provided by levels of DNA synthesis. To achieve this, the processing protocol for the assay was altered to allow incubation of nuclei immobilised on coverslips in the γH2AX mouse monoclonal antibody and a complementary secondary antibody concurrent with staining of BdUTP with streptavidin-FITC. To maximise detection of BdUTP a short incubation of 1 hour was used for primary and secondary antibodies, with streptavidin-FITC being included in both steps. Using this method both BdUTP and phosphorylated H2AX could be clearly visualised in nuclei. As expected the level of phosphorylated H2AX was significantly greater in damaged nuclei compared to naive nuclei, reflecting the presence of etoposide induced double strand breaks (Figures 3.3c and 3.3d).

3.4.2 Extracts from etoposide-treated cells induce the DDR in the absence of physical damage

The proof of concept and optimization experiments described so far demonstrate that inhibition of DNA replication and induction of H2AX phosphorylation are stable *in vitro* even when soluble signalling molecules in the naive extracts used are initially

inactive. It seems likely that the presence of DSBs in damaged nuclei activates soluble cytosolic factors in these extracts as it would in an intact cell, allowing propagation of damage signalling. To ask whether this soluble damage signalling and its impact on nuclear functions such as DNA replication can be uncoupled from the damage itself, the effect of damage-activated extract on naive nuclei was examined.

Exposure of naive nuclei to activated extract suppressed DNA replication elongation compared to extract from untreated cells, confirming the presence of soluble signalling molecules able to inhibit DNA replication *in vitro* in damage-activated extract. Furthermore this was accompanied by phosphorylation of H2AX in naive nuclei (Figures 3.4a and 3.4b), showing that the presence of physical damage is not required for the early stages of DDR signalling to be activated.

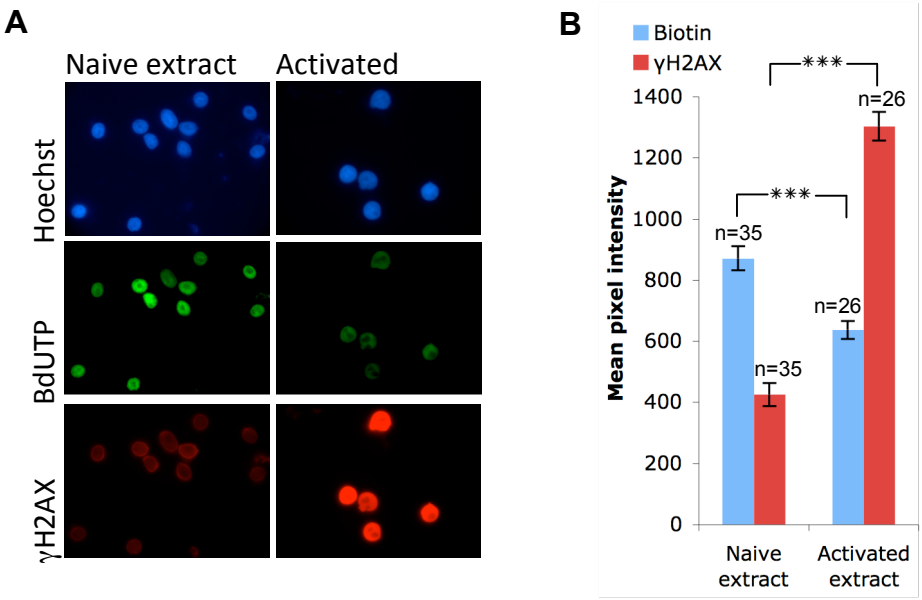

Figure 3.4 Damage-activated extract activates the DNA damage response in naïve nuclei

a) Fluorescent images of sites of DNA replication and phosphorylated H2AX in naïve S phase HeLa-S3 nuclei incubated in naïve and damage-activated S phase HeLa-S3 extract. Reactions were processed as described in the methods (Section 2.7). BdUTP incorporation was visualised using streptavidin-fluorescein (green) and H2AX phosphorylation with mouse monoclonal anti-phospho H2AX (Ser139) antibody, and anti-mouse Alexa 568 conjugated secondary antibody. Nuclei were counterstained with Hoechst 33258 (blue).

b) Quantification of BdUTP incorporated into nuclear DNA (blue) and H2AX phosphorylation (red) in cell-free reactions in which naïve nuclei are incubated in naïve and damage-activated extract. Histogram shows average fluorescent intensity with standard error of the mean and is representative data from one of five experiments. Asterisks represent the p-value found by t-test assuming unequal variances: ✳ = 0.05>p>0.01; ✳✳ = 0.01>p>0.001; ✳✳✳ p<0.001. n = number of nuclei quantified per sample.

Marker	Initiation in naive extract	Initiation in activated extract	Mean decrease in DNA replication initiation	Total No. of nuclei scored
BdUTP	0.150	0.110	27%	225
BdUTP	0.149	0.113	24%	411
BdUTP	0.157	0.133	15%	227
BdUTP	0.184	0.094	49%	216
Total	**0.160 ±0.0082**	**0.113 ±0.008**	**29% ∗**	**1079**

Table 3.1 Replication initiation is inhibited in naïve G1 phase nuclei when incubated in damage-activated extract

Naïve Gl phase HeLa-S3 nuclei were incubated in naïve and damage-activated S phase HeLa-S3 extract. Reactions were processed as described in the methods (Section 2.7), and nuclei displaying BdUTP incorporation were scored by eye. Table displays the proportion of nuclei undergoing initiation under each condition in four separate experiments, and the mean decrease in initiation between paired reactions. Total mean values are displayed with standard error of the mean. Asterisks represent the p-value found by paired t-test: ✳ = 0.05>p>0.01.

When this experiment was extended to monitor the effect on initiation of DNA replication rather than elongation from pre-initiation replicons, a significant effect was also recorded. Using synchronized replication competent G1 phase nuclei, activated extract inhibited initiation of DNA replication by up to 49% compared to naive extract (Table 3.1). Incubation in activated extract resulted in consistent lower levels of initiation across multiple batches of G1 nuclei compared to naive extract.

3.4.3 Contrasting effects of the PIKK inhibitors wortmannin & LY294002 upon H2AX phosphorylation

The cellular response to double strand breaks is dependent upon and mediated by the PIKKs, ATM, ATR and DNA-PK. To ask whether the PIKKs are required *in vitro* for damage-activated extract to induce H2AX phosphorylation and restraint of DNA replication, a pair of well-characterised PIKK inhibitors was used. Activated extracts were supplemented with these inhibitors prior to incubation with naive nuclei so that both extract and nuclei-derived kinases would be silenced.

3.4.3.1 Inhibition of DNA replication and H2AX phosphorylation by activated extract is PIKK-dependent

Wortmannin is an irreversible inhibitor of the PIKKs which modifies protein structure by covalently binding to kinases (Norman, Shih et al. 1996). In the presence of 200μM wortmannin, a concentration known to affect all PIKKs (Rodriguez-Bravo, Guaita-Esteruelas et al. 2006), H2AX phosphorylation was dramatically inhibited in naive nuclei (Figure 3.5). In addition, nuclei displayed on average a 46% increase in BdUTP

incorporation indicating that DDR-mediated restraint of DNA synthesis was blocked (Table 3.2). LY294002 is a competitive and reversible inhibitor of the PIKKs (Vlahos, Matter et al. 1994). When damage-activated extract was supplemented with either 50μM or 200μM LY294002, BdUTP incorporation in naive nuclei increased by an average of 10% and 52% respectively, however at both concentrations H2AX phosphorylation rose by over 30% (Figure 3.5a; Table 3.2).

3.4.3.2 PIKK inhibitors stimulate DNA replication elongation in naive nuclei & extracts

Naive nuclei were also incubated in naive extract supplemented with either 200μM wortmannin or 200μM LY294002. Under these circumstances both inhibitors stimulated BdUTP incorporation above levels observed in naive nuclei incubated in naive extract alone (Table 3.3), but only wortmannin abolished base levels of H2AX phosphorylation (Figure 3.6). Only a single replicate was carried out using LY294002, but a contrasting effect upon H2AX phosphorylation was seen compared to naive

Condition	Concentration	Marker	Mean untreated pixel intensity	Sample size	Mean treated pixel intensity	Sample size	Percentage change
naive/activated	200uM Wortmannin	BdUTP	709.55	44	1141.79	56	60.92%
naive/activated	200uM Wortmannin	BdUTP	982.75	46	1107.48	52	12.69%
naive/activated	200uM Wortmannin	BdUTP	251.00	47	376.37	39	49.95%
naive/activated	200uM Wortmannin	BdUTP	242.62	28	538.04	45	121.76%
naive/activated	200uM Wortmannin	BdUTP	419.81	40	520.50	37	23.99%
naive/activated	200uM Wortmannin	BdUTP	575.38	46	904.59	38	57.22%
naive/activated	200uM Wortmannin	BdUTP	695.93	38	1080.32	29	55.23%
		Total	**553.86 ±101.82**	**289**	**809.87±122.12**	**296**	**46.22% ****
naïve/activated	200uM Wortmannin	H2AX	652.14	28	249.14	45	-53.70%
naïve/activated	200uM Wortmannin	H2AX	341.52	40	59.70	37	-82.52%
naïve/activated	200uM Wortmannin	H2AX	320.87	46	41.14	38	-87.18%
naïve/activated	200uM Wortmannin	H2AX	444.76	38	74.87	29	-83.17%
		Total	**411.30 ±50.19**	**152**	**106.21 ±48.14**	**149**	**-74.18% *****
naive/activated	50uM LY294006	BdUTP	575.38 ±25.44	46	663.05 ±36.96	34	15.24% *
naive/activated	50uM LY294006	BdUTP	695.93 ±18.38	38	743.49 ±45.83	21	6.83%
naive/activated	50uM LY294006	H2AX	320.87 ±11.90	46	443.94 ±28.06	34	38.36% ***
naive/activated	50uM LY294006	H2AX	444.76 ±17.15	38	576.27 ±31.52	21	29.57% ***
naive/activated	200uM LY294006	BdUTP	695.93 ±18.58	38	1064.32 ±49.29	33	52.93% ***
naive/activated	200uM LY294006	BdUTP	245.62 ±8.44	44	370.56 ±9.12	34	50.87% ***
naive/activated	200uM LY294006	H2AX	444.76 ±17.15	38	556.24 ±21.46	33	25.06% ***
naive/activated	200uM LY294006	H2AX	209.99 ±12.72	44	313.79 ±16.70	34	49.43% ***

Table 3.2 PIKK inhibitors alleviate the block on DNA synthesis elongation imposed on naïve S phase nuclei by damage-activated extract
Naïve S phase HeLa-S3 nuclei were incubated in damage-activated S phase HeLa-S3 extract supplemented with either 200μM wortmannin, 50μM LY294002 or 200μM LY294002. Reactions were processed as described in the methods (Section 2.7), and mean pixel intensities of BdUTP incorporation and H2AX phosphorylation for each sample recorded using Openlab. Table displays the mean pixel intensity of these markers with standard error of the mean and the percentage change in fluorescence between control reactions and reactions treated with inhibitor. Asterisks represent the p-value found by paired t-test (total values) or t-test assuming unequal variances (individual replicates): ✳ = 0.05>p>0.01; ✳✳ = 0.01>p>0.001; ✳✳✳ p<0.001.

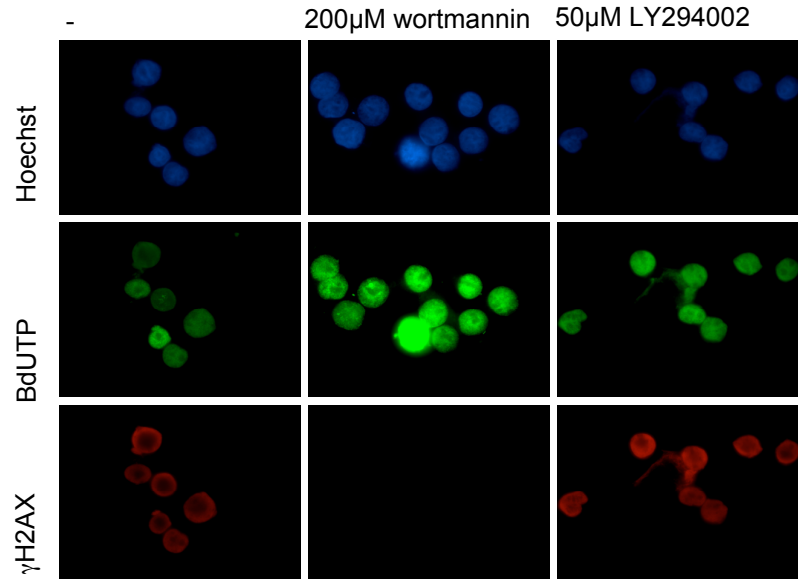

Figure 3.5 PIKK inhibitors alleviate the block on DNA synthesis elongation imposed on naïve S phase nuclei by damage-activated extract

Fluorescent images of sites of DNA replication and phosphorylated H2AX in naïve S phase HeLa-S3 nuclei incubated in damage-activated S phase HeLa-S3 extract supplemented with either 200μM wortmannin or 50μM LY294002. Reactions were processed as described in the methods (Section 2.7). BdUTP incorporation was visualised using streptavidin-fluorescein (green) and H2AX phosphorylation with mouse monoclonal anti-phospho H2AX (Ser139) antibody, and anti-mouse Alexa 568 conjugated secondary antibody. Nuclei were counterstained with Hoechst 33258 (blue).

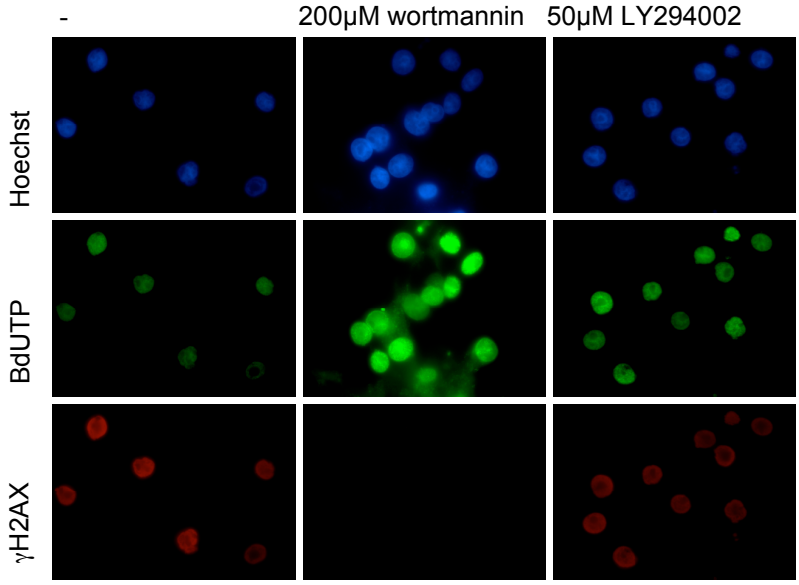

Figure 3.6 PIKK inhibitors stimulate DNA synthesis elongation in naïve S phase nuclei incubated with naïve extract

Fluorescent images of sites of DNA replication and phosphorylated H2AX in naïve S phase HeLa-S3 nuclei incubated in naïve S phase HeLa-S3 extract supplemented with either 200μM wortmannin or 50μM LY294002. Reactions were processed as described in the methods (Section 2.7). BdUTP incorporation was visualised using streptavidin-fluorescein (green) and H2AX phosphorylation with mouse monoclonal anti-phospho H2AX (Ser139) antibody, and anti-mouse Alexa 568 conjugated secondary antibody. Nuclei were counterstained with Hoechst 33258 (blue).

Condition	Concentration	Marker	Mean untreated pixel intensity	Sample size	Mean treated pixel intensity	Sample size	Percentage change
naïve/naïve	200uM Wortmannin	BdUTP	1466.59	32	1538.92	32	4.93%
naïve/naïve	200uM Wortmannin	BdUTP	1411.12	35	1561.62	53	10.67%
naïve/naïve	200uM Wortmannin	BdUTP	555.53	41	764.13	59	37.55%
naïve/naïve	200uM Wortmannin	BdUTP	503.62	32	738.84	49	46.71%
		Total	**984.21±262.94**	**140**	**1150.88±230.69**	**193**	**16.93%**
naïve/naïve	200uM Wortmannin	H2AX	349.45 ±19.00	35	96.28 ±7.23	28	-72.45% ***
naïve/naïve	200uM Wortmannin	H2AX	337.46 ±23.70	32	189.19 ±23.91	49	-43.94% ***
naive/naive	50uM LY294006	BdUTP	503.62 ±18.58	32	721.78 ±28.32	33	43.32% ***
naive/naive	50uM LY294006	H2AX	337.46 ±23.70	32	350.52 ±12.87	33	3.90%

Table 3.3 PIKK inhibitors stimulate DNA synthesis elongation in naïve S phase nuclei incubated with naïve extract

Naïve S phase HeLa-S3 nuclei were incubated in naïve S phase HeLa-S3 extract supplemented with either 200µM wortmannin, 50µM LY294002 or 200µM LY294002. Reactions were processed as described in the methods (Section 2.7), and mean pixel intensities of BdUTP incorporation and H2AX phosphorylation for each sample recorded using Openlab. Table displays the mean pixel intensity of these markers with standard error of the mean and the percentage change in fluorescence between control reactions, and reactions treated with inhibitor. Asterisks represent the p-value found by paired t-test (total values) or t-test assuming unequal variances (individual replicates): ✳ = 0.05>p>0.01; ✳✳ = 0.01>p>0.001; ✳✳✳ p<0.001.

nuclei in damage-activated extract. When incubated in naive extract, nuclei displayed constant levels of H2AX phosphorylation whether the inhibitor was added to the reaction or not (Table 3.3).

3.4.4 Damaged nuclei condition cellular extract to inhibit DNA replication

It has already been shown that activation of the DNA damage response is sustained in damaged nuclei when incubated in naive extract, and hypothesized that this is due to activation of soluble damage signalling *in vitro* by these nuclei. To test whether signals generated by damaged nuclei can activate the DDR in naive extract, naive extracts were exposed to nuclei containing etoposide-induced DSBs, during a "pre-conditioning reaction" before being cleared of nuclei by centrifugation. These "pre-conditioned" extracts were then incubated with naive nuclei to test their effect on DNA synthesis and H2AX phosphorylation. A significant suppression in capacity to support elongation of DNA synthesis was evident, compared to mock treated extract pre-exposed to naive nuclei (Figures 3.7a and 3.7b; Table 3.4). Thus events that activate the DDR as well as some of the consequences of DDR activation can be reconstituted *in vitro*.

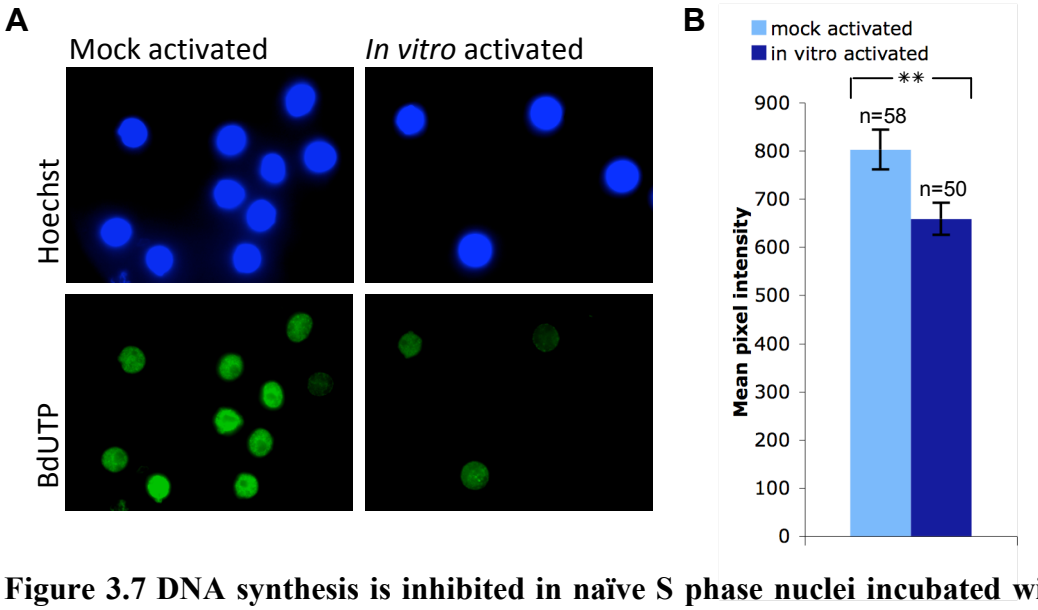

Figure 3.7 DNA synthesis is inhibited in naïve S phase nuclei incubated with S phase extract preconditioned by exposure to damaged nuclei

Naïve S phase HeLa-S3 extract was preincubated in either naïve or damaged S phase nuclei, before recovery by centrifugation to create mock activated or *in vitro* activated extracts.

a) Fluorescent images of sites of DNA replication in naïve S phase HeLa-S3 nuclei incubated with mock and *in vitro* activated extract. Reactions were processed as described in the methods (Section 2.7). BdUTP incorporation was visualised using streptavidin-fluorescein (green). Nuclei were counterstained with Hoechst 33258 (blue).

b) Quantification of BdUTP incorporated into nuclear DNA (blue) in cell-free reactions in which naïve nuclei are incubated in mock and *in vitro* activated extract. Histogram shows average fluorescent intensity with standard error of the mean, and is representative data from one of two independent experiments. N = number of nuclei quantified per sample. Asterisks represent the p-value found by single factor ANOVA: ✳✳ = 0.01>p>0.001;

3.4.5 Cell free nuclei present an unique global pattern of H2AX phosphorylation

One of the characteristic features of H2AX phosphorylation in damaged cells is its focal nature. These foci are specifically induced at the site of double strand breaks, and the number of them has previously been shown to correlate to the number of DNA lesions present in the nucleus (Sedelnikova, Rogakou et al. 2002). However the H2AX phosphorylation imposed by damage-activated cytosolic extract upon naive nuclei is not constrained to foci. Instead, a global pattern of phosphorylation is displayed, which is not evident in nuclei prior to incubation in cytosolic extract (Figures 3.8a and 3.8b). As this is induced independent of the presence of physical damage, a global pattern is not unexpected and implies that targeting of the kinases is impaired. However the presence of physical damage does not restore focal H2AX phosphorylation because a global pattern is also observed in damaged nuclei *in vitro* (Figure 3.3c).

Figure 3.8 Global H2AX phosphorylation develops over the course of cell-free reactions and is independent of DNA synthesis

a) Immunofluorescence images of H2AX phosphorylation in an etoposide-treated HeLa-S3 cell and a naïve S phase HeLa-S3 nucleus after 30 minutes incubation in damage-activated extract. H2AX phosphorylation was detected with mouse monoclonal anti-phospho H2AX (Ser139) antibody, and anti-mouse Alexa 568 conjugated secondary antibody.

b) Immunofluorescence images of initial states of H2AX phosphorylation (red) in naïve and damaged S phase HeLa-S3 nuclei. Nuclei were counterstained with Hoechst 33258 (blue).

c) Fluorescence images of BdUTP incorporation (green) and H2AX phosphorylation (red) in individual naïve S phase HeLa-S3 nuclei after 2 or 30 minutes incubation in naïve or damage-activated S phase HeLa-S3 extract. BdUTP was detected using fluorescein streptavidin. Nuclei were counterstained with Hoechst 33258 (blue).

d) Fluorescence images of BdUTP incorporation (green) and H2AX phosphorylation (red) in individual naïve S phase HeLa-S3 nuclei over 30 minutes incubation in damage-activated S phase HeLa-S3 extract supplemented with 200μM aphidicolin. Nuclei were counterstained with Hoechst 33258 (blue).

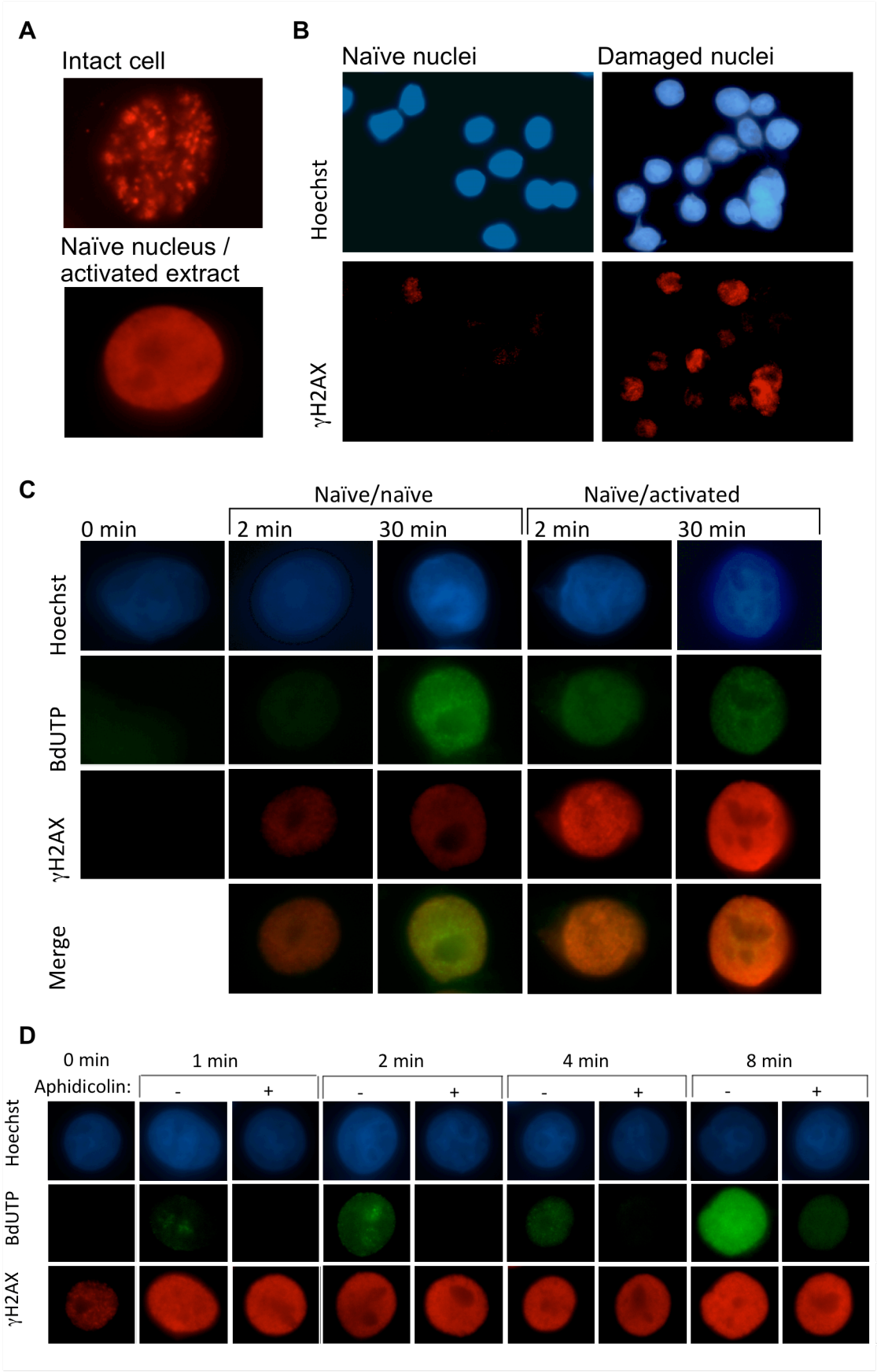
A
Intact cell
Naïve nucleus /
activated extract
B
Naïve nuclei
Damaged nuclei
Hoechst
γH2AX
C
Naïve/naïve
Naïve/activated
0 min
2 min
30 min
2 min
30 min
Hoechst
BdUTP
γH2AX
Merge
D
0 min
1 min
2 min
4 min
8 min
Aphidicolin:
-
+
-
+
-
+
-
+
Hoechst
BdUTP
γH2AX

3.4.5.1 Extract-induced global H2AX phosphorylation develops rapidly in vitro

To examine the development of global H2AX phosphorylation in naive nuclei, a time course was carried out over the course of a 30 minute cell-free incubation, combining naive nuclei with either naive or damage-activated extracts. The presence of any extract induced global H2AX phosphorylation in nuclei within 2 minutes of exposure, with greater levels of phosphorylation observed in those incubated in activated extract. The intensity of H2AX phosphorylation did not increase greatly between the 2 minute interval and the end of the 30 minute incubation (Figure 3.8c).

3.4.5.2 Extract-induced H2AX phosphorylation is independent of DNA replication

In an intact cell that has suffered DNA damage, ATM exclusively phosphorylates H2AX at the site of double strand breaks, which then act as a barrier to DNA replication elongation. However, ATM and H2AX phosphorylation have been found to also play a role in regulation of DNA replication (Shechter, Costanzo et al. 2004). This suggests two possible explanations for the global pattern of H2AX phosphorylation observed: either the removal of barriers to the propagation of H2AX phosphorylation, or the indiscriminate targeting of DNA damage signalling to all ongoing replication forks in the absence of DSBs. In order to test whether ongoing replication forks propagate H2AX phosphorylation in vitro, damage-activated extracts were supplemented with aphidicolin, an inhibitor of DNA replication, before incubation with naive nuclei. In the presence of 1mM aphidicolin, incorporation of biotinylated-dUTP into nuclear DNA was substantially reduced, but patterns of H2AX phosphorylation were unaltered, displaying global phosphorylation within 1 minute of exposure to activated extract (Figure 3.8d).

Marker	Mean mock-activated pixel intensity	Mean *in vitro*-activated pixel intensity	Total No. of nuclei	Percentage decrease
BdUTP	803.01 ±41.66	659.40 ±33.27	108	17.98% **
BdUTP	1179.39 ±47.44	1010.19 ±58.58	71	14.35% *
			Average decrease	**16.17%**

Table 3.4 DNA synthesis is inhibited in naïve S phase nuclei incubated with S phase extract preconditioned by exposure to damaged nuclei
Naïve S phase HeLa-S3 nuclei were incubated in either mock or *in vitro* activated extract. Reactions were processed as described in the methods (Section 2.7), and mean pixel intensities of BdUTP incorporation for each sample recorded using Openlab. Table displays the mean pixel intensity of BdUTP with standard error of the mean and the percentage change in intensity between control reactions, and reactions treated with *in vitro* activated extract. Asterisks represent the p-value found by t-test assuming unequal variances: : ✳ = 0.05>p>0.01; ✳✳ = 0.01>p>0.001;

3.5 Discussion

Work in this chapter shows that cell-free approaches can be adapted as the basis of DDR signalling activation assays, using phosphorylation of H2AX as a direct marker and inhibition of DNA synthesis elongation as a surrogate marker. From the experiments described here, it can be concluded that:

- Inhibition of DNA synthesis and induction of H2AX phosphorylation are maintained in nuclei from damaged cells, even when activated cytosolic factors are replaced with naive cytosol.

- Treating nuclei with damage-activated extract induces H2AX phosphorylation and inhibits DNA synthesis in both S and G1 phase nuclei, in the absence of DNA lesions.

- DSB-containing nuclei are able to activate soluble components of DNA damage signalling *in vitro*, reconstituting upstream events of the DDR as well as downstream phosphorylation of H2AX.

- Both induction of H2AX phosphorylation and inhibition of DNA synthesis *in vitro* are dependent on PIKK activity. H2AX phosphorylation occurs independently of DNA synthesis.

These conclusions give rise to some interesting questions about the nature of DNA damage response signalling in this system and in general, which are discussed below.

3.5.1 Nuclei in cytosolic extract display a base level of H2AX phosphorylation

When naive nuclei were incubated in naive extract, a base level of global H2AX phosphorylation was observed. This phosphorylation was lower than that observed when damaged or damage-activated components were used, but was clearly induced by the exposure of nuclei to cytosolic extract. Not all naive nuclei were free of focal H2AX phosphorylation upon harvesting, but those foci induced by thymidine exposure and the physical stress of cell lysis were minimal, and present at a far lower frequency than in nuclei from cells treated with etoposide. When a double strand break occurs *in vivo*, a positive feedback loop is formed between γH2AX, MDC1 and ATM, propagating spread of H2AX phosphorylation throughout megabase-size regions of chromatin (Lou,

Minter-Dykhouse et al. 2006). It seems likely that with the absence of cell membranes, soluble DDR signalling proteins in the cytosolic extract surrounding the nuclei allow this feedback mechanism to generate a disproportionate imposition of H2AX phosphorylation throughout the entire population.

The nature of the cell line used to generate nuclei and extracts may also contribute to this base level of H2AX phosphorylation. The S3 HeLa cell line is a subclone of the HeLa cell line, which was derived from a human epithelial cervical cancer. Constitutive phosphorylation of H2AX, ATM, Chk2 and p53 is a common feature of the early stages of cancer (Bartkova, Hořejši et al. 2005; Gorgoulis, Vassiliou et al. 2005; Srivastava, Gochhait et al. 2008), and might be partly responsible for the small proportion of nuclei displaying γH2AX foci following harvesting. An initial experiment was carried out to investigate whether this base level of H2AX phosphorylation was observed in nuclei from non-cancerous cells using undamaged S phase WI38 nuclei. These nuclei did support DNA elongation, and appeared to show a drop in BdUTP incorporation when incubated in damage-activated extract compared to naive extract, but levels of H2AX phosphorylation were high in both samples. Nuclei that had not been exposed to extract were also visualised, however very low numbers of these nuclei were retained upon the polylysine-coated coverslips used. Unlike S3 HeLa nuclei, the few attached WI38 nuclei displayed no initial H2AX phosphorylation, suggesting that this phosphorylation was not due to nuclei from healthy cell lines being less able to withstand the preparation conditions. Instead it is more likely to result from the use of cytosolic extract from cancerous cells, which contain physiological alterations and mutations conferring resilience to damage signalling pathways that are not found within the WI38 cell line.

The less robust nature of WI38 cells and their slow doubling time, meant that while a small number of nuclei could be harvested relatively easily on a one off basis, applying damage treatments and growing cells up in bulk to harvest cytosolic extract was not feasible. Given these factors, previous optimisation of the harvesting and assay protocol for S3 HeLa cells, and that S3 HeLa nuclei and extracts display a clear differential in H2AX phosphorylation and BdUTP incorporation when components from etoposide-treated cells are used, experimentation was continued using this cell line regardless of the base level of H2AX phosphorylation shown.

3.5.2 Induction of H2AX phosphorylation in the absence of DNA lesions

These data show that damage-activated extracts contain soluble signalling molecules that are able to target chromatin regardless of the presence of physical DNA damage, inhibiting DNA synthesis in both S and G1 phase naive nuclei. Furthermore in S phase nuclei effective phosphorylation of H2AX is induced in the absence of DNA lesions (G1 nuclei were not examined). A recent paper has been published demonstrating the induction of local H2AX phosphorylation in the absence of damage when proteins in the DDR signalling pathway were fused to chromatin for a prolonged period (Soutoglou and Misteli 2008). Soutoglou and Misteli concluded that the stable association of repair factors with chromatin is required for triggering, amplifying and maintaining DDR signalling, which is consistent with these results. The H2AX phosphorylation observed in my experiments takes place far more rapidly than that previously observed, and occurs throughout the nucleus, reflecting the mass of activated signalling factors present in damage-activated extracts compared to the specific targeting of a small region of chromatin.

3.5.3 Recreation of multiple stages of DNA damage response signalling

Damaged nuclei were also used to activate signalling in naive extract, to produce "*in vitro* activated extract", which was then shown to inhibit BdUTP incorporation and induce H2AX phosphorylation in naive nuclei. While these experiments confirm the ability of DSB-containing nuclei to activate soluble components of the DDR pathway *in vitro*, the drop in biotinylated-dUTP incorporation was less than half of that produced by extracts harvested directly from etoposide treated cells. Thus *in vitro* induction of the DDR does not occur with the same efficiency when reconstituted *in vitro*. For this reason, directly damage-activated extracts were used for the majority of experiments, rather than further investigating the capacity of pre-conditioned extract.

3.5.4 H2AX phosphorylation and inhibition of DNA synthesis are both regulated by PIKKs but are independent of each other

H2AX phosphorylation induced by activated extract appears to localise with sites of replication elongation during the early stages of cell-free reactions. Recent research has suggested roles for ATM, ATR and H2AX in regulation of DNA replication initiation and elongation, and at first glance could present an explanation for this observation (Marheineke and Hyrien 2004; Shechter, Costanzo et al. 2004). However, when

damage-activated extracts are supplemented with aphidicolin no decrease in H2AX phosphorylation is observed, showing that phosphorylation is not propagated by ongoing replication forks.

3.5.4.1 Disruption of DDR signalling targeting

The fact that the H2AX phosphorylation observed by Soutoglou (Soutoglou and Misteli 2008) was restrained to the areas in which proteins such as NBS1, MRE11 and MDC1 were fused to chromatin, suggests that the global H2AX phosphorylation observed in the cell-free system may be due to disruption of DDR signalling targeting leading to binding of these proteins across the entirety of the chromatin. This would not require any reliance upon DNA synthesis, although the areas where DNA is unwound for replication may prove more accessible and be targeted first in the absence of physical DNA lesions, explaining the initial co-localisation with sites of replication observed. As the cell-free reaction progresses, H2AX phosphorylation is likely to spread out from these areas due to the feedback mechanisms previously described, leading to saturation of the chromatin, and overwriting the initial fine focal pattern. While H2AX phosphorylation in the cell-free system is not linked to DNA synthesis, the stimulation of BdUTP incorporation by PIKK inhibitors in naive nuclei and extract, as well as in nuclei treated with damage-activated extract, is consistent with a role for ATM and γH2AX in the control of DNA replication elongation.

3.5.4.2 Deregulation of DNA damage detection and repair from delayed DNA synthesis in the presence of LY294002

While wortmannin abolished H2AX phosphorylation and stimulated BdUTP incorporation, treatment with LY294002 stimulated BdUTP incorporation without any negative effect on H2AX phosphorylation. Furthermore, in reactions containing damage-activated extracts, levels of H2AX phosphorylation showed a significant increase. It is known that unlike the G1-S and G2-M checkpoints, in which progress through the cell cycle is actively delayed until set events have been completed, the intra-S phase checkpoint does not operate by bringing an abrupt halt to DNA replication, but rather by slowing the rate at which it occurs, allowing damage to be repaired (Rhind and Russell 2000; Willis and Rhind 2009). As such, the fact that DNA synthesis is continuing in the presence of H2AX phosphorylation is not unusual - this is routinely observed in the experiments in this chapter - but the significant increase in rate suggests

LY24002 induces deregulation of the mechanisms linking DNA damage detection and repair with slowed replication rates.

H2AX phosphorylation can be mediated by one or more of ATM, ATR and DNA-PK, dependent on the cause of damage. Phosphorylation of ATM in response to etoposide treatment is well documented, however the ATR-dependent Chk1 pathway is also activated in HeLa cells in response to 15μM etoposide treatment (Fu, Wan et al. 2008; Jamil, Mojtabavi et al. 2008; Rudolf, Cervinka et al. 2009; Nam, Doi et al. 2010). Furthermore, siRNA inhibition of DNA-PK in HeLa cells has been shown to increase sensitivity to etoposide treatment (Tian, Chen et al. 2007), suggesting that all three kinases play a role in the response to etoposide-induced double strand breaks.

While wortmannin and LY294002 are both known inhibitors of the PIKK family, they have different modes of action, and vary considerably in effectiveness. Wortmannin inhibits DNA-PK, ATM and ATR at a concentration of 200μM (Sarkaria, Tibbetts et al. 1998; Rodriguez-Bravo, Guaita-Esteruelas et al. 2006). LY294002 is an effective inhibitor of DNA-PK, with an IC50 of 1-5μM, however studies examining its effects on ATM have given contradictory results. In a 2004 study characterising purified ATM, Goodarzi reports that LY294002 inhibits ATM with an IC50 of 6μM (Cheatham, Vlahos et al. 1994), however in an *in vitro* study Stiff shows that treatment with LY294002 inhibits DNA-PK dependent H2AX phosphorylation in ATM-deficient chicken cells, but does not prevent phosphorylation in ATM-competent cells lacking DNA-PK (Stiff, O'Driscoll et al. 2004). A concentration of 1mM LY294002 is required to effectively inhibit ATR (Hall-Jackson, Cross et al. 1999). It seems consistent with Stiff's findings that the concentrations used for this chapter (50 and 200μM) inhibit DNA-PK, but not ATM or ATR, alleviating restrictions on DNA synthesis without affecting early DDR signalling. Future work would benefit from analysis with an antibody for phosphorylated ATM in order to clarify this point. Stimulation of BdUTP incorporation by LY294002 suggests that inhibition of the ATR signalling pathway is not required to relieve restraints upon DNA synthesis during S phase, and that this may also apply to ATM.

Previous results suggest that activated soluble signalling elements present in damage-activated extracts are most easily able to bind to regions of the chromatin where the DNA is being unwound to allow replication. If LY294002 is alleviating signalling

pathways that restrain DNA synthesis without inhibiting the phosphorylation of H2AX and consequent downstream DDR signalling, then ongoing DNA replication elongation may provide more sites to which activated DDR proteins can bind, and from which H2AX phosphorylation can spread leading to greater levels of nuclear γH2AX.

3.5.5 Potential applications of the cell-free system

In addition to the biological implications already discussed, this cell-free system has potential for a number of research applications.

3.5.5.1 Assay for inhibitors

Use of wortmannin and LY294002 has shown that we can see an effect of PIKK inhibitors upon the DDR using this system. These results demonstrate how this cell-free system can be used as a simple screening tool for small molecule inhibitors of the DNA damage response in a system that is uncomplicated by the presence of damage, and which is isolated from the process of DNA repair. Soluble factors present in activated extracts recreate both G1/S and intra-S phase checkpoints, and upstream events that signal the activation of soluble components of the DDR have also been reconstituted *in vitro*, providing multiple targets against which inhibitory small molecules could be selected. The University of York has patent protected this system (reference number 3079P/GB), and its value as a screening tool in comparison to existing assays is discussed in greater detail in the final discussion (Chapter 6). While phosphorylation of H2AX acts as a clear and reproducible marker of early DDR signaling, the system can also potentially be used in combination with other antibodies, such as those for phosphorylated ATM, ATR, Chk1 and Chk2, to more closely dissect whereabouts in these pathways inhibitors are acting.

3.5.5.2 Studying the role of Ciz1 in the DNA damage response

This cell-free system can be used to investigate the roles of novel proteins implicated in the DNA damage response. Such applications include examining the effect of titrating proteins into cell-free reactions and asking if an effect on H2AX phosphorylation or DNA synthesis is shown, and use of damage-activated extracts to modify substrates of ATM and ATR *in vitro*. This system has been used to investigate the role of Ciz1 in the DNA damage response, and use of it for this purpose is discussed in Chapters 4 and 5.

Chapter 4

CHARACTERISATION OF CIZ1'S SQ/TQ MOTIFS

4.1 Introduction

A role for Ciz1 in regulation of DNA replication has been established by the Coverley laboratory (Coverley, Marr et al. 2005; Ainscough, Rahman et al. 2007), but evidence has also been found implicating it in the DNA damage response. Experiments have previously suggested a correlation between Ciz1 overexpression and induction of H2AX phosphorylation, and Ciz1 is commonly misspliced in cancerous cells (Rahman, Ainscough et al. 2007). Most notably, Ciz1 contains a number of SQ/TQ motifs, which are commonly phosphorylated by ATM and ATR (Kim, Lim et al. 1999; O'Neill, Dwyer et al. 2000). These motifs are often found in clusters and their presence is thought to be indicative of DNA damage response proteins (Traven and Heierhorst 2005). Human Ciz1 contains 21 S/TQ motifs, and mouse Ciz1 contains 18 grouped in 3 clusters. One of the SQ motifs in human Ciz1 has already been shown to be phosphorylated in response to ionising radiation (Matsuoka, Ballif et al. 2007), however this particular site is not present in mammalian homologues. This chapter uses the cell free system described in Chapter 3 along with other tools to investigate whether SQ/TQ motifs in the murine splice variant, ECiz1, are phosphorylated as part of the DNA damage response.

4.2 Aims

This chapter aimed to use the cell free system and other methods to investigate phosphorylation of Ciz1 in response to DNA damage.

Goals were:

- To carry out bioinformatic characterisation of Ciz1 SQ/TQ motifs
- Detection and dissection of SQ/TQ phosphorylation in Ciz1

4.3 Experimental design

To adapt the cell free system to carry out phosphorylation assays, GST-tagged Ciz1 protein and protein fragments were attached to GST beads and incubated in naive or damage-activated extracts (Figure 4.1), before being separated out by centrifugation and run on western blot. Phospho-(Ser/Thr) ATM/ATR substrate antibody was then used to identify phosphorylated protein. Full length murine GST-ECiz1, an N-terminal fragment GST-ECiz1 N442 and a C-terminal fragment GST-ECiz1 C274 were used for these experiments.

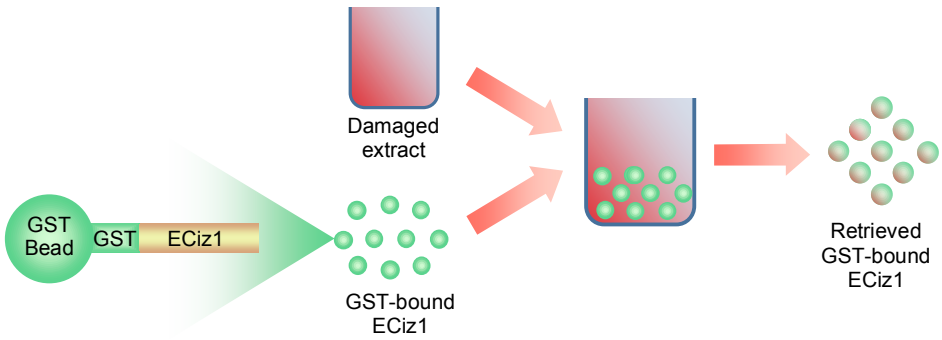

Figure 4.1 Diagram of GST-ECiz1 phosphorylation assay

4.4 Results

4.4.1 Bioinformatic analysis of Ciz1 SQ/TQ sites

4.4.1.1 SQ/TQ motifs form clusters within Ciz1

Clustering of SQ/TQ motifs is a common feature of DDR proteins, and their presence is thought to be indicative of potential involvement in the response. Using a stringent definition of an SQ/TQ cluster domain (SCD), in which there are 5 or more SQ/TQ motifs, separated by no more than 35 amino acids each, 1% of all mammalian and yeast proteins contain one or more SCDs. In 2002, 10% of these SCD-containing proteins had been identified as having a role in the DDR (Schwartz, Duong et al. 2002). Not only does human Ciz1 contain an SCD in exon 8 by this definition, but also two other smaller clusters of SQ/TQ motifs spread across the protein. Different exons of both human and mouse Ciz1 were grouped into sections of the protein with approximately equal sequence lengths, as displayed in Figure 4.1, and the statistical likelihood of the number of motifs falling in each section analysed using the chi-squared test. p-values were significant in both human and mouse for exon 8, and in mouse for exons 14-17, showing it to be statistically unlikely that motifs are evenly spread across the protein by chance, and reinforcing the idea that clustering of SQ/TQ motifs is occurring in Ciz1.

4.4.1.2 SQ/TQ motif frequency in Ciz1 is comparable with that of known DDR proteins

The statistical likelihood of an SQ/TQ motif occurring is one in every two hundred amino acid residues. Human Ciz1 contains 21 SQ/TQ motifs, equivalent to one site every 43 residues. This frequency is higher than that seen in the known DDR proteins BRCA1, 53BP1, CREB-binding protein and MDC1, which vary between one every 61 residues, and one every 93 (Table 4.2). If this is compared to proteins with no suspected

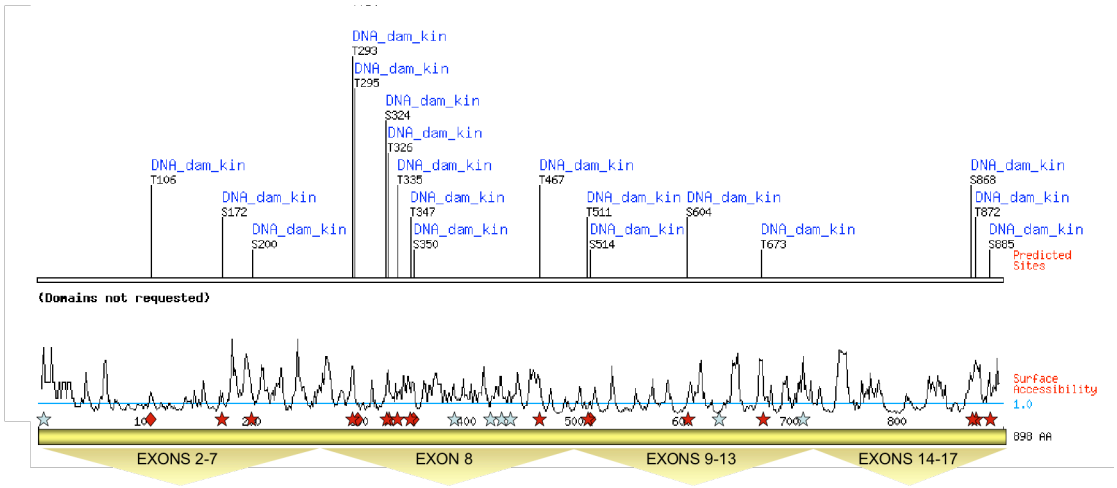

Figure 4.2 Predicted ATM & DNA-PK phosphorylation sites in human Ciz1

The amino acid sequence of human Ciz1 was input to Scansite. Here the predicted ATM and DNA-PK binding sites are overlaid against predicted surface accessibility of individual amino acid residues, and known SQ/TQ sites in Ciz1. SQ/TQ motifs are displayed as stars, while other phosphorylation sites are diamonds. Predicted phosphorylation sites are shown in red.

HUMAN CIZ1					
Exons	**SQ/TQ sites**	**Expected sites**	**Exon length**	**χ^2**	**P**
2-7	3	6.17	264	3.68	0.0551
8	10	5.47	234	5.16	0.0231
9-13	5	5.07	217	0.08	0.7773
14-17	3	4.28	183	0.79	0.3741

MOUSE CIZ1					
Exons	**SQ/TQ sites**	**Expected sites**	**Exon length**	**χ^2**	**P**
2-7	3	5.25	261	7.01	0.0081
8	10	3.04	151	19.24	<0.0001
9-13	4	4.97	247	0.45	0.5
14-17	0	3.75	186	5.61	0.0179

Table 4.1 Chi square analysis of SQ/TQ motif distribution throughout human and mouse Ciz1 shows statistically significant clustering of sites

Protein name	Protein length	SQ/TQ sites	Amino acids per SQ/TQ site	Identified role in DNA damage response?
Ciz1	898	21	42.8	*None*
53BP1	1972	32	61.6	*Recruited to DSBs, mediates AT M-autophosphorylation*
BRCA1	1863	20	93.2	*Substrate of ATM*
CREB-binding protein	2442	36	67.8	*Activates genotoxic stress-coupled gene transcription during oxidative stress and DNA damage*
MDC1	2089	33	63.3	*Substrate of ATM, recruited to H2AX foci*
Caspase-activated nuclease	338	1	338	*None*
Actin	375	1	375	*None*
Ribonuclease III	1374	3	458	*None*

Table 4.2 Frequency of SQ/TQ motifs in Ciz1 is comparable to that in known DDR proteins

involvement in the PIKK pathways, such as actin 1, ribonuclease III and caspase-activated nuclease, a considerable drop in frequency is seen, with over 300 amino acid residues per motif.

4.4.1.2 SQ/TQ motif frequency in Ciz1 is comparable with that of known DDR proteins

The statistical likelihood of an SQ/TQ motif occurring is one in every two hundred amino acid residues. Human Ciz1 contains 21 SQ/TQ motifs, equivalent to one site every 43 residues. This frequency is higher than that seen in the known DDR proteins BRCA1, 53BP1, CREB-binding protein and MDC1, which vary between one every 61 residues, and one every 93 (Table 4.2). If this is compared to proteins with no suspected involvement in the PIKK pathways, such as actin 1, ribonuclease III and caspase-activated nuclease, a considerable drop in frequency is seen, with over 300 amino acid residues per motif.

4.4.1.3 Scansite predicts phosphorylation of Ciz1 SQ/TQ motifs

Scansite is a program that predicts sites within an amino acid sequence which are likely to be targeted by protein kinases, using a matrix of selectivity values to assess likelihood of phosphorylation of short sequences (Obenauer, Cantley et al. 2003). It also predicts corresponding surface accessibility of amino acids, based solely on sequence. The Scansite motif search operates at three different stringencies set by the percentile of variation from a library of known motifs that the protein falls into compared to all other vertebrate proteins contained in SwissProt. These percentiles are the top 0.2% (high), 1% (medium) and 5% (low) of sequence matches. At varying stringencies, human Ciz1 is predicted to contain between 1 and 18 potential DNA damage kinase phosphorylation motifs, the majority of which are SQ/TQ sites. Figure 4.1 displays the location of all SQ/TQ motifs in human Ciz1, highlighting the fourteen ScanSite predicts to be phosphorylated by the DNA damage kinases, ATM or DNA-PK, in a low stringency search. Also shown are four serine and threonine residues predicted to be targeted by ATM and DNA-PK by this search, which are not immediately followed by glutamine. Lending credence to the efficacy of ScanSite's search is the fact that the site identified as most likely to be phosphorylated is the threonine residue identified by Matsuoka (Matsuoka, Ballif et al. 2007), which it predicts to be a substrate of DNA-PK.

4.4.2 Confirmation of ECiz1 phosphorylation *in vitro*

In Chapter 3 it was demonstrated that soluble PIKK-mediated DDR signalling proteins are present in cytosolic extract from etoposide-treated cells, and capable of phosphorylating H2AX in undamaged nuclei. Here, these extracts are used to demonstrate PIKK-dependent phosphorylation of SQ/TQ motifs in Ciz1.

4.4.2.1 ECiz1 SQ/TQ motifs are phosphorylated by exposure to damage-activated extract

In order to investigate phosphorylation of Ciz1 *in vitro*, a GST-tagged murine embryonic splice variant of Ciz1 was used. ECiz1 is found in 11 day mouse embryos, and has been shown to stimulate DNA synthesis initiation and elongation and to form

foci within the nuclei (Coverley, Marr et al. 2005; Rahman, Ainscough et al. 2007). Unlike full length Ciz1, ECiz1 can be expressed and purified in bacteria easily. As ECiz1 is a murine splice variant, it does not contain a homologue of the motif identified by Matsuoka, but does contain 13 other SQ/TQ motifs (Figure 4.3a). GST-tagged ECiz1 was bound to GST beads and incubated for thirty minutes in these damage-activated extracts, which were prepared and supplemented as for the assays described previously. When retrieved and probed by Western blot for phosphorylated SQ/TQ motifs, ECiz1 incubated in damage-activated extract displayed a clear band compared to that incubated in naive extract, or untreated ECiz1, and of identical size to that detected when probed with the anti-Ciz1 antibody 1793 (Figure 4.3b).

4.4.2.2 Phosphorylation of SQ/TQ motifs in ECiz1 is dependent on PIKKS

To verify the PIKK-dependent nature of the SQ/TQ phosphorylation observed in Figure 4.3b, damage-activated extracts were supplemented with either 200μM wortmannin or 200μM LY294002 prior to incubation with GST-ECiz1. When treated with either PIKK inhibitor, phosphorylation could not be detected (Figure 4.3c). In Chapter 3.5.4.2 the properties of LY294002 in the cell free system are discussed and it is established that they are consistent with inhibition of DNA-PK but not ATM or ATR, while wortmannin inhibits all three. As both inhibitors prevent phosphorylation of ECiz1 by damage-activated extracts, it suggests that this phosphorylation is dependent upon DNA-PK, rather than upon ATM or ATR. This could potentially be tested using a DNA-PK specific inhibitor.

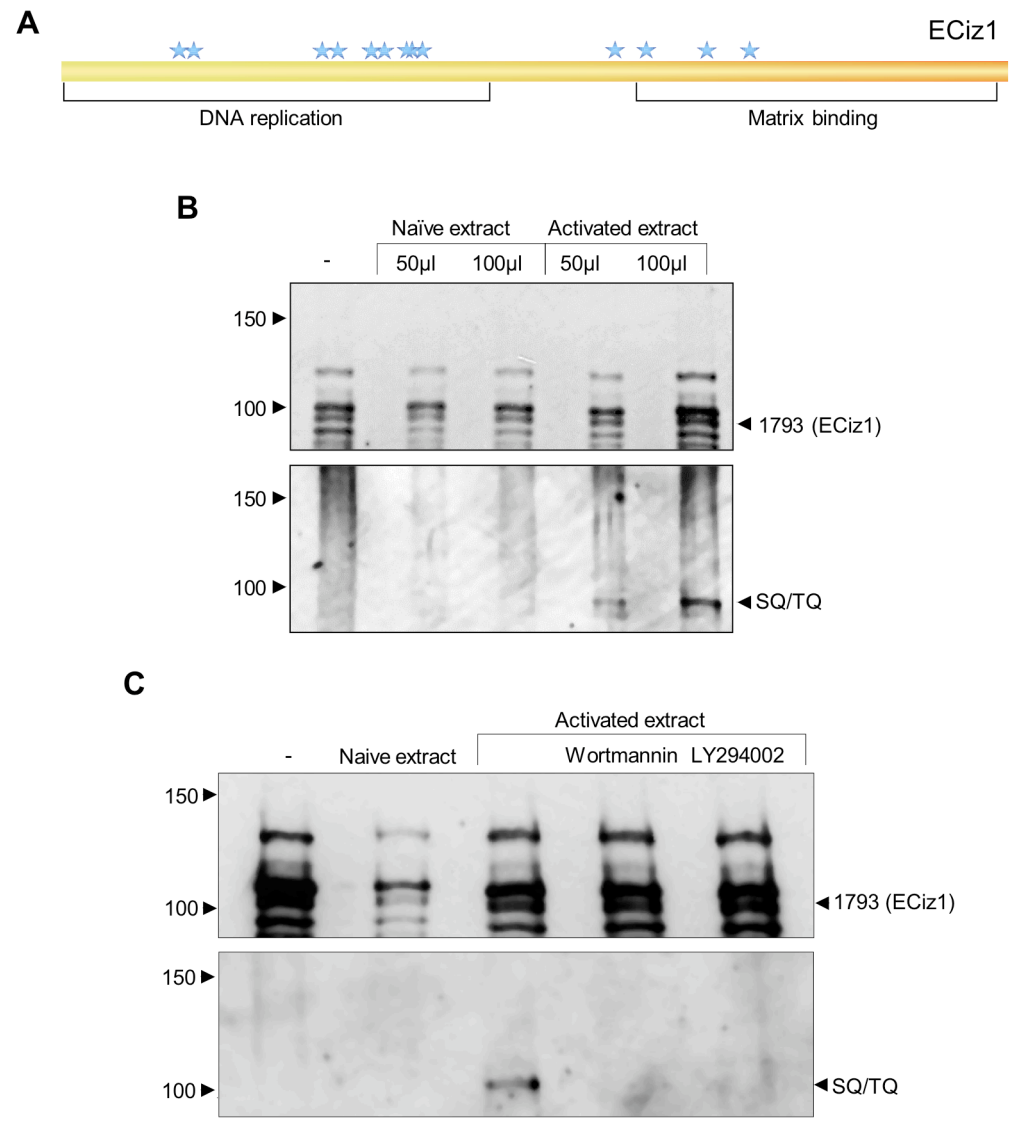

Figure 4.3 GST-ECiz1 is phosphorylated in a PIKK-dependent manner when exposed to damage-activated extract

a) Schematic of ECiz1 showing functional domains and SQ/TQ motifs marked as stars.

b) Purified GST ECiz1 was incubated in naïve and damage-activated S phase HeLa extract at 37°C. Reactions were processed as described in the methods (Section 2.7) and retrieved protein was added directly to 2x loading buffer. Protein bands were separated by 6.5% SDS-PAGE, and analysed using antibodies raised against Ciz1 and phosphorylated SQ/TQ sites.

c) Purified GST ECiz1 was incubated in damage-activated S phase HeLa extract supplemented with 200µM wortmannin or 200µM LY294002 at 37°C. Reactions were processed as described in the methods (Section 2.7) and retrieved protein was added directly to 2x loading buffer. Protein bands were separated by 6.5% SDS-PAGE, and analysed using antibodies raised against Ciz1 and phosphorylated SQ/TQ sites.

4.4.3 Locating phosphorylated motifs in ECiz1

Of the 13 SQ/TQ sites spread across ECiz1, 10 are predicted to be ATM or DNA-PK phosphorylation sites by a low stringency ScanSite search (Figure 4.4a). To establish which section of the protein was being phosphorylated two fragments of ECiz1, GST ECiz1-N442 (N442) and GST ECiz1-C274 (C274), were used (Figure 4.4b).

4.4.3.1 SQ/TQ phosphorylation is only detected in vitro in the C-terminus of ECiz1

GST-tagged N442 and C274 were incubated in damage-activated extract before retrieval by centrifugation, and probed by Western blot for SQ/TQ phosphorylation. While the 1793 antibody could be used to detect N442, as this is an antibody against the N-terminal region of the protein, it could not be used to detect C-terminal regions. Instead an anti-GST antibody was used to detect the GST-tag in fragment C274. No phosphorylation could be observed in N442, however C274 displayed a phosphorylated band of identical size to that found by the anti-GST antibody (Figures 4.4c and d). When damage-activated extract was supplemented with 200μM wortmannin prior to incubation, the intensity of this phosphorylated band was considerably diminished (Figure 4.4d).

4.4.3.2 Mutation of serine and threonine residues in the C-terminus of ECiz1 shows little effect upon overall phosphorylation levels in vitro

Following detection of SQ/TQ phosphorylation in C274, a GST-tagged construct with three of the four SQ/TQ motifs in the C-terminal region of ECiz1 replaced by AQ, rendering them unable to be phosphorylated, was generated by PCR point mutation (Figure 4.4b). This construct, GST ECiz1 AQ1-3 (AQ1-3), was used to purify protein that could be used for cell-free assays. When AQ1-3 was incubated with damage-activated extract SQ/TQ phosphorylation could still be detected compared to untreated protein (Figure 4.4e). While this phosphorylation is at a slightly lower intensity than that observed in an unaltered GST-ECiz1 control, the quality of the blot and intensity of the 1793 bands produced by sheer quantity of protein purified make it difficult to tell whether this is due to lower levels of AQ1-3 retrieved, or a genuine decrease in phosphorylation.

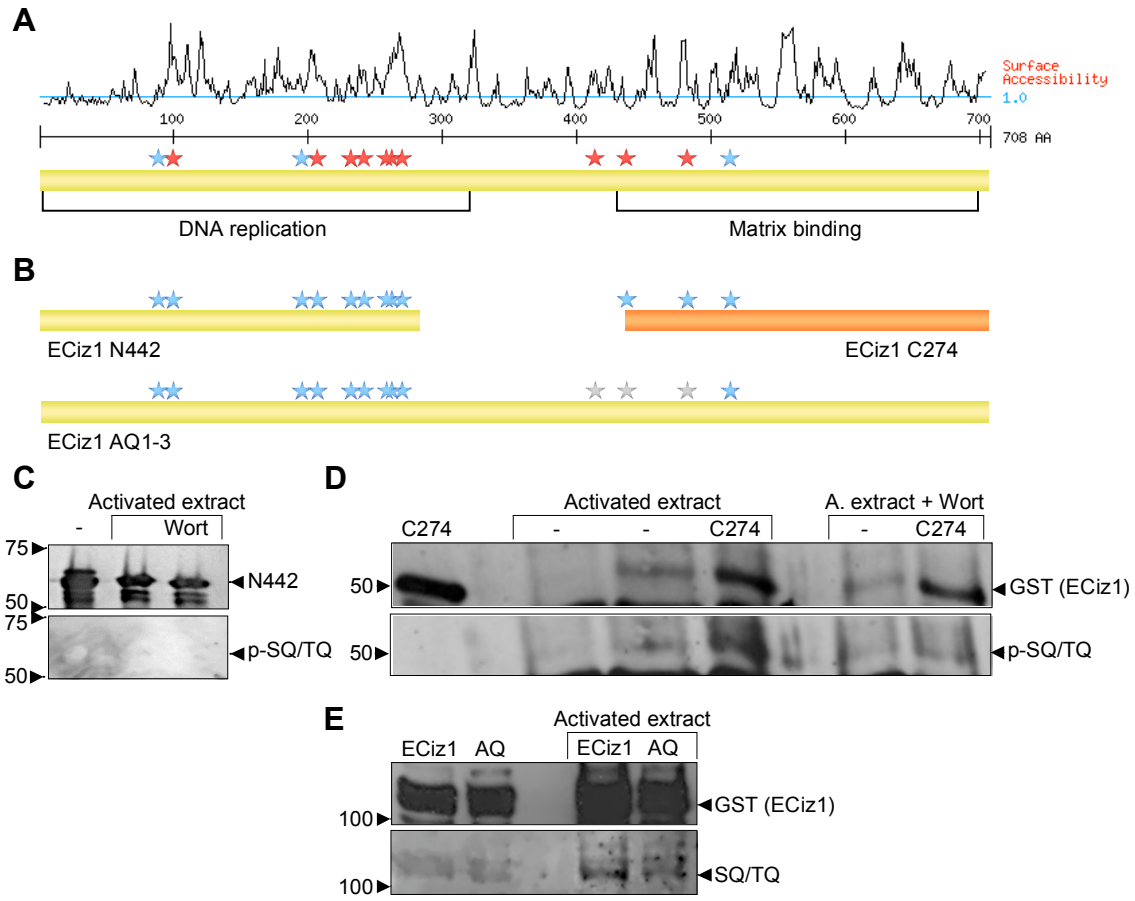

Figure 4.4 ECiz1 fragment C274 is phosphorylated in a PIKK-dependent manner when exposed to damage-activated extract

a) Schematic of ECiz1 showing predicted DDR motifs and functional domains against predicted surface accessibility of individual amino acid residues. SQ/TQ motifs predicted to be phosphorylated by ATM or DNA-PK by Scansite are marked in red.

b) Schematics of constructs used for fragment phosphorylation assays. GST ECiz1 N442 and C274 fall within the replication and anchor domains of ECiz1 respectively. The SQ/TQ motifs mutated to prevent phosphorylation in GST ECiz1 AQ1-3 are marked in grey.

c) Purified GST ECiz1 N442 was incubated in naïve and damage-activated S phase HeLa extract. Reactions were processed as described in the methods (Section 2.7) and retrieved protein was added directly to 2x loading buffer. Protein bands were separated by 6.5% SDS-PAGE, and analysed using antibodies raised against Ciz1 and phosphorylated SQ/TQ sites.

d) Purified GST ECiz1 C274 was incubated in naïve and damage-activated S phase HeLa extract. Reactions were processed as described in the methods (Section 2.7) and retrieved protein was added directly to 2x loading buffer. Protein bands were separated by 6.5% SDS-PAGE, and analysed using antibodies raised against GST and phosphorylated SQ/TQ sites.

e) Purified GST ECiz1 AQ1-3 was incubated in naïve and damage-activated S phase HeLa extract. Reactions were processed as described in the methods (Section 2.7) and retrieved protein was added directly to 2x loading buffer. Protein bands were separated by 6.5% SDS-PAGE, and analysed using antibodies raised against GST and phosphorylated SQ/TQ sites.

4.4.4 SQ/TQ motifs in Ciz1 fragments are not detectably phosphorylated when cells are exposed to etoposide

As an alternative approach to detecting SQ/TQ phosphorylation across different regions of Ciz1, NIH3T3 cells transfected with GFP-tagged N-terminus N442 or C-terminus C274 Ciz1 were allowed to express for 20.5 hours prior to a 3 hour treatment with 20μM etoposide. NIH3T3 cells were used as they are easily transfected using an Amaxa Nucleofector kit, unlike HeLa-S3 cells which displayed a very low transfection efficiency. Fragments of Ciz1 were used rather than full length Ciz1, in an attempt to reflect the difference in SQ/TQ phosphorylation seen between N- and C-terminal regions in section 4.4.3.1. Cells were then stained for SQ/TQ phosphorylation by immunofluorescence using the phospho-SQ/TQ antibody described previously. While detectable nucleus-wide SQ/TQ phosphorylation was successfully induced by damage, no difference in phosphorylation could be seen between GFP-expressing and

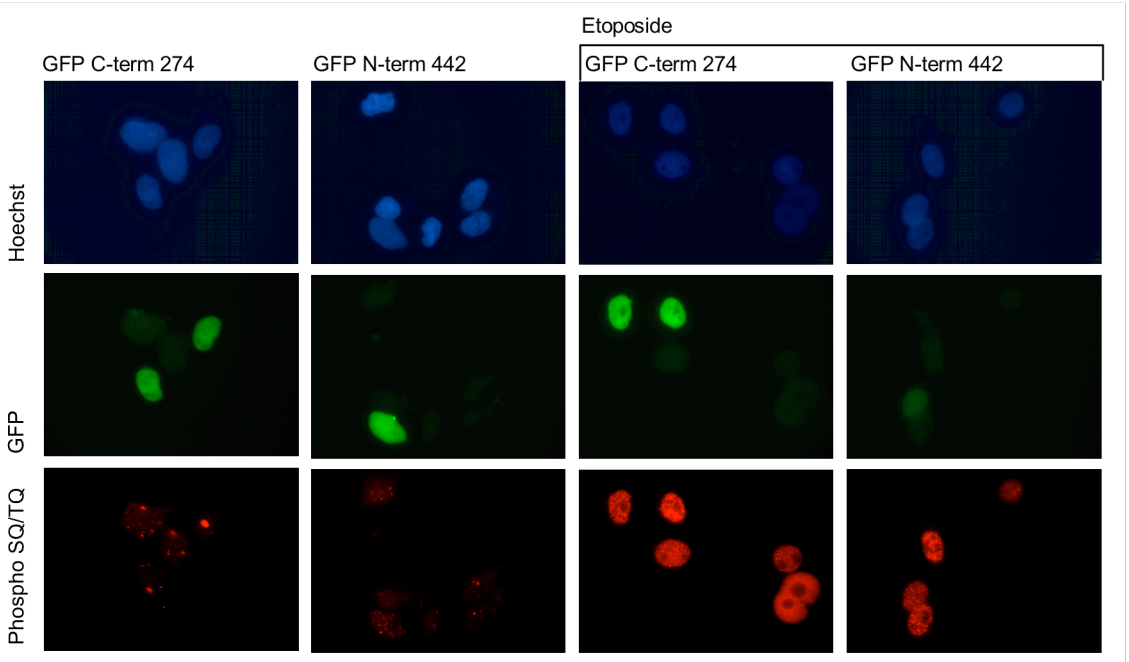

Figure 4.5 SQ/TQ motif phosphorylation is not altered in NIH3T3 cells transfected with GFP-Ciz1-C274 and GFP-Ciz1-N442

Immunofluorescence images showing GFP-tagged Ciz1 fragments and phosphorylation of SQ/TQ motifs in NIH3T3 cells with and without etoposide treatment. Cells were transfected with either GFP-Ciz1-C274 or GFP-Ciz1-N442 by Amaxa and allowed to express for 20 hours before 2 hours treatment with 20μM etoposide. Cells were washed in 0.1% Triton X-100 for 10 seconds, and then rinsed once in PBS before fixation with PFA. GFP fluorescence is shown in green. Phosphorylated SQ/TQ motifs were detected using mouse monoclonal anti-phospho-(Ser/Thr) ATM/ATR substrate 2851S antibody (red) and anti-mouse Alexa 568 conjugated secondary. Nuclei were counterstained with Hoechst 33258 (blue).

untransfected cells with either protein fragment, in either control or etoposide-treated cells (Figure 4.5). Without a specific antibody against modified Ciz1 SQ/TQ motifs, it is difficult to search for phosphorylation *in vivo*. This experiment relies upon addition of large quantities of truncated protein to cells, and the failure to detect phosphorylation of either ECiz1 fragment may reflect preferential interaction of PIKKs with correctly targeted and processed endogenous Ciz1 over partial proteins with potentially disrupted structure.

4.5 Discussion

Work in this chapter shows that damage-activated cell-free extracts in combination with phosphorylation sensitive antibodies can be used to carry out DDR signalling activation assays upon purified proteins. The PIKK-dependent nature of the phosphorylation induced is verified by the use of the inhibitors wortmannin and LY294002, the inhibitory properties of which were validated in chapter 3. Using this system to investigate Ciz1, it can be concluded that ECiz1 is phosphorylated by soluble DDR signaling elements present in damage-activated cytosolic HeLa extract, and that this phosphorylation can be traced to the C-terminal region of the protein. These conclusions give rise to the question of what role phosphorylation of SQ/TQ motifs in Ciz1 might play, and whether any clues as to this can be gained from examination of Ciz1's structural features and known functions, or from any similarities to proteins with known DNA damage response roles. The restrictions of the system used, and their implications for detection of modified proteins should also be considered.

4.5.1 Obstacles to detection of phosphorylated SQ/TQ motifs

Large scale screens have been carried out to identify substrates of the PIKK family which display phosphorylated SQ/TQ motifs in response to both ionising radiation and UV exposure (Matsuoka, Ballif et al. 2007; Stokes, Rush et al. 2007). While three main types of SCD-containing proteins have been identified - mediators linking ATM/ATR to other proteins, CHK1&2-like kinases and checkpoint effectors with roles in DNA repair or cell cycle arrest (Zhou and Elledge 2000; Nyberg, Michelson et al. 2002) - these studies implicate proteins in many processes in the DNA damage response, ranging from the predictable such as oncogenesis, transcriptional regulation and cell cycle regulation, through to more diverse pathways such as immunity, developmental processes and intracellular protein transport. In one of these studies phosphorylation of a Ciz1 TQ motif was detected in response to ionizing radiation, however this motif is only found in human Ciz1 (Matsuoka, Ballif et al. 2007). This chapter confirms phosphorylation of one or more SQ/TQ motifs in murine ECiz1 in response to etoposide-induced double strand break, and traces this phosphorylation to the C-terminus of the protein. However mutation of three out of the four C-terminal SQ/TQ motifs does not eliminate phosphorylation of ECiz1 in damage-activated extract.

4.5.1.1 Varying efficacy of phospho-specific antibodies

While phosphorylation of SQ/TQ motifs in the N-terminal fragment N442 could not be detected following incubation in damage-activated extract, modification of this region cannot be ruled out. The anti-phospho SQ/TQ antibody was raised against synthetic phospho-(Ser/Thr) ATM/ATR substrate peptides, and preferentially targets phospho-serine/threonine residues preceded by leucine or other hydrophobic amino acids at the -1 position and followed by glutamine at the +1 position, making it unlikely to bind phosphorylated motifs preceded by a non-hydrophobic residue. Using a non-protein specific antibody increases the chance of binding, but also has a risk of missing phosphorylated motifs due to regional variation in structure, charge and hydrophobicity.

By way of example, the Matsuoka study used a total of sixty eight phospho-(Ser/Thr) targeting antibodies including the Cell Signaling antibody used here. Of these only one bound to a Ciz1 peptide, an anti-Phospho RPA32 (S33) Antibody (Bethyl Laboratories) (Matsuoka, Ballif et al. 2007). The failure of the Cell Signaling antibody to detect this modification may be due to peptide size and structure, but reflects the fact that while this antibody is well-characterised and commonly used for DDR research, one antibody cannot be relied upon to detect all modified motifs within a protein. Given that truncation of ECiz1 to create the N442 fragment may cause changes in folding, affecting surface accessibility of motifs and the ability of the antibody to bind, it is not certain that continued phosphorylation of ECiz1 AQ1-3 solely reflects the one unmutated motif remaining in the C-terminus of the protein.

4.5.1.2 Limitations of using a single DNA damaging agent

As demonstrated by the wide variety of proteins in which phosphorylation occurs, SQ/TQ modification is a widespread feature of DNA damage signalling, and has been shown to operate via several mechanisms. Phosphorylated SCDs in both mediators and Chk2-like kinases commonly bind to forkhead-associated (FHA) domains in other molecules and proteins, facilitating recruitment, oligomerization and auto-phosphorylation of checkpoint kinases (Xu, Tsvetkov et al. 2002; Lou, Minter-Dykhouse et al. 2003). However as FHA domains only require one phosphorylated threonine residue to bind to, SQ motifs are redundant for this purpose. Evidence has been found that SQ/TQ motifs also bind to BRCA1 C-terminal (BRCT) domains (Manke, Lowery et al. 2003; Furuya, Poitelea et al. 2004), and along with the fact that

serine phosphorylation in SQ motifs has been observed *in vivo* (Gatei, Zhou et al. 2001), suggests that FHA domain interaction is not the sole mode of action of SQ/TQ motif function.

Further evidence for the sophisticated nature of SQ/TQ-dependent signalling is given by the range of requirements for activation of downstream signalling. In the yeast protein's Chk2 homologue, Rad53, and its precursor, Rad9, individual SQ/TQ motifs are redundant, and a threshold of SQ/TQ phosphorylation across the protein must be reached in order for signalling to be propagated further (Schwartz, Duong et al. 2002; Lee, Schwartz et al. 2003). By contrast, in mammalian Chk2 SQ/TQ motifs have been found to have individual importance (Melchionna, Chen et al. 2000). One of the best characterised SCD-containing proteins, BRCA1, takes this to extremes, with the SQ/TQ motif required for downstream signalling to occur not only reliant upon the type of DNA damage experienced but the current stage of the cell cycle (Gatei, Zhou et al. 2001; Xu, O'Donnell et al. 2002). The experiments here have only examined etoposide-induced DSB signalling in cytosolic extracts from S phase cells, and it is not unlikely that were different sources of damage to be utilised, variations in SQ/TQ phosphorylation across ECiz1 might be observed.

4.5.2 Functional domains of ECiz1

As limited knowledge is available about general mechanisms of phosphorylation-dependent SQ/TQ signalling, it is impossible to state a clear cut function of the phosphorylated motifs in Ciz1 and ECiz1. However it is possible to examine known features of the protein and speculate upon their impact upon the DNA damage response. A number of key features of Ciz1 have previously been identified, and the protein divided into two main regions: the N-terminal domain, required for stimulation of DNA replication initiation and ongoing synthesis (Coverley, Marr et al. 2005; Copeland, Sercombe et al. 2010), and the C-terminal domain, which is vital for recruitment of Ciz1 to nuclear foci (Ainscough, Rahman et al. 2007). As detectable SQ/TQ phosphorylation has been limited to the C-terminus to date, discussion will focus on the features of this region.

4.5.2.1 Matrix binding region

While it was originally expected that any SQ/TQ phosphorylation found in ECiz1 would be traced to the N-terminal region of the protein, due to its involvement in replication, the presence of a nuclear matrix binding domain in the C-terminus gives rise to the possibility that SQ/TQ phosphorylation might affect Ciz1's DNA replication stimulating properties by modulating its recruitment to the nuclear matrix. The nuclear matrix binding domain spans amino acids 708 to 830, and in its absence, recruitment of Ciz1 to DNAse and high salt-resistant nuclear structures is abolished (Ainscough, Rahman et al. 2007). During S phase these matrix-associated foci have been shown to co-localise with newly synthesised DNA, and evidence suggests that they coordinate delivery of cyclin A to the pre-replication complex (Copeland, Sercombe et al. 2010). Ciz1 has also been shown to stimulate DNA replication elongation during S phase, and given the slowing of DNA synthesis is an integral part of the response to DNA damage, inhibiting Ciz1's ability to bind to the nuclear matrix could contribute to this. Alternatively, should Ciz1 possess an active role in DNA damage signalling, phosphorylation of this domain might induce recruitment of Ciz1 to nuclear matrix foci of DDR proteins as has already been observed in the cases of Rad51, Rad54, BRCA1 and BRCA2 (Mladenov, Anachkova et al. 2006).

4.5.2.2 C2H2 zinc finger

The C-terminal region of Ciz1 also contains a zinc finger domain, the function of which has not yet been identified. Initially zinc fingers were thought to be primarily involved in DNA binding, however evidence has been accumulating for RNA and protein binding too (Pieler and Bellefroid 1994; Brown 2005; Gamsjaeger, Liew et al. 2007). A variety of different zinc finger domains exist, however that found in Ciz1 is a "classical" C2H2 domain. C2H2 zinc finger domains are commonly found in oncogenes and tumour suppressors, and their damage and distortion in DDR proteins due to presence of toxic metal ions, or dietary zinc deficiency is thought to be a factor in carcinogenesis (Witkiewicz-Kucharczyk and Bal 2006).

There are three distinct classes of C2H2 zinc fingers – triple-C2H2, multiple-adjacent-C2H2 and separated-pair-C2H2 (Iuchi 2001). Triple and separated pair zinc fingers are only capable of binding one ligand at a time, whereas multiple adjacent zinc fingers can bind multiple substrates. Ciz1 contains a triple-C2H2 zinc finger, similar to those found

in the C-terminal region of Krüppel-like factors (KLFs). Krüppel-like factors regulate transcription of cell cycle control factors and act as tumour suppressors, especially in endocrine-linked malignancies (Simmen, Pabona et al. 2010). A number of the KLF family proteins regulate $Cipl^{p21}$ activity, and recently erythroid Krüppel-like factor (EKLF) has been shown to bind directly to $Cip1^{p21}$ (Rowland and Peeper 2006; Choi, Kim et al. 2009; DiFeo, Martignetti et al. 2009; Siatecka, Lohmann et al. 2010). One of these proteins, Krüppel-like factor 6 also displays misregulation of alternate splicing in a number of cancers (DiFeo, Martignetti et al. 2009). This is of interest given Ciz1's initial discovery due to its interaction with $Cip1^{p21}$, and research suggesting Ciz1 stimulates proliferation of oestrogen-stimulated breast cancer cells (Mitsui, Matsumoto et al. 1999; den Hollander and Kumar 2006; den Hollander, Rayala et al. 2006). Krüppel-like factor 8 is a regulator of cyclin D1, and requires two nuclear localisation sequences (NLS) in order to be recruited to the nucleus (Mehta, Lu et al. 2009). One of these sequences is located in the N-terminus of the protein, adjacent to the only two SQ motifs in the protein. The second NLS is spread across the two C-terminal C2H2 zinc fingers. However no sequence homology of the N-terminal NLS is shared with Ciz1 and despite the similarities described here, the KLF family contain few SQ/TQ motifs, with no report of any connection to the DNA damage response.

4.5.2.3 Matrin 3 homologous domain

The other major feature identified in the C-terminus of Ciz1 is a Matrin 3 homologous (MH3) domain (Mitsui, Matsumoto et al. 1999). This domain spans residues 782 through to 835, and has also been found in the C-terminal regions of matrin 3 and NP220. It contains unique motifs which have not been observed in any other nuclear proteins. Little is known of the function of NP220, however from structural analysis it is expected to be a RNA splicing protein (Okumara, Nogami et al. 1998). More is known about matrin 3, an abundant nuclear protein which has been shown to interact with proteins in the chromatin remodelling, RNA processing, translation, transcription, apoptosis, DNA replication and DNA repair pathways (Zeitz, Malyavantham et al. 2009). Matrin 3 has been found to be phosphorylated in response to DNA damage in two separate studies, and interacts with SFPQ and NONO, two proteins which stimulate ligation of broken DNA and associate with proteins involved in non-homologous end joining (Bladen, Udayakumar et al. 2005; Matsuoka, Ballif et al. 2007; Salton, Lerenthal et al. 2010). No detailed dissection of the different regions of matrin 3 has

been carried out in connection with its role in the DNA damage response, however the similarities suggest that presence of the MH3 domain in Ciz1 may be relevant.

4.5.3 Implications of LY294002 inhibition of ECiz1 phosphorylation

Phosphorylation of Ciz1 in the cell free system is affected by both wortmannin and LY294002. In Chapter 3 it was shown that LY294002 does not affect the H2AX response, and in fact stimulates its phosphorylation in reactions containing activated extracts. While this amplification of DDR signalling is not expected in a reaction lacking nuclei entirely, ATM or ATR-mediated phosphorylation of Ciz1 is not consistent with inhibition of SQ/TQ phosphorylation by LY294002. I would therefore suggest that Ciz1 is not directly involved in the initial amplification of signalling upon detection of DNA damage, and instead propose a model where Ciz1 is involved in the pathways slowing DNA synthesised following detection, and is phosphorylated by DNA-PK, rather than by ATM or ATR. Given that wortmannin is a broad inhibitor of the PIKK family of proteins, and the inconsistencies in the literature over LY294002's precise targets, future study of *in vitro* phosphorylation of Ciz1's SQ/TQ motifs could benefit from dissection with more specific inhibitors such as KU-55933 (ATM) and NU7026 (DNA-PK), which are becoming increasingly commercially available. This would confirm identification of the precise PIKK by which Ciz1 is phosphorylated, and improve understanding of the pathways in which it is involved.

Chapter 5

CHARACTERISATION OF EXPRESSION OF CIZ1 IN RELATION TO THE DNA DAMAGE RESPONSE

5.1 Introduction

In Chapter 4 phosphorylation of SQ/TQ motifs present in mouse ECiz1 was confirmed, and traced to the C-terminus of the protein. A number of possible functions for C-terminal phosphorylation were posited, including modulation of nuclear matrix binding. Previous work done in this laboratory shows that Ciz1's capacity to bind to the nuclear matrix is impaired in most cancer cell lines [Sercombe *et al*, submitted], and that this is modulated during development [Munkley, unpublished]. Furthermore preliminary work suggested that overexpression of Ciz1 promotes phosphorylation of H2AX [Rahman, unpublished]. Here, the effect of DNA damage induction upon Ciz1, and of Ciz1 overexpression upon the DDR are examined.

5.2 Aims

- Do double strand breaks or inhibition of the DNA damage response affect Ciz1 expression?

- Do double strand breaks or inhibition of the DNA damage response affect Ciz1 nuclear matrix binding?

- Does Ciz1 co-localise with known DNA damage response and cell cycle proteins following induction of double strand breaks?

- Can induction of H2AX phosphorylation in response to Ciz1 overexpression be confirmed?

- Does recombinant Ciz1 affect the response to DNA damage in cell free reactions?

5.3 Experimental Design

Ciz1 expression and localisation were studied by immunofluorescence in a variety of cell lines, by using etoposide and wortmannin to induce or inhibit the DDR, and in the cell free system by addition of purified ECiz1 to isolated nuclei and damage-activated cell extracts. Etoposide concentrations were initially determined by a combination of literature search and titration into cultured NIH3T3 cells to establish what concentration was necessary to induce H2AX phosphorylation at levels detectable by Western blot

following a two hour incubation. H2AX phosphorylation was examined by immunofluorescence and Western blot in NIH3T3 cells overexpressing GFP-tagged Ciz1. Examination of expression of Ciz1 mRNA following etoposide treatment was carried out by real time PCR (RT-PCR). A panel of healthy and tumour-derived cell lines were used for these experiments. While ideally the same cell lines would have been used for all experiments, lines varied in their ability to tolerate damage treatments, growing time and general vigour. These factors influenced choice of cell lines for individual experiments. Limitations of these varying approaches are discussed.

5.4 Results

5.4.1 Ciz1 localisation does not alter in response to etoposide or wortmannin treatment in two cancer cell lines

HeLa-S3 and U2OS cells are two cell lines originating from cervical cancer and osteosarcoma tumours respectively, and are commonly used in DDR research. U2OS cells contain a functional p53 gene capable of inducing an apoptotic response to UV exposure (Allan and Fried 1999), whereas no p53 cDNA can be amplified from HeLa-S3 cells (Jia, Osada et al. 1997). The HeLa-S3 cell line was used to harvest nuclei and cytosolic extracts for the cell free experiments and Ciz1 phosphorylation assays described in Chapters 2 and 3.

To examine whether the phosphorylation of Ciz1 observed *in vitro* by damage-activated extracts reflects detectable alterations in endogenous Ciz1, HeLa-S3 and U2OS cells were treated for 2 hours with 2μM or 20μM etoposide and washed in 0.1% Triton X-100 before fluorescent microscopy was used to visualise endogenous Ciz1 and nuclear H2AX phosphorylation by immunofluorescence. All cell lines displayed focal H2AX phosphorylation in response to double strand break induction, with levels of phosphorylation correlating to etoposide concentration. Predictably, when cells were exposed to 200μM wortmannin during etoposide treatment H2AX phosphorylation was not detected (Figure 5.1a and b). In both HeLa-S3 and U2OS cells Ciz1 displayed the focal nuclear pattern previously characterised (Ainscough, Rahman et al. 2007; Rahman, Ainscough et al. 2007), but no variation in localisation or intensity of staining was detected in response to either etoposide or wortmannin treatment.

Ciz1 can be seen in the nucleus in two forms - as distinct replication foci, and also as a low level background stain. When the focal staining was enhanced digitally and

Figure 5.1 Ciz1 does not co-localise with phosphorylated H2AX in etoposide-treated HeLa-S3 cells or U2OS cells

Immunofluorescence images showing Ciz1 and phosphorylated H2AX in HeLa-S3 and U2OS cells treated with etoposide and wortmannin. Cells were treated for 1.5 hours with either 2μM or 20μM etoposide, in the presence and absence of 20μM wortmannin. Cells were washed in 0.1% Triton X-100 for 10 seconds, and then rinsed once in PBS before fixation with PFA. Ciz1 was detected using rabbit Ciz1 1793 polyclonal antibody (green) and anti-rabbit FITC conjugated secondary antibody. phosphorylated H2AX was detected using mouse monoclonal anti-phospho H2AX (Ser139) antibody (red) and anti-mouse Alexa 568 conjugated secondary. Nuclei were counterstained with Hoechst 33258 (blue).

a) Ciz1 and phosphorylated H2AX in etoposide and wortmannin-treated HeLa-S3 cells.

b) Ciz1 and phosphorylated H2AX in etoposide and wortmannin-treated U2OS cells.

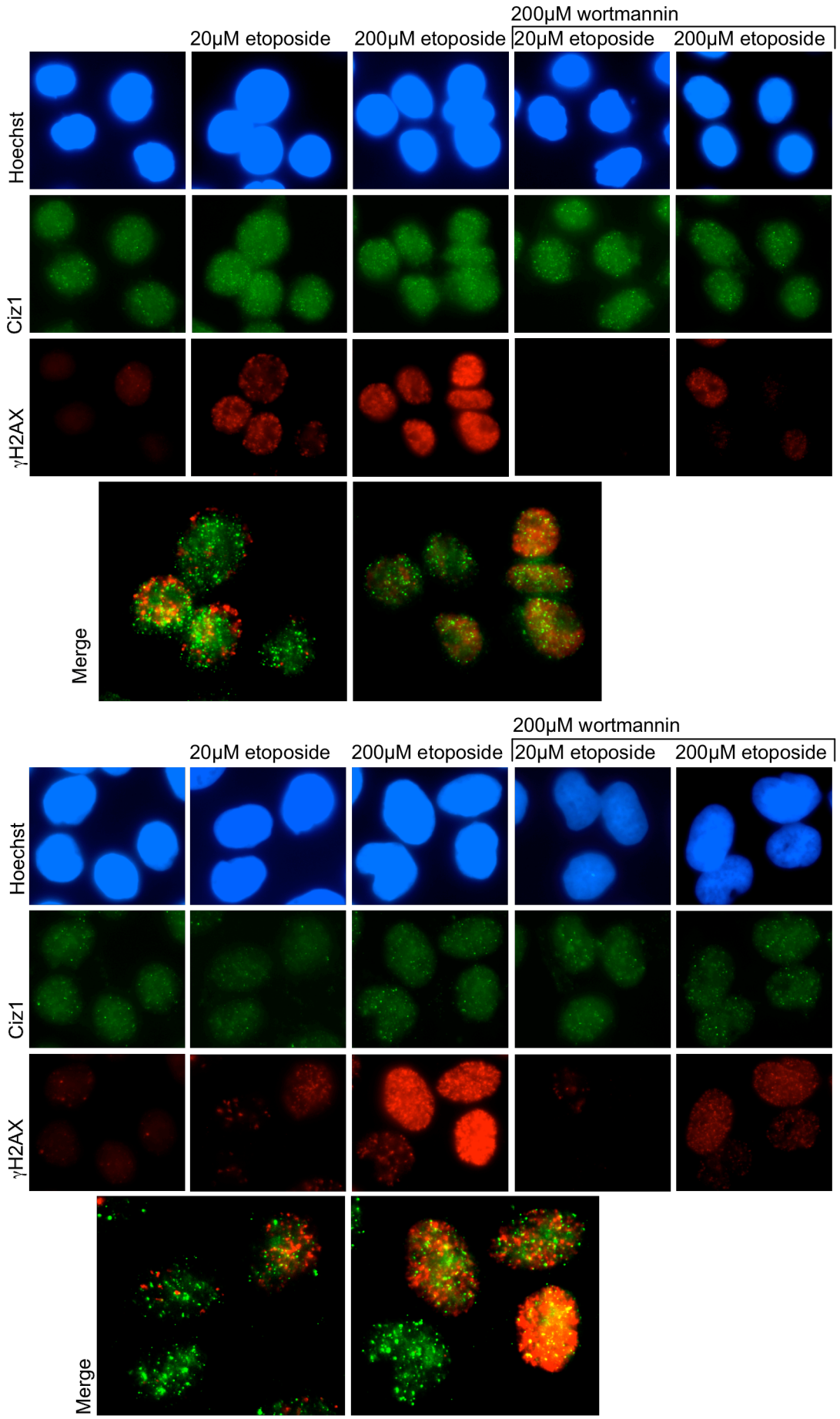
200μM wortmannin
20μM etoposide
200μM etoposide
20μM etoposide
200μM etoposide
Hoechst
Ciz1
γH2AX
Merge
200μM wortmannin
20μM etoposide
200μM etoposide
20μM etoposide
200μM etoposide
Hoechst
Ciz1
γH2AX
Merge

examined for co-localisation, a small proportion of Ciz1 foci coincided with γH2AX foci, but only in cells in which γH2AX had been propagated throughout the majority of the nucleus. In instances where γH2AX foci were less numerous, reflecting a lower level of DSBs, no co-localisation could be observed. It can be concluded that Ciz1 replication foci are not the same as γH2AX sites.

5.4.2 Ciz1's matrix binding properties may be affected by etoposide treatment in healthy cell lines

The failure of U2OS and HeLa-S3 cells to display any alteration in levels of Ciz1 expression in response to etoposide treatment in 5.4.1 does not rule out a role for Ciz1 in the DDR, but does suggest that phosphorylation of Cizl by the PIKKs does not target it for degradation. The use of only a detergent wash prior to visualisation could fail to reveal transition of protein from soluble or chromatin bound to the nuclear matrix, or vice versa.

Developing upon this first experiment, and looking specifically at Ciz1's matrix binding properties, cells were treated with 20μM etoposide for 2 hours before fluorescent microscopy was used to visualise Ciz1 and nuclear H2AX phosphorylation by immunofluorescence. Following an initial wash with 0.1% Triton-X100 as in the previous experiment, cells were treated with DNase I to strip chromatin and bound proteins from nuclei. Mouse NIH3T3 cells, which are derived from non-cancer cell lineages, were used in this experiment. Etoposide treatment induced H2AX phosphorylation, which was extracted from nuclei when DNase was applied. Multiple Ciz1 foci were also displayed, prior to DNase treatment, a small proportion of which were retained. However no difference was displayed between Ciz1 levels in control and etoposide-treated cells in either sample (Figure 5.2).

5.4.3 Ciz1 overexpression does not induce H2AX phosphorylation in NIH3T3 cells

Experiments previously carried out by Faisal Rahman in the Coverley laboratory had suggested that Ciz1 overexpression induced H2AX phosphorylation. Two approaches were taken to try to confirm this observation.

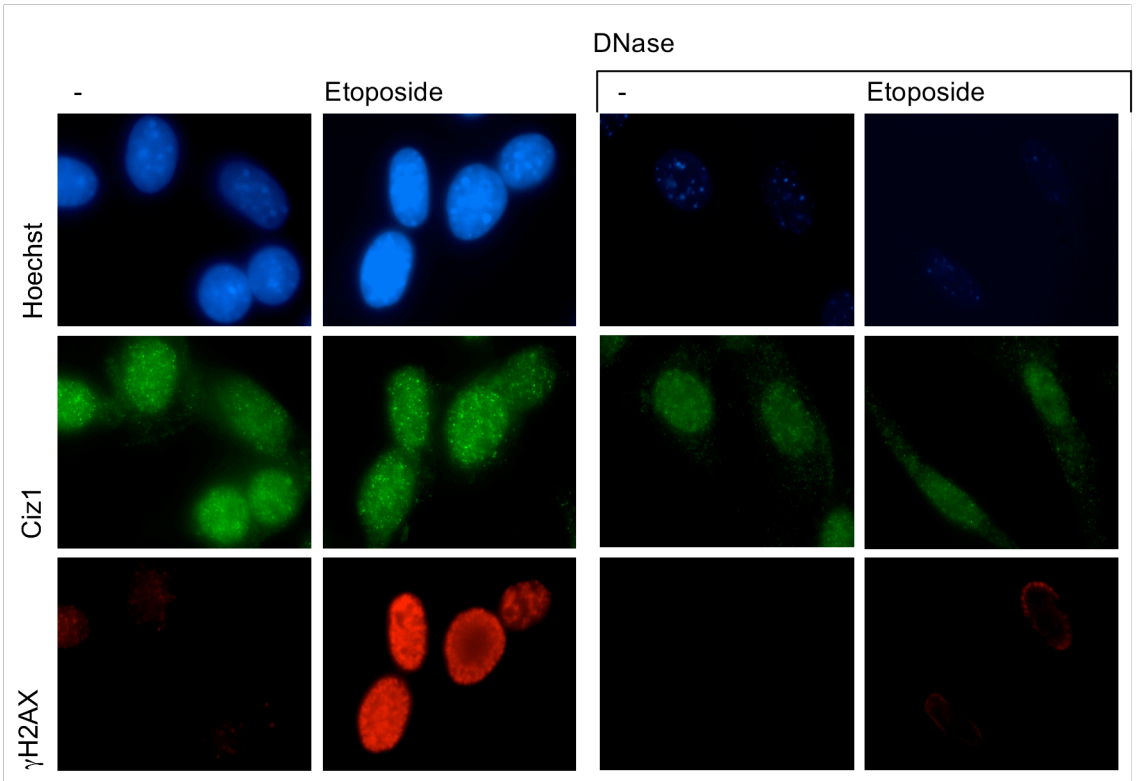

Figure 5.2 Etoposide treatment does not alter levels of DNAse-resistant Ciz1 protein in NIH3T3 cells

Immunofluorescence images showing Ciz1 and phosphorylated H2AX in NIH3T3 cells. Cells were treated for 2 hours with 20μM etoposide, then incubated in CSK with 0.1m NaCl and 0.1% Triton X-100 for 5 minutes, washed 3 times in DNAse buffer and incubated for 30 minutes in 1:20 DNAse. Cells were rinsed twice in PBS before fixation with PFA. Ciz1 was detected using rabbit Ciz1 1793 polyclonal antibody (green) and anti-rabbit FITC conjugated secondary antibody. Phosphorylated H2AX was detected using mouse monoclonal anti-phospho H2AX (Ser139) antibody (red) and anti-mouse Alexa 568 conjugated secondary. Nuclei were counterstained with Hoechst 33258 (blue).

5.4.3.1 Ciz1 overexpression does not induce H2AX phosphorylation

Amaxa and lipid transfection methods were used to examine levels of H2AX phosphorylation following transient transfection of NIH3T3 cells with GFP-Ciz1. Initially a Western blot approach was used, however original transfection approaches were too harsh, and led to induction of H2AX phosphorylation in both GFP control and Ciz1 populations (Figure 5.3a). The lipid transfection method was adapted to incorporate a shorter incubation period of 3 hours in order to reduce damage to the cells. To compensate for the resulting decrease in transfection efficiency immunofluorescence was used to directly examine H2AX phosphorylation in individual cells. This method clearly showed no increase in H2AX phosphorylation in the GFP-Ciz1 transfected population compared to the GFP control, and much lower levels of phosphorylation in both transfected populations compared to an etoposide-treated control (Figure 5.3b).

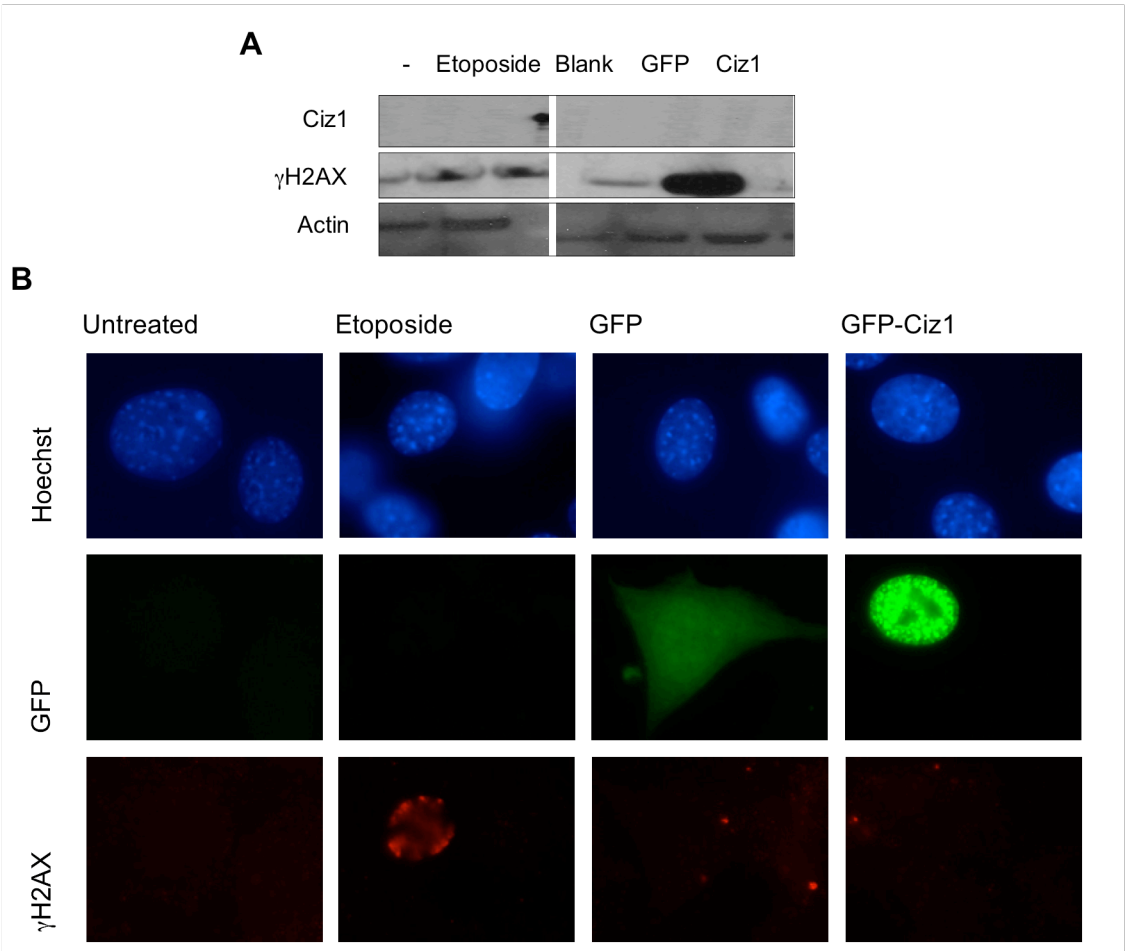

Figure 5.3 H2AX phosphorylation is not induced by Ciz1 overexpression
a) NIH3T3 cells were transfected with Ciz1, no vector and GFP controls by Amaxa. Cells were allowed to express for 20 hours, before scrape harvesting from equal-sized plates. Protein was separated by 6.5% SDS polyacrylamide gel and detected using using mouse monoclonal anti-phospho H2AX (Ser139) antibody, rabbit polyclonal anti-Ciz1 1793 antibody and mouse monoclonal anti-actin antibody.
b) Immunofluorescence images showing GFP and H2AX phosphorylation in NIH3T3 cells. Cells were either treated with 20μM etoposide for 2 hours, or transfected by TransIT-3T3 with GFP or GFP-Ciz1 for 2 hours, and then allowed to express for 20 hours. Cells were washed in 0.1% Triton X-100 for 10 seconds, and then rinsed once in PBS before fixation with PFA. GFP fluorescence is shown in. Phosphorylated H2AX was detected using mouse monoclonal anti-phospho H2AX (Ser139) antibody (red) and anti-mouse Alexa 568 conjugated secondary. Nuclei were counterstained with Hoechst 33258 (blue).

5.4.3.2 Addition of 10nM ECiz1 to cell free reactions does not induce H2AX phosphorylation

To confirm this result in the absence of trauma caused to cells by transfection, the effect of exposing isolated nuclei to purified ECiz1 protein was examined. In Chapter 3 it was confirmed that the DNA damage signalling pathways inducing H2AX phosphorylation in these nuclei are intact, and Chapter 4 demonstrated the ability of damage-activated extracts to phosphorylate purified ECiz1. Therefore it seemed likely that if increasing

the quantity of Ciz1 in cells has an effect on H2AX phosphorylation, it could be recapitulated in the system.

Cell free reactions were carried out in which populations of naive G1 phase nuclei or S phase nuclei were incubated in naive S phase extract supplemented with 10nM ECiz1 for 30 minutes (Figure 5.4a). Reactions were then separated out on a 6.5% gel and probed by Western blot for γH2AX and phosphorylated ATM. While base levels of γH2AX varied between nuclei, no difference in phosphorylation of either H2AX or ATM could be seen in nuclei exposed to ECiz1 (Figure 5.4c).

5.4.4 Titration of ECiz1 into cell free reactions with etoposide-treated extracts inhibits DNA synthesis

The cell free system allows use of two different measures of response to the DNA damage response, the first of which – H2AX phosphorylation – does not appear to be affected by Ciz1. As discussed in Chapter 4, inhibition of Ciz1 phosphorylation by LY294002 implicates it in the pathways constraining DNA synthesis, rather than in initiation and propagation of DNA damage signalling.

Previous work by the Coverley lab has shown that addition of 1nM ECiz1 to naive cell free reactions stimulates initiation of DNA synthesis, while lower and higher levels of 0.1nM and 10nM have no effect (Coverley, Marr et al. 2005). Purified ECiz1 was titrated into cell free reactions containing S phase naive nuclei and damage-activated cytosolic extract at concentrations of 0.1nM, 1nM and 10nM, to examine whether addition of exogenous Ciz1 alleviated the drop in DNA synthesis seen in damage-activated extract (Figure 5.4b). Three replicates with a total of eight paired reactions were carried out, and although there was not a consistent level of BdUTP incorporation in the presence of ECiz1, only in one instance could any increase be seen, and this was negligible at 0.53% (Table 5.1). Of these eight sets of reactions, half displayed a drop in BdUTP incorporation of more than twelve percent, two of which were found to be highly significant by t-test (p-values of 0.00026 and $2.34xE^{-5}$) .

5.4.5 Effect of etoposide on expression of Ciz1 replication domain and anchor domain transcript

The nucleotide sequences of eukaryotic protein-coding genes contain both introns, regions of DNA that are not present in mature mRNA, and exons, regions that are

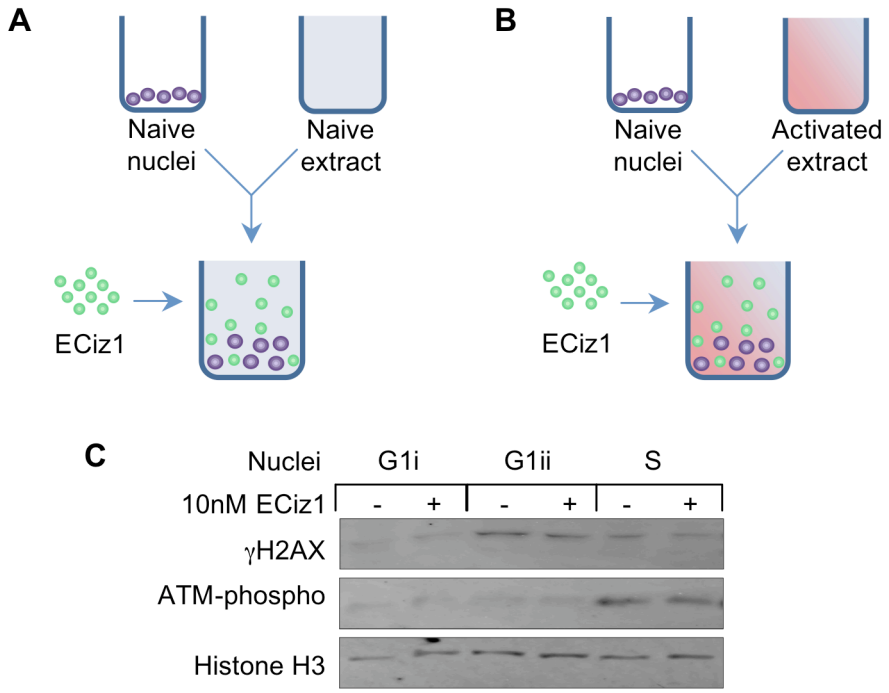

Figure 5.4 Addition of 10nM ECiz1 to cell-free reactions does not induce phosphorylation of H2AX or ATM

a) Schematic showing addition of Ciz1 to naïve nuclei and extract.

b) Schematic showing addition of Ciz1 to naïve nuclei and damage-activated extract.

c) Three batches of naïve nuclei were incubated in damage-activated S phase HeLa extract supplemented with 10nM ECiz1. Two paired reactions were carried out using G1 phase nuclei (G1i & G1ii), and one using S phase nuclei. Reactions were added directly to SDS-PAGE loading buffer and run on a gel before being probed by Western Blot for phosphorylated H2AX and ATM.

Condition	Concentration	Mean untreated pixel intensity	Sample size	Mean treated pixel intensity	Sample size	Percentage change
naive/activated	0.1nM ECiz1	697.71 ±50.25	51	493.49 ±25.55	34	-29.27% ***
naive/activated	0.1nM ECiz1	718.66 ±54.12	27	661.03 ±30.14	60	-8.02%
naive/activated	0.1nM ECiz1	578.46 ±56.90	14	581.50 ±72.95	20	0.53%
naive/activated	1nM ECiz1	697.71 ±50.25	51	606.35 ±39.43	36	-13.10%
naive/activated	1nM ECiz1	718.66 ±54.12	27	628.20 ±42.82	49	-12.69%
naive/activated	10nM ECiz1	697.71 ±50.25	51	695.22 ±56.18	45	-0.06%
naive/activated	10nM ECiz1	718.66 ±54.12	27	437.67 ±30.39	60	-39.10% ***
naive/activated	10nM ECiz1	578.46 ±56.90	14	572.14 ±90.36	16	-1.10%

Table 5.1 Titration of ECiz1 into cell free reactions impairs BdUTP incorporation in damage-activated extracts

Naïve S phase HeLa nuclei were incubated in damage-activated S phase HeLa extract supplemented with either 0.1nM, 1nM or 10nM ECiz1. Reactions were processed as described in the methods (Section 2.7), and mean pixel intensities of BdUTP incorporation for each sample recorded using Openlab. Table displays the mean pixel intensity of BdUTP fluorescence with standard error of the mean and the percentage change in intensity between control reactions, and reactions treated with ECiz1. Asterisks represent the p-value found by t-test assuming unequal variances: ✳✳✳ $p<0.001$.

preserved throughout mRNA processing and go on to be translated into amino acids for inclusion in the final protein. These exons act as modules, allowing editing of one gene to suit a multitude of cellular conditions and fates. This ability to mix and match sections of a protein is known as alternative splicing, and occurs in approximately 70% of human genes.

Ciz1 undergoes extensive alternative splicing, with several exons that are commonly altered in cancerous cells (Rahman, Ainscough et al. 2007), and variation in expression of the N and C-terminuses of the protein has been observed in a range of human cancers [Sercombe et al, submitted] and during cellular differentiation [Jennifer Munkley, unpublished]. While no variation in total protein could be seen in response to etoposide treatment, it seemed possible that changes in expression of the different regions of the protein could be going unreported. WI38 and U2OS cells were treated for up to 4 hours with 20μM etoposide prior to RNA extraction and generation of cDNA. RT-PCR was then used to examine levels of replication domain (RD) N-terminus and anchor domain (AD) C-terminus Ciz1 using primers for exons 7 and 16 (Figure 5.5a).

Five timepoints were taken, ranging from untreated cells through to four hours etoposide exposure. In WI38 cells a drop in levels of exon 7 mRNA was observed following treatment, while levels of exon 16 mRNA rose, peaking one hour after etoposide was added and then beginning to drop again (Figure 5.5a). Conversely in U2OS cells, levels of both exons decreased following etoposide treatment (Figure 5.5b). These opposing trends continued when levels of relative expression of the two exons were compared; in WI38 cells etoposide treatment increased levels of exon 16 mRNA compared to exon 7 mRNA, while the ratio of exon 16 to exon 7 mRNA fell in U2OS cells (Figures 5.5a and b).

5.4.6 Ciz1 does not co-localise with PCNA, p21 or MDC1 following etoposide treatment

One of the key features of double strand breaks is the rapid recruitment of proteins in both the DNA damage detection and repair pathways, forming discrete foci of signalling and repair factors (Belyaev 2010; Costes, Chiolo et al. 2010). As such, a common indicator of involvement in the DDR is localisation to these foci, frequently referred to as ionising radiation-induced foci (IRIF), following DNA damage. While the distribution of foci formed by signaling factors following etoposide treatment will vary

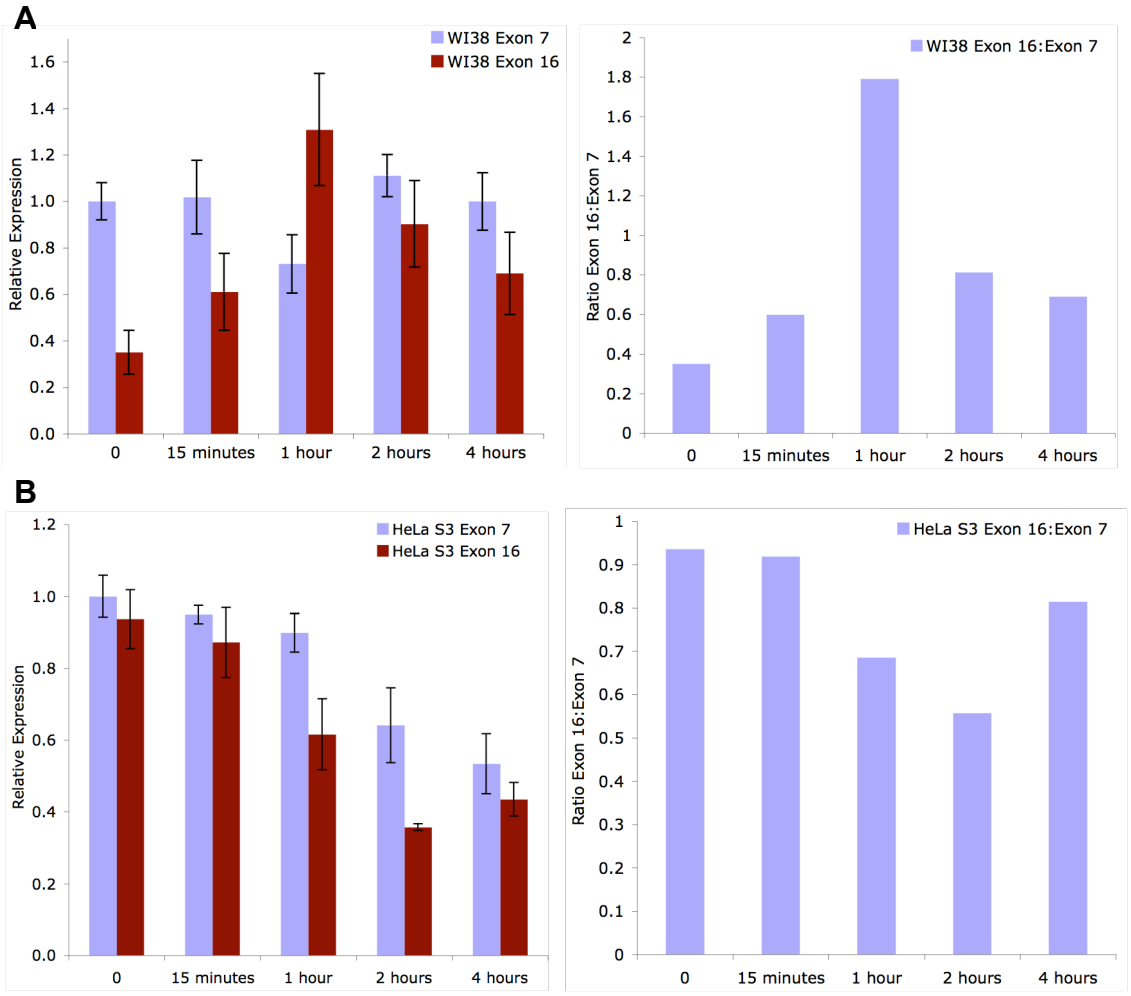

Figure 5.5 Levels of Ciz1 exon 16 mRNA decrease in WI38 cells following etoposide treatment, but increase in the cervical cancer cell line, HeLa-S3

Real time PCR analysis of Ciz1 expression in WI38 and HeLa-S3 cells following addition of 20μM etoposide to culture medium. TaqMan probes located within exon 7 and exon 16 were used to detect replication domain and anchor domain mRNA levels respectively. Relative levels are displayed for each exon, as well as a ratio of exon 16 expression compared to exon 7.

a) Relative and proportional expression of Ciz1 exon 7 and exon 16 mRNA in WI38 cells over 4 hours following addition of 20μM etoposide to culture medium.

b) Relative and proportional expression of Ciz1 exon 7 and exon 16 mRNA in HeLa-S3 cells over 4 hours following addition of 20μM etoposide to culture medium.

from that of IRIF due to both the nature of break induced and the S phase specific timing of damage, the content of the foci should not vary. Immunofluorescence was used to compare localisation of Ciz1 with that of three known checkpoint and signalling proteins, two of which have prior links with Ciz1.

5.4.6.1 PCNA

Proliferating cell nuclear antigen (PCNA) is a processivity factor for DNA polymerases δ and ε, increasing the rate of incorporation of nucleotides during DNA synthesis

(Bravo, Frank et al. 1987; Burgers 1991). Outside S phase PCNA normally exists as a detergent-soluble monomer, however during S phase it forms a detergent-insoluble trimer that associates with replication forks, encircling dsDNA and facilitating loading of polymerases (Krishna, Kong et al. 1994; Ellison and Stillman 2003). When cycling cells are treated with DNA damaging agents, PCNA becomes insolubly bound to chromatin, forming foci at the sites of damage (Essers, Theil et al. 2005), and has been shown to be involved in nucleotide excision repair (NER), base excision repair (BER) and mismatch repair (Nichols and Sancar 1992; Matsumoto, Kim et al. 1994; Umar, Buermeyer et al. 1996). These foci do not only form in the presence of single strand breaks, but have been shown to occur in an ATM-independent fashion in response to DSBs (Balajee and Geard 2001). Localisation of PCNA with Ciz1 has previously been observed in a small proportion of cycling cells (Coverley, Marr et al. 2005), therefore PCNA was chosen as an initial protein to compare to Ciz1 following etoposide treatment.

HeLa-S3 and NIH3T3 cells were treated with 2μM or 20μM etoposide for up to 3 hours prior to washing in 0.1% Triton X-100, before fluorescent microscopy was used to visualise Ciz1 and PCNA by immunofluorescence. Co-localisation between Ciz1 and PCNA could not be observed under any conditions in either cell line (Figures 5.6a and b).

5.4.6.2 p21

Ciz1 was initially discovered because of its interaction with p21, binding to the protein via a site located somewhere in the 150 amino acids surrounding the first C-terminal zinc finger motif. This study also suggested that Ciz1 may mediate localisation of p21, speculating that it could transport the protein from the nucleus into the cytoplasm in response to DNA damage (Mitsui, Matsumoto et al. 1999). Transcription of p21 is stimulated by p53, inhibiting CDK activity and preventing progression from G1 to S phase (Bartek and Lukas 2001). H2AX has been shown to stabilise and increase p21 levels as part of the p53 pathway, diverting the fate of the cell from apoptosis caused by degradation of p21 (Allan and Fried 1999; Fragkos, Jurvansuu et al. 2009). P21 is also a regulator of PCNA, preventing initiation of DNA synthesis by competitively inhibiting interaction with DNA polymerases (Moldovan, Pfander et al. 2007). Co-localisation of p21 can also be observed with ATR, phosphorylated ATM, phosphorylated H2AX,

Figure 5.6 Ciz1 does not co-localise with PCNA following etoposide treatment in NIH3T3 and HeLa-S3 cells

Cells were washed in 0.1% Triton X-100 for 10 seconds, and then rinsed once in PBS before fixation with PFA. Ciz1 was detected using rabbit polyclonal anti-Ciz1 1793 antibody (green) and anti-rabbit FITC conjugated secondary antibody. PCNA was detected using mouse monoclonal anti-PCNA antibody (red) and anti-mouse Alexa 568 conjugated secondary.

a) Immunofluorescence images showing Ciz1 and PCNA in NIH3T3 cells. Cells were treated for up to 3 hours with 20μM etoposide.

b) Immunofluorescence images showing Ciz1 and PCNA in HeLa-S3 cells. Cells were treated for 2 hours with either 2μM or 20μM etoposide.

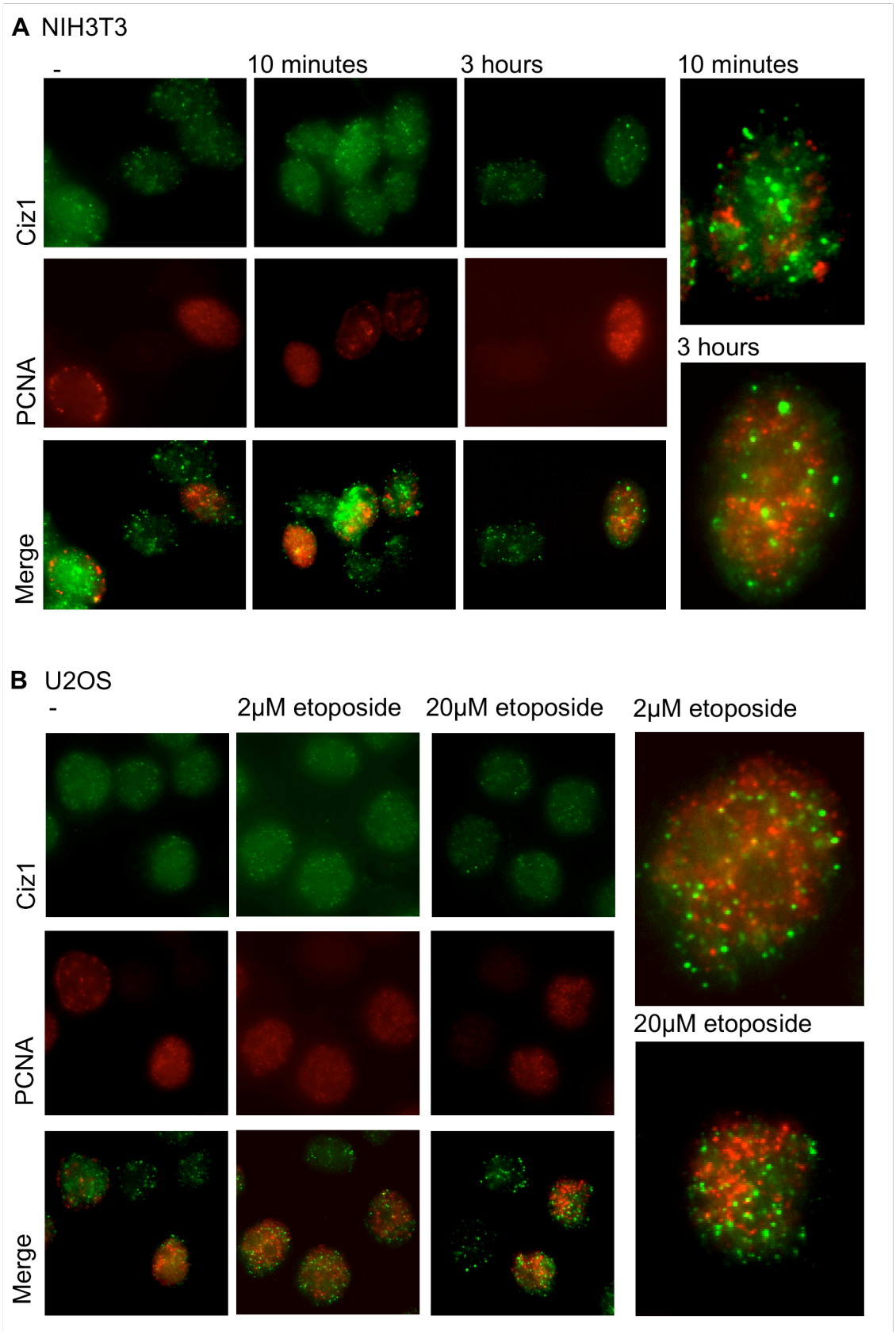
A NIH3T3
-
10 minutes
3 hours
10 minutes
Ciz1
PCNA
3 hours
Merge
B U2OS
-
2μM etoposide
20μM etoposide
2μM etoposide
Ciz1
PCNA
20μM etoposide
Merge

53BP1 and BRCA1 in bystander cells adjacent to cells containing DNA damage (Burdak-Rothkamm, Rothkamm et al. 2008).

NIH3T3 cells were treated with 20μM etoposide for up to 2 hours prior to washing in 0.1% Triton X-100, before fluorescent microscopy was used to visualise Ciz1 and p21 by immunofluorescence. No co-localisation could be observed between Ciz1 and p21 (Figure 5.7).

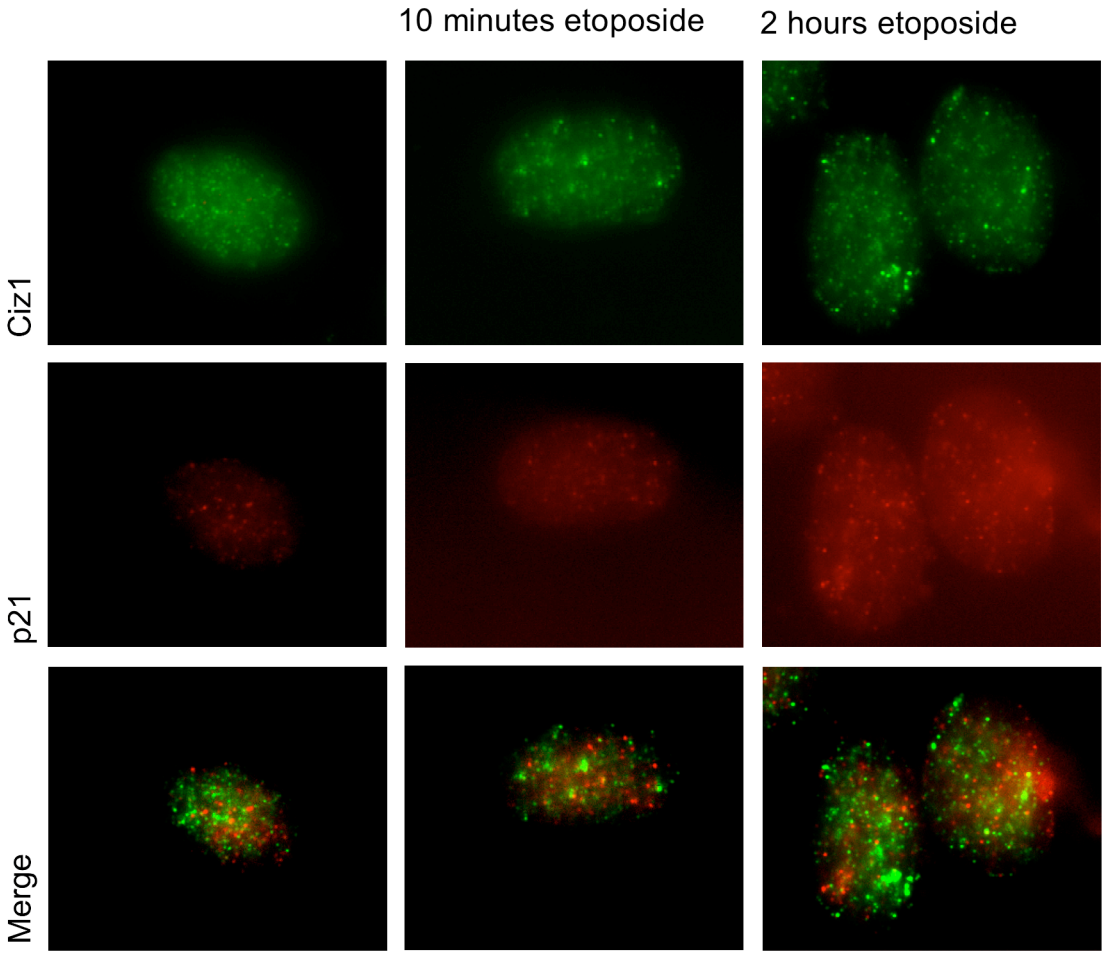

Figure 5.7 Ciz1 does not co-localise with p21 following etoposide treatment in HeLa-S3 cells

Immunofluorescence images showing Ciz1 and p21 in HeLa-S3 and U2OS cells. Cells were treated for up to 2 hours with 20μM etoposide, washed in 0.1% Triton X-100 for 10 seconds, and then rinsed once in PBS before fixation with PFA. Ciz1 was detected using rabbit polyclonal anti-Ciz1 1793 antibody (green) and anti-rabbit FITC conjugated secondary antibody. p21 was detected using mouse monoclonal anti-p21 antibody (red) and anti-mouse Alexa 568 conjugated secondary.

5.4.6.3 MDC1

Mediator of the DNA damage checkpoint 1 (MDC1) binds to the C-terminus of phosphorylated H2AX, recruiting the Mre11-Rad50-Nbs1 complex to sites of double strand breaks (Lukas, Melander et al. 2004; Stucki, Clapperton et al. 2005). While this interaction between γH2AX and MDC1 is dispensable for the recruitment of DNA damage signalling and repair proteins such as 53Bp1 and BRCA2 to lesions, it is vital for their formation into stable foci (Celeste, Fernandez-Capetillo et al. 2003; Stewart, Wang et al. 2003). MDC1 has also been implicated in non-homologous end joining repair of chromosome ends with defective telomeres (Dimitrova and de Lange 2006), but this is the extent of its identified involvement in DNA repair so far. Due to its role in recruiting and stabilising DDR proteins, MDC1 seemed a good target to compare against Ciz1. As the MDC1 antibody used was raised against rabbit, a mouse monoclonal antibody raised against the C-terminus of Ciz1 was used to visualise Ciz1 expression.

D3T3 cells were treated with 20μM etoposide for 2 hours prior to washing in 0.1% Triton X-100, before fluorescent microscopy was used to visualise Ciz1 and MDC1 by immunofluorescence. Following etoposide-treatment no obvious change in either protein could be seen, and no co-localisation was observed between the two (Figure 5.8).

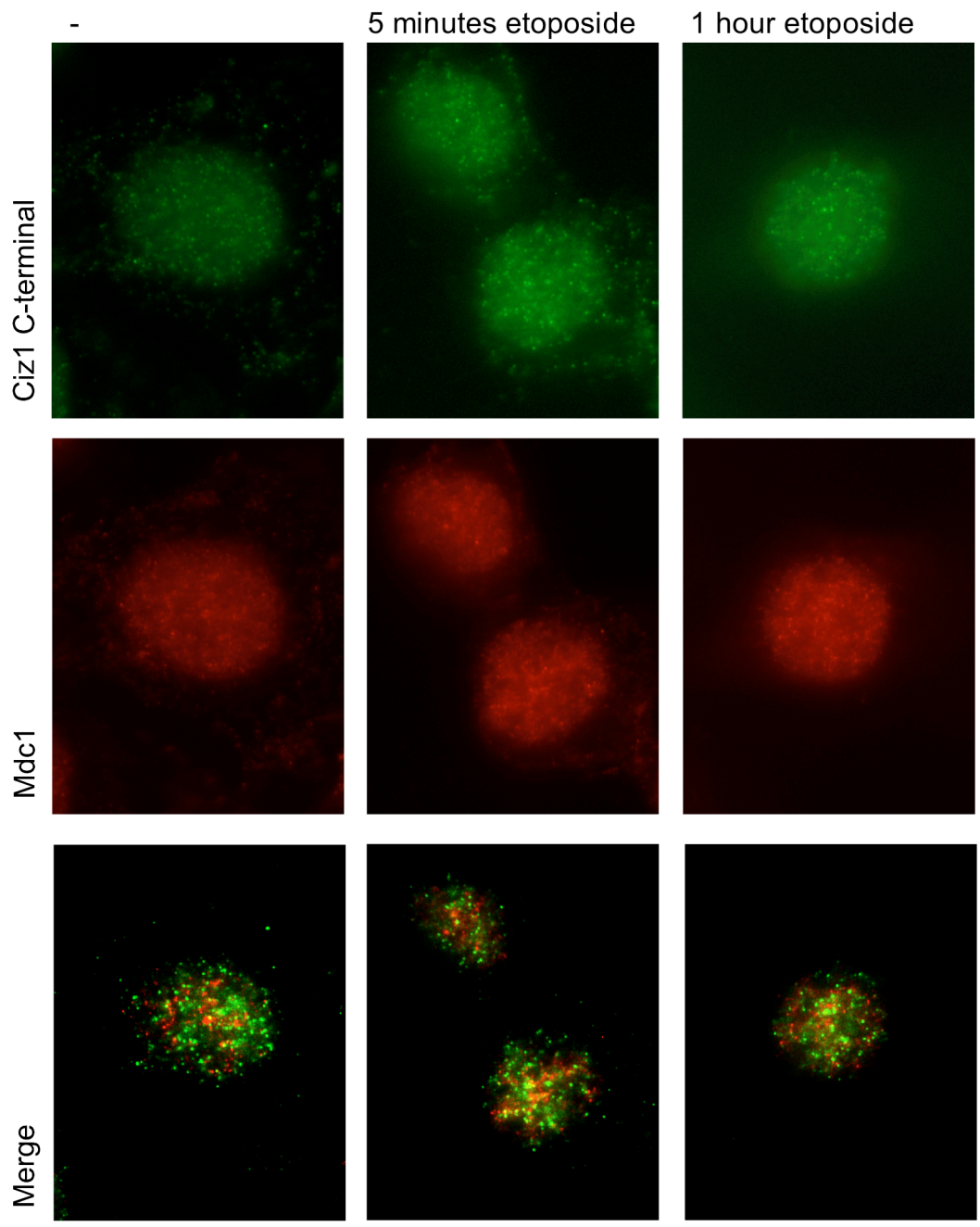

Figure 5.8 Ciz1 does not co-localise with MDC1 following etoposide treatment in D3T3 cells

Cells were treated for 2 hours with either 2μM or 20μM etoposide, washed in 0.1% Triton X-100 for 10 seconds, and then rinsed once in PBS before fixation with PFA. Ciz1 was detected using mouse monoclonal anti-Ciz1 C-terminal TED antibody (green) and anti-mouse Alexa 568 conjugated secondary antibody. MDC1 was detected using rabbit polyclonal anti-MDC1 antibody (red) and anti-rabbit FITC conjugated secondary.

5.5 Discussion

In this chapter both live cells, and the cell free system described in chapter 3 were used to ask two main questions – what is the effect of DSB induction upon Ciz1 expression and transcription, and can a measurable effect of excess Ciz1 upon DNA damage signalling be observed? From these experiments we can draw the following conclusions:

- Overexpression of Ciz1 in intact cells and addition of excess ECiz1 to isolated nuclei in cell free reactions does not induce H2AX phosphorylation; however supplementation of cell free reactions containing damage-activated extract with ECiz1 further inhibits DNA synthesis in naïve nuclei.

- No change can be observed in overall Ciz1 protein levels or in its nuclear matrix binding following etoposide treatment in either a healthy or tumour-derived cell line.

- Ciz1 does not co-localise with PCNA, p21 or MDC1 in response to etoposide treatment.

- Ciz1 transcript expression responds to etoposide treatment: exon 7 mRNA dropped in both WI38 and U2OS cells. In the normal cell line this was accompanied by a rise in exon 16 transcript levels, whereas in the tumour-derived line exon 16 transcript fell.

While these conclusions do not provide a simple explanation for Ciz1's role in the DNA damage response, they do support the PIKK-dependent phosphorylation of Ciz1 observed in Chapter 4, and further implicate the C-terminal domain of Ciz1. As such a number of avenues are opened up for discussion and speculation.

5.5.1 Ciz1 is likely to be a non-IRIF-associated DDR protein

The evidence collected so far – Ciz1's failure to promote γH2AX foci, associate with known DDR proteins, or to display any change in spatial location, levels or nuclear binding following etoposide treatment – rule out a role in propagation of initial DDR signalling fairly conclusively. It is important to note that while the formation of damage-induced γH2AX foci is a major method by which DNA damage is detected and

repaired, there are a number of proteins that do not form discernable foci, including Chk1, Chk2, p53, Cdc25a, DNA-PK and SMC1 (Bekker-Jensen, Lukas et al. 2006), and that recruitment to IRIF is neither an essential, nor a defining feature of DDR proteins. Furthermore, while phosphorylation of SQ/TQ motifs is indicative of involvement in the DDR, it does not always affect recruitment to damage foci - this is independent of SCD phosphorylation in BRCA1 (Cortez, Wang et al. 1999; Kitagawa, Bakkenist et al. 2004). In short, while the failure of Ciz1 to associate with IRIF makes involvement in early stages of DDR signalling unlikely, it does not rule out involvement in the response altogether. Given the PIKK-dependent phosphorylation of Ciz1 observed in response to DDR induction both *in vitro* here and in intact cells in the Matsuoka study (Matsuoka, Ballif et al. 2007), combined with the changes in mRNA expression seen following etoposide treatment, it seems likely that Ciz1 may instead be involved in the response at a different level.

5.5.2 Non-IRIF-associated proteins have a number of known roles in the DDR

If Ciz1 is a non-IRIF-associated DNA damage response protein, the question is raised of what role it might play. The roles of known non-IRIF-associated proteins will be discussed briefly.

5.5.2.1 Regulation of cell cycle checkpoints

Two key non-IRIF-associated proteins are the checkpoint kinases, Chk1 and Chk2. Chk1 and Chk2 are activated by ATR and ATM respectively following DNA damage, and go on to play a variety of roles in the response, but do not form cytologically discernible foci. Isoforms of Cdc25, a phosphatase required for successful transition between the G1 and S phases of the cell cycle, are phosphorylated by Chk1 and Chk2 in response to DNA damage either inactivating them, inducing export from the nucleus or inducing degradation of the protein (Furnari, Blasina et al. 1999; Lopez-Girona, Furnari et al. 1999; Xiao, Chen et al. 2003). Again, despite its important role in the DDR, no accumulation of Cdc25 can be seen at DSBs. Another pair of non-IRIF-associated proteins, DNA-PK and its partner Ku70 were implicated in DSB-induced inhibition of DNA synthesis in Chapter 3.

5.5.2.2 Transcription of DSB-induced genes and induction of apoptosis

E2F1 is a member of the E2F family of transcription factors, which regulate genes involved in cell cycle control. Once activated by DNA damage, both Chk1 and Chk2 phosphorylate E2F1 and its partner pRB (Stevens, Smith et al. 2003; Urist, Tanaka et al. 2004; Inoue, Kitagawa et al. 2007), with E2F1 also known to be a substrate of DNA-PK (Watanabe, Shinohara et al. 2003). In addition to regulating expression of genes such as cyclin E, p107, CDC6 and ribonucleotide reductase, which are required for successful transition between phases of the cell cycle, E2F1 has been shown to stimulate transcription of ATM, Chk1, Apaf1, p73 and ARF, which are involved in DNA damage detection, repair and apoptosis (Polager, Kalma et al. 2002; Stevens and La Thangue 2004). Chk1 and Chk2 also influence the p53-mediated apoptotic pathway, by phosphorylating both p53 (another protein which does not localise in response to DNA damage) and other components of the pathway (Stracker, Usui et al. 2009).

5.5.2.3 Chromatin modification and DNA repair

SMC1 and SMC3 are two components of the cohesin complex, which maintains sister chromatid cohesion and is required for successful repair of double strand breaks (Atienza, Roth et al. 2005). Damage-induced phosphorylation of SMC1 and SMC3 are also involved in checkpoint signalling (Kim, Xu et al. 2002; Yazdi, Wang et al. 2002; Luo, Li et al. 2008), but while modification of SMC1 is only seen in the vicinity of DNA lesions, the protein can be found across the entire nucleus, with no overall shift in localisation (Bekker-Jensen, Lukas et al. 2006). Additionally, activated Chk1 modifies chromatin structure by cessation of normal phosphorylation of histone H3, providing a physical block to transcription of cell cycle modulators such as cyclin B1 and CDK1 by preventing interaction of GCN5 with their promoter elements (Shimada and Nakanishi 2008; Shimada, Niida et al. 2008).

In summary, non-IRIF-associated DDR proteins tend to either be effectors playing roles in cell cycle arrest or transcription, or mediators that exploit this lack of localisation to allow them to connect downstream signalling molecules at the site of DSBs with effectors throughout the entire nucleus. Like Cdc25, p21, and the CDK and cyclin families, Ciz1 already possesses a well-characterised role in cell cycle progression, and inhibition of its phosphorylation by LY294002 implies a connection to DNA-PK. I

would therefore suggest that Ciz1 may play a role in control of cell cycle during the DDR, and shall go on to explore this idea in greater depth in Chapter 6.

Chapter 6

GENERAL DISCUSSION

The aim of this thesis was to investigate Ciz1's involvement in the DDR, first by establishing whether it is phosphorylated by the PIKKs in response to etoposide treatment, and then by attempting to identify a role for the protein within the DDR process. Several approaches were taken, one of which, the development of a cell free approach to study the DNA damage response, has had significant implications in its own right. As such this chapter will cover two main elements: applications of the new developments to this system and speculation upon Ciz1's role in the DDR.

6.1 Development of the cell free system as a tool to study the DDR

Chapter 3 dealt in detail with adaptation and characterisation of a cell free system previously used to carry out studies of DNA replication initiation and elongation to permit study of the events resulting from etoposide-induced DNA damage. When reconstituted *in vitro*, the PIKK-dependent signalling that takes place as a consequence of DSB formation can be isolated from and manipulated separately to DNA damage itself and also isolated from the process of DNA repair. Soluble factors present in damage-activated extracts recreate both G1/S and intra-S phase checkpoints, impinging on initiation and elongation of DNA synthesis respectively. Finally, upstream events that signal the activation of soluble components of the DDR have also been reconstituted in vitro. Two uses of the system have been illustrated in Chapters 3 and 4; firstly for study and dissection of the DDR signalling pathways, and secondly as a screening tool to assess potential inhibitors of the PIKKs and other molecules in these pathways.

6.1.1 Use of the cell free system to draw biological conclusions about the DDR

Use of the cell free system to study DDR pathways can be divided into two main examples. These consist of the use of the two biological markers to draw conclusions about the effect of different inhibitors upon the two main pathways that constitute the DDR, and use of cell free extracts to study damage-induced phosphorylation of Ciz1.

6.1.1.1 Contrasting biological markers allow dissection of the different pathways of the DDR

In Chapter 3 use of two PIKK inhibitors with different substrate specificities demonstrated the systems capacity to be used to draw biological conclusions. While wortmannin and LY294002 both removed the block on DNA synthesis imposed by

activated extract they differed in their impact on H2AX phosphorylation. Wortmannin caused a reduction in phosphorylation of H2AX, but treatment with LY24002 led to an increase over that imposed by activated extract alone. Thus, phosphorylation of H2AX is uncoupled from ongoing DNA synthesis. This is consistent with published observations, which suggest that the DDR chiefly slows DNA synthesis during S phase by inhibition of origin firing (Larner, Lee et al. 1999), with ongoing synthesis being routinely observed at a low rate in damage-activated extracts used in Chapter 3.

Furthermore, by examining the effect of the two inhibitors upon H2AX phosphorylation, it was possible to clarify conflicting results that had been seen when using LY294002 as part of previous *in vitro* and cellular studies (Cheatham, Vlahos et al. 1994; Stiff, O'Driscoll et al. 2004). From observations here it seems likely that while LY294002 interacts with purified ATM *in vitro*, in a cellular context it does not affect ATM signalling, possibly due to altered folding and modification of protein produced by bacterial purification. Lastly the preservation of H2AX phosphorylation seen with LY24002 suggests that DNA damage detection is uncoupled from inhibition of DNA synthesis, and that DNA-PK helps to slow DNA replication in damaged cells in a manner that is independent of ATM and ATR.

6.1.1.2 Use of soluble DDR factors to phosphorylate SQ/TQ motifs

Chapter 4 then goes on to document use of the cell free system as an assay for phosphorylated SQ/TQ motifs, allowing identification of PIKK substrates. This assay possesses the advantage that it permits study of a specific protein rather than the somewhat scattershot approach used in the mass spectrometry assays described in Chapter 4 (Matsuoka, Ballif et al. 2007; Stokes, Rush et al. 2007). Additionally, this method only requires synthesis of the target protein and not of phosphorylated ATM and ATR, and the use of damage-activated cytosolic extract is more representative of an *in vivo* environment than purified protein interaction assays.

6.1.2 Potential for the cell free system to be used as an assay for DDR inhibitors

As demonstrated by the use of wortmannin and LY294002 in Chapter 3, the cell free system also serves as an assay for potential DDR inhibitors. In recognition of the advantages provided by the cell free system, a patent has been submitted by the University of York for the technology (Patent No. GB0903373.9), and funding has been

allocated by the University Research Innovation Office's Strategic Initiative Fund for further development of the system as a high throughput assay.

6.1.2.1 Need for targeted cancer treatments

In the past decade there has been a switch in focus to development of targeted therapies that exploit specific differences between cancer and healthy cells, driven by the severe side effects of conventional chemotherapies and radiotherapies. The number of documented genetic and epigenetic differences is escalating as a result of intensive research (Collins and Barker 2007), offering a raft of new potential therapeutic targets.

With detailed and specific knowledge of specific pathways and players comes the opportunity to design very specific chemical inhibitors. Structure-based drug design takes key altered proteins, and uses knowledge of their crystal structure to design inhibitors that can specifically target tumour cells. Protein kinases are a classic example of this, as they are easily purified in quantity, involved in many critical pathways, and their targets are frequently mutated in cancers (Eglen and Reisine 2009). A number of inhibitors of tyrosine receptor kinases have been approved for clinical use, including tarceva and iressa, and cyclin dependent kinase inhibitors such as alvocidib and seliciclib have been entered into phase II and III trials (Hidalgo, Siu et al. 2001; Wakeling, Guy et al. 2002; Shapiro 2006).

6.1.2.2 PIKKs are a good target for selective treatments

One class of protein kinases which has been identified as holding therapeutic potential, is the PIKK family. Blocking PIKKs increases sensitivity of cells to radiation, increasing effectiveness of radiotherapy (McKenna and Muschel 2003), and is likely to increase the efficacy of chemotherapies that act by creating DNA damage. While wortmannin and LY294002 are useful research tools, they are not ideal for clinical purposes as they show effects on other kinases and have concentration and stability issues.

Through high throughput screening a number of classes of PIKK inhibitors have been discovered and are in clinical trials. These efforts have chiefly focused on the PI3K-AKT-MTOR pathway, due to its frequent deregulation in tumour cells and role in regulating cell growth and survival (Workman, Clarke et al. 2010). However its

involvement in a range of pathways from glucose metabolism to haematopoietic stem cell regulation means that chronic inhibition could lead to serious side effects (Zhang, Grindley et al. 2006; Sopasakis, Liu et al. 2010). The more specialised roles of the PIKKs ATM and ATR present a more focused avenue for drug discovery, however as we learn more about their role in regulating the DNA replication fork (Shechter, Costanzo et al. 2004) it is becoming evident that their inhibition may have undesirable effects.

6.1.2.3 Benefits of the cell free system as an assay

Progress of research into the oncogenome over the past decade has been facilitated by the availability of high-throughput technologies such as fluorescence *in situ* hybridisation, high-throughput DNA sequencing and chromatin immunoprecipitation microarrays. In order to exploit the role of protein kinases in cancer, a number of gene-focused bio-assays have been developed to look for substrates and downstream signalling partners (Eglen and Reisine 2009). This has led to generation of cell-based assays, such as bioluminescence resonance energy transfer and protein fragment-complementation which are also able to screen libraries of inhibitors for specific protein kinases (Moll, Prinz et al. 2006; Prinz, Diskar et al. 2006; Stefan, Aquin et al. 2007). These assays are useful tools, but have the drawback that they require tagging of the target kinase, and only permit study of an individual, rather than an entire pathway. Development of new high throughput technologies, for both genome & proteome characterisation and for drug discovery, is of great importance in understanding and treating cancer. This cell free approach offers a highly focused biological assay, with multiple fluorescent outputs, that is amenable to high-throughput format. Furthermore, in addition to reconstituting and isolating the role of known DDR players such as ATM and ATR, it also offers access to as yet unidentified players whose inhibition could have potent and selective effects on the cell's response to DNA damage.

6.2 Involvement of Ciz1 in the DDR

In Chapters 4 and 5, variations of the properties of Ciz1 in response to DSB induction were studied, both within the cell free system and in intact cells. These experiments gave rise to the following conclusions:

- Ciz1 is phosphorylated in response to DDR activation

- Ciz1 phosphorylation is inhibited by LY294002 treatment, and is therefore likely to be DNA PK-induced, and part of the pathways leading to inhibition of DNA synthesis

- Ciz1 is not recruited to IRIF

- Nuclear matrix binding of Ciz1 is not altered by DSB induction

- Ciz1 does not induce ATM-mediated early DDR signalling, or stimulate H2AX phosphorylation

- Expression of Ciz1 C-terminal mRNA increases following DSB induction in a healthy human lung fibroblast cell line. Contrastingly, C-terminal mRNA levels fall in a human osteosarcoma cell line under the same conditions

Given these results and pre-existing knowledge about Ciz1, I shall go on to speculate upon Ciz1's role in the DDR and how it can be tested. This section will focus upon two main questions: how could DDR activation affect spatial organisation of Ciz1 in the nucleus, and how might Ciz1's existing role in control of DNA replication initiation tie in with the DDR?

6.2.1 Spatial organisation of DDR proteins - where can we place Ciz1?

Proteins involved in the DDR can be divided into two main classes - proteins present in a fixed format throughout chromatin which are only activated following modification induced by proximity to a lesion, and proteins that alter location in response to damage (Bekker-Jensen, Lukas et al. 2006). Those proteins that relocalise in response to DNA damage can be assigned three main targets:

- DSB-flanking chromatin (MDC1, MRN complex, 53BP1, BRCA1, ATM). These proteins are signal amplification and recruitment factors, forming classic IRIF. IRIF can cover up to a megabase, and are visible by fluorescent microscopy (Bekker-Jensen, Lukas et al. 2006).

- ssDNA containing microcompartments (ATR, RPA, Rad51, Rad52, BRCA2, FANCD2). These proteins are recruited to repair centres for individual breaks and their foci are visible by fluorescent microscopy.

- Unprocessed DSB and partially processed DSB intermediates, suggesting direct interaction with DNA ends (DNA-PK, Ku70, SMC1/3 cohesin containing complex). These foci are generally outside the resolution achievable by fluorescent microscopy, unless massive damage outside the scope of normal physiological conditions is inflicted.

As recruitment of Ciz1 to IRIF at DSB-flanking chromatin has already been ruled out, it seems likely that Ciz1 either falls either into the first class of nuclear-bound locally activated proteins, or that similar to DNA-PK, it is recruited to microcompartments at the sites of unprocessed breaks which are beyond the resolution of light microscopy. Should it be that Ciz1 localisation is unaffected by DNA damage, but that SQ/TQ modification is induced by nearby breaks, a phospho-specific antibody for Ciz1 would be required to detect this phosphorylation. If it is instead the case that Ciz1 localisation does change but at a lower resolution than can be visualised, it is possible that application of a dose of etoposide sufficient to induce massive disruption of DNA could result in visible co-localisation of Ciz1 with DNA-PK. In this instance the methods used by Bekker-Jensen *et al* to induce DSBs by intense laser irradiation could also reveal Ciz1 localisation at the sites of unprocessed breaks, with the advantage that damage is constrained to a limited section of the nucleus, rather than spread throughout it as with use of chemical or ionising radiation-induced damage.

6.2.2 Ciz1 may inhibit DNA synthesis in response to DNA damage via its role in controlling DNA replication initiation

At the end of chapter 5 I suggested that Ciz1 might play a role in cell cycle control during the DNA damage response. This idea is supported by several pieces of evidence - firstly inhibition of its phosphorylation in damage-activated extract supplemented with LY294002. As discussed earlier in this chapter and chapter 3, LY294002 alleviates inhibition of DNA synthesis in damage-activated extracts without reducing H2AX phosphorylation. It seems likely that proteins affected by LY294002 contribute to restraint of DNA replication. It is known that formation of DSBs mainly inhibits DNA synthesis by inducing a drop in origin firing throughout S phase (Larner, Lee et al. 1999). Ciz1 has a characterised role in the events leading up to licensing of replication origins that may well contribute to this decrease.

6.2.2.1 Sequential activation of cyclins E and A plays an important role in initiation of DNA replication

Control of DNA initiation and transition from G1 to S phase is controlled in part by cyclin E and cyclin A, in combination with their protein kinase partner CDK2. In addition to controlling transcription of S phase proteins, cyclin E facilitates MCM loading during pre-RC assembly and in concert with CDK2 promotes licensing of DNA replication origins (Jackson, Chevalier et al. 1995; Coverley, Laman et al. 2002; Geng, Lee et al. 2007; Chuang, Teixeira et al. 2009). Cyclin A-CDK2 activates existing pre-RC complexes, and stimulates DNA synthesis elongation, promoting S phase (Coverley, Laman et al. 2002; Yam, Fung et al. 2002; Woo and Poon 2003). Cyclin A-CDK2 also phosphorylates CDC6, leading to its export from the nucleus to cytoplasm, preventing formation of new pre-RC and thereby avoiding rereplication (Petersen, Lukas et al. 1999). CDK2-dependent functions of cyclins E and A rely upon the interaction with CDK2 causing CDK2 to enter an active conformation, exposing the active site of the protein to ATP. With these important roles in pre-RC assembly and activation and prevention of rereplication, cyclin E and cyclin A must bind to CDK2 in the correct order for DNA replication to be carried out properly.

6.2.2.2 Ciz1 is a platform for sequential cyclin E and A loading onto the nuclear matrix

Cyclins interact with inhibitors, activators and substrates using binding sequences known as Cy motifs (Wohlschlegel, Dwyer et al. 2001). Ciz1 contains five Cy motifs, three within its replication domain, and two in its anchor domain (Figure 6.1a). While little is known of the function of the C-terminal Cy motifs (one of which is located just after the third C2H2 zinc finger) the interactions of the N-terminal Cy motifs with cyclins E and A have been characterised by this laboratory. Via these N-terminal motifs, Ciz1 binds cyclins E and A, and works in cooperation with cyclin A/CDK2 to promote DNA replication initiation (Copeland, Sercombe et al. 2010). Cyclin E binds to Ciz1 at Cy-ii, but can be displaced by cyclin A, which binds to both Cy-ii and Cy-iii. Immobilisation of cyclin E upon the nuclear matrix is independent of Ciz1, but immobilisation of cyclin A is disrupted by depletion of Ciz1.

Given the temporally distinct nature of cyclin E and A expression (Sherr 1995) Copeland proposes a model in which Ciz1 becomes bound to cyclin E during pre-RC assembly during late G1 phase, before recruitment of cyclin A to Ciz1 displaces cyclin E, regulating their sequential roles at pre-RC complexes (Figure 6.1b). While the C-

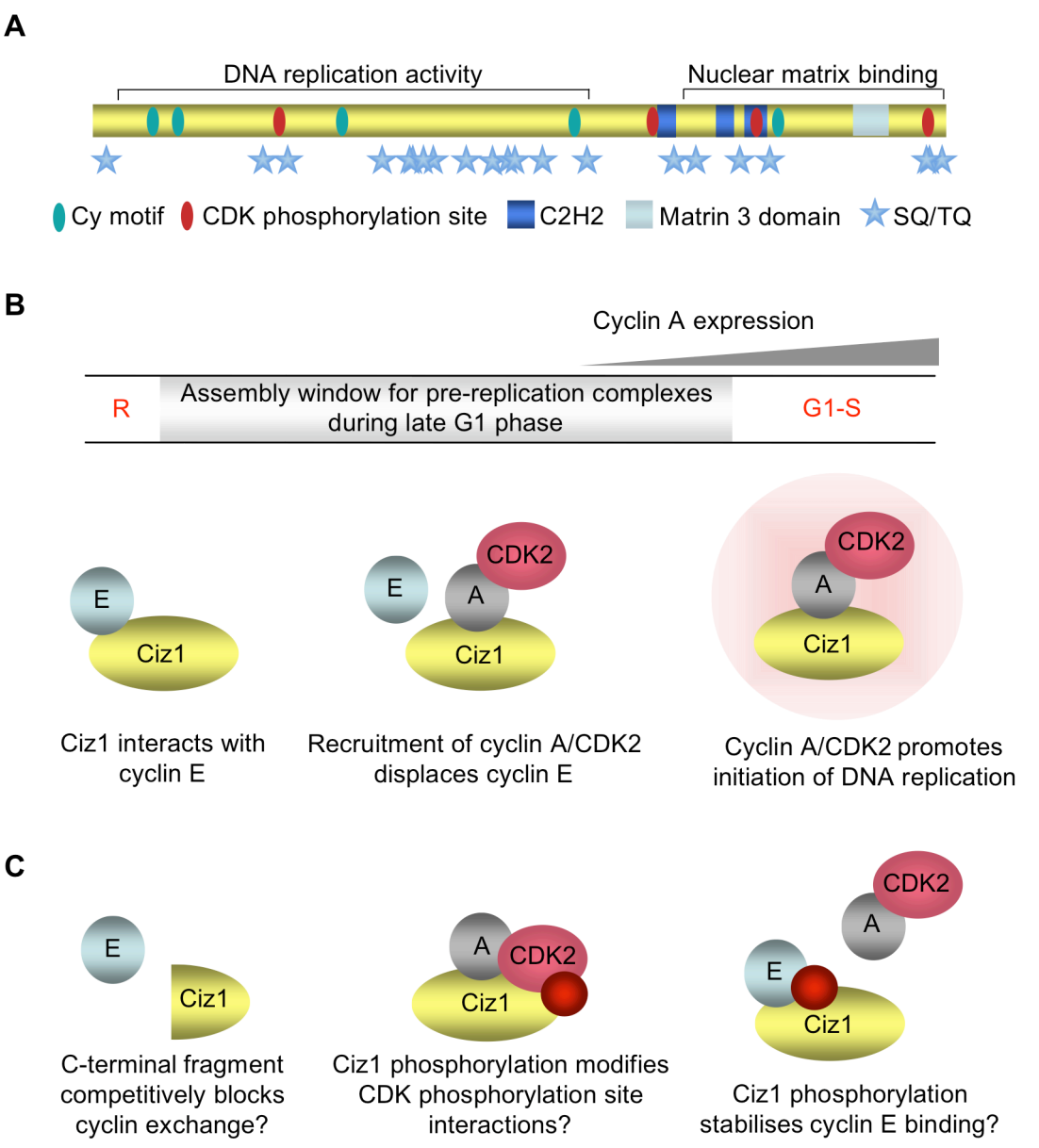

Figure 6.1 Model of Ciz1 interactions with cyclin E and cyclin A/CDK2 during initiation of DNA replication

a) Diagram of full length human Ciz1 displaying SQ/TQ motifs and functional sites

b) Model of Ciz1 interactions with cyclin E and cyclin A/CDK2 during initiation of DNA replication. Copeland's data suggests that Ciz1 would interact with cyclin E via Cy-ii during mid G1 phase. As cyclin A levels rise in late-G1 phase, cyclin E would be displaced from Cy-ii by cyclin A. Interaction with Ciz1 could localize cyclin A/CDK2 complexes to sites that contain cyclin E, promoting phosphorylation of nearby substrates.

c) Three possible models for Ciz1-mediated inhibition of DNA synthesis initiation following activation of DDR signalling.

terminal region of the protein is not required for interaction with either cyclin, this model also suggests that the matrix-binding properties of Ciz1 may support delivery of cyclin A to replication factories. Once bound to Ciz1 at these sites, cyclin A-CDK2 is able to locally promote initiation of DNA replication. This model is supported by observation of co-localisation between Ciz1 and cyclin A in cycling cells [Nikki Copeland; unpublished], and describes a Ciz1-dependent step in origin licensing and firing which could be modulated in response to DNA damage.

6.2.3 Three models for Ciz1-mediated inhibition of origin firing

DNA PK is a member of the PIKK family, and forms a trimer with two Ku units in presence of DNA (Dvir, Peterson et al. 1992; Downs and Jackson 2004). Autophosphorylation of DNA-PK in response to ionising radiation is dependent both on Ku and upon MDC1, and leads to co-localisation with γH2AX and 53BP1 (Chan, Chen et al. 2002; Lou, Chen et al. 2004). While ATM and DNA-PK both phosphorylate H2AX in a redundant fashion following exposure to ionising radiation, DNA-PK is not capable of phosphorylating downstream signalling proteins such as Chk2, NBS1, CtIP, BLM, and p53 (Stiff, O'Driscoll et al. 2004). Tellingly, DNA-PK is preferentially autophosphorylated in response to replication-associated DSBs as opposed to ionising radiation induced breaks during S phase (Chen, Chan et al. 2005). As etoposide induces DSBs by stalling the replication fork, DNA-PK should be active in both the damage-activated extract and *in vivo* experiments described here (Li and Liu 2001). As discussed in chapter 3, it seems likely that DNA-PK is the LY294002-inhibited component of the DDR responsible for restraining DNA synthesis in the cell free system, and that it is also the protein responsible for phosphorylation of ECiz1 in damage-activated cytosolic extract observed in chapter 4. Based upon the results in this thesis, I propose a model in which DNA-PK phosphorylates Ciz1 in response to double strand break signalling, which then causes Ciz1 to modulate origin firing via its interactions with cyclins E and A, and CDK2. As yet there is little evidence as to how Ciz1 would do this, but existing knowledge of its function gives us three possible explanations that could be tested (Figure 6.1c).

6.2.3.1 Preferential recruitment of C-terminal fragments to unfired origins?

In chapter 5, RT-PCR data suggested a rise in expression of Ciz1 C-terminal mRNA following etoposide treatment in a normal cell line. This uncoupled expression of

different regions of Ciz1 mRNA is not unusual - there are a large number of splice variants of the protein, and variation in N and C-terminal expression has been previously observed in several biological contexts. Heather Sercombe found uncoupled expression of the two ends of Ciz1 in a range of tumour cells, with transcription of C-terminal exons exceeding N-terminal mRNA in stage I through to III tumours, but with the balance reversing to favour the replication domain of Ciz1 in metastatised tissue [Sercombe et al, submitted]. Similar uncoupling has also been seen in differentiating tissue, with increased expression of C-terminal mRNA as human urothelial cells are stimulated to differentiate [Jennifer Munkley, unpublished].

The 1793 antibody commonly used to study Ciz1 expression is specific to the N-terminus of the protein, and antibodies targeting the C-terminus have only recently been developed. There is therefore very limited knowledge about levels of expression and localisation of the nuclear matrix binding region at the protein level. However overexpression of recombinant GFP-tagged C-terminus Ciz1 has shown that it competitively disrupts nuclear binding of full length endogenous Ciz1, and that this affects assembly of pre-RC (Sercombe et al, submitted). Newly produced Ciz1 is recruited to replication factories during early-mid G1 phase and is required for progression into S phase (Coverley, Marr et al. 2005; Ainscough, Rahman et al. 2007). This raises the question of whether the observed increase in C-terminal mRNA could represent an increase in translated splice variants with a dysfunctional N-terminal region that might preferentially be recruited during G1 phase. Lacking the N-terminal Cy motifs shown to be required for interaction with cyclins E and A, cyclin exchange would be unable to occur, and cyclin A/CDK2 would be unable to stimulate DNA synthesis initiation (Figure 6.1c). While no decrease was seen in nuclear matrix-bound N-terminus Ciz1 following etoposide treatment, this is not necessarily incompatible with C-terminus recruitment. This model could be tested by comparison of cyclin A co-localisation with Ciz1 N & C-terminal regions by immunofluorescence following etoposide treatment.

6.2.3.2 Ciz1 DNA replication activity is modulated by CDK2 phosphorylation sites

The ability of Ciz1 to stimulate DNA replication initiation *in vitro* has already been mentioned. In the cell free system, this effect peaks at a concentration of 1nM, with any increase causing numbers of initiating nuclei to fall. In addition to Cy motifs, Ciz1 contains a number of possible CDK-phosphorylation sites, through which members of

the CDK family commonly phosphorylate substrates (Figure 6.1) (Endicott, Noble et al. 1999). When one of these sites, threonine 191/2, is replaced with two alanine residues rendering it unable to be phosphorylated, initiation does not fall when the threshold level of 1nM Ciz1 is exceeded, but remains at an increased level (Coverley, Marr et al. 2005). Modulation of Ciz1's capacity to stimulate initiation can also be achieved by inactivating the CDK phosphorylation site threonine 293 (Coverley, Marr et al. 2005). If phosphorylation of these sites by CDK2 is required for promotion of initiation by Ciz1 in concert with cyclin A/CDK2, it is possible that phosphorylation of nearby SQ/TQ motifs (Figure 6.1a) could effect conformational changes within Ciz1 that prevent access to CDK phosphorylation sites (Figure 6.1c).

This model could potentially be tested by titrating purified Ciz1 phosphorylated *in vitro* by damage-activated extract into cell free initiation assay reactions, and asking whether the initiation profile mimics those seen using CDK phosphorylation site mutants. Alternatively, point mutation could be used to edit the SQ/TQ motifs adjacent to CDK phosphorylation sites so that they are either constitutively phosphorylated or incapable of phosphorylation, and these mutants used to generate initiation profiles. Neither method would give evidence for a direct link between CDK2 and Ciz1, but could provide an indication whether this avenue is worth investigating further.

6.2.3.3 Stabilisation of cyclin E-Ciz1 interactions following DNA damage induction?

One clear method of delaying initiation would be if phosphorylation of SQ/TQ motifs within Ciz1 stabilised its binding to cyclin E, leading to retention of the protein at pre-replication complexes (Figure 6.3c). This could be effected either by direct interaction with cyclin E, or by conformational change inactivating the Cy-iii motif which is required by cyclin A, but not cyclin E, to bind to Ciz1 (Copeland, Sercombe et al. 2010). In addition to altering rates of DNA synthesis stabilisation of cyclin E at replication factories could also provide positive feedback, promoting earlier stages of DDR signalling. Cyclin A has been shown to act as a negative regulator of CDC6 as well as promoting its export from the nucleus (Petersen, Lukas et al. 1999; Coverley, Laman et al. 2002). CDC6 is required for Chk1 activation (Clay-Farrace, Pelizon et al. 2003; Oehlmann, Score et al. 2004), so disruption of cyclin A/CDK2 activity by competition for CDK2 by cyclin E could help sustain Chk1 signalling.

Again, this model can be tested using immunofluorescence techniques. If cyclin E and Ciz1 are stabilised at replication factories, co-localisation of the two should be seen as with cyclin A and Ciz1. If DSB induction results in a stabilisation of cyclin E and Ciz1 interaction, then such a co-localisation should be prolonged into S phase following etoposide treatment. The cell free system also provides the opportunity to use damage-activated extracts to create phosphorylated Ciz1 *in vitro*, which could then be used to ask whether sequential addition of cyclin E and cyclin A still shows the displacement of cyclin E characterised by Copeland's study, or whether cyclin E maintains a stable interaction with Ciz1.

6.2.4 Conclusions

While it is difficult to choose one specific model for Ciz1's involvement in the DDR without further experimentation, current literature does provide some insight as to which might be correct. Research into the response to UV induced DNA damage, shows that exposure has both increased transcription of cyclin E and stabilised the protein during S phase (Carcagno, Ogara et al. 2009; Lu, Liu et al. 2009). Furthermore, PIKK-dependent artemis-mediated degradation of cyclin E is known to contribute to recovery from the S phase checkpoint (Wang, Zhang et al. 2009). When the amino acid residues responsible for this degradation were inactivated by point mutation, lower levels of cyclin A bound to CDK2 could be retrieved by immunoprecipitation. Given Ciz1's role in mediating cyclin exchange, this evidence provides strong support for a model in which PIKK-dependent phosphorylation of SQ/TQ leads to stabilisation of cyclin E upon the pre-replication complex, preventing initiation of DNA synthesis.

ABBREVIATIONS

53BP1	Tumour protein p53 binding protein 1
AD	Anchor domain
Apaf1	Apoptotic peptidase activating factor 1
AQ	Alanine glutamine
ATM	Ataxia telangectasia mutated
ATP	Adenosine triphosphate
ATR	Ataxia telangectasia mutated related
ATRIP	ATR interacting protein
BdUTP	Biotinylated dUTP
BER	Base excision repair
BLM	Bloom syndrome protein
BRCA1	Breast cancer 1
BRCA2	Breast cancer 2
BRCT	Breast cancer 1 C-terminal domain
BSA	Bovine serum albumin
C2H2	Cys 2 His 2 zinc finger
CAPS	3-(Cyclohexylamino)-1-propanesulfonic acid
Cdc25	Cell division cycle 25
CDC6	Cell division cycle 6
CDK	Cyclin dependent kinase
CDK1	Cyclin dependent kinase 1
CDK2	Cyclin dependent kinase 2
cDNA	Complementary DNA
Chk1	Checkpoint kinase 1
Chk2	Checkpoint kinase 2
Ciz1	p21 cip1-interacting zinc finger protein
CPK	Creatine phosphokinase
CREB	cAMP response element-binding protein
CSK buffer	Cytoskeletal buffer
Ct	Cycle threshold
CtBP	C-terminal binding protein
CtIP	CtBP-interacting protein
CTP	Cytidine triphosphate
Cy	Cyclin binding motif
dATP	Deoxyadenosine triphosphate
dCTP	Deoxycytidine triphosphate
DDR	DNA damage response
dGTP	Deoxyguanosine triphosphate
DLC1	Dynein light chain 1
DMEM	Dulbecco's modified eagle medium
DMSO	Dimethyl sulfoxide
DNA	Deoxyribonucleic acid
DNA-PK	DNA-dependent protein kinase
dNTP	Deoxyribonucleotide triphosphate
DSB	Double strand break
DTT	Dithiothreitol
dTTP	Deoxythymidine triphosphate
E2F1	E2F transcription factor 1
ECiz1	Embryonic Ciz1
EDTA	Ethylenediaminetetraacetic acid
EGTA	Ethylene glycol tetraacetic acid
EKLF	Erythroid Krüppel-like Factor
ERE	Estrogen response element
ERH	Enhancer of rudimentary homolog
Erα	Estrogen receptor alpha
EST	Expressed sequence tag
FANCD2	Fanconi anemia group D2 protein
FCS	Foetal calf serum

FHA	Forkhead-associated domain
FITC	Fluorescein isothiocyanate
G1 phase	Growth phase 1
G2 phase	Growth phase 2
GFP	Green fluorescent protein
γH2AX	Phosphorylated histone H2AX
GST	Glutathione S-transferase
GTP	Guanosine triphosphate
H2AX	Histone H2A variant x
HR	Homologous recombination
IC50	Half maximal inhibitory concentration
ICL	Interstrand crosslink
IPTG	Isopropyl β-D-1-thiogalactopyranoside
IR	Ionising radiation
IRIF	Ionising radiation induced foci
KLF	Krüppel-like factor
Ku70	Ku autoantigen protein p70
LB	Luria-Bertani medium
M	Mitosis
MCM	Mini chromosome maintenance protein
MDC1	Mediator of DNA damage checkpoint protein 1
MH3	Matrin 3 homologous domain
MMR	Mismatch repair
MRN	Mre11-Rad50-Nbs1 complex
mRNA	Messenger RNA
MTOR	Mammalian target of rapamycin
NER	Nucleotide excision repair
NHEJ	Non-homologous end joining
NLS	Nuclear localisation signal
p21	Cyclin-dependent kinase inhibitor 1
p53	Tumour protein 53
PAGE	Polyacrylamide gel electrophoresis
PBS	Phosphate buffered saline
PCNA	Proliferating cell nuclear antigen
PCR	Polymerase chain reaction
PFA	Paraformaldehyde
PIKK	Phosphoinositide-3-kinase-related protein kinase
PMSF	Phenylmethanesulfonylfluoride
pRB	Retinoblastoma protein
pre-RC	Pre-replication complex
RD	Replication domain
RNA	Ribonucleic acid
RPA	Replication protein A
RT-PCR	Real time PCR
S phase	Synthesis phase
SCD	SQ/TQ cluster domain
SDS	Sodium dodecyl sulfate
SEM	Standard error of the mean
SFPQ	Splicing factor, proline- and glutamine-rich
siRNA	Small interfering RNA
SMC1	Structural maintenance of chromosomes 1
SMC3	Structural maintenance of chromosomes 3
SQ	Serine glutamine
SSB	Single strand break
ssDNA	Single stranded DNA
TBS	Tris buffered saline
TQ	Threonine glutamine
Tris	Tris(hydroxymethyl)aminomethane
UTP	Uridine triphosphate

REFERENCES

Abraham, R. T. (2001). "Cell cycle checkpoint signaling through the ATM and ATR kinases." Genes Dev **15**(17): 2177-96.

Agarwal, M. L., A. Agarwal, et al. (1995). "p53 controls both the G2/M and the G1 cell cycle checkpoints and mediates reversible growth arrest in human fibroblasts." Proc Natl Acad Sci U S A **92**(18): 8493-7.

Ahn, J. Y., X. Li, et al. (2002). "Phosphorylation of threonine 68 promotes oligomerization and autophosphorylation of the Chk2 protein kinase via the forkhead-associated domain." J Biol Chem **277**(22): 19389-95.

Ainscough, J. F.-X., F. A. Rahman, et al. (2007). "C-terminal domains deliver the DNA replication factor Ciz1 to the nuclear matrix." Journal of Cell Science **120**(1): 115-125.

Allan, L. A. and M. Fried (1999). "p53-dependent apoptosis or growth arrest induced by different forms of radiation in U2OS cells: p21WAF1/CIP1 repression in UV induced apoptosis." Oncogene **18**(39): 5403-12.

Andegeko, Y., L. Moyal, et al. (2001). "Nuclear retention of ATM at sites of DNA double strand breaks." J Biol Chem **276**(41): 38224-30.

Arias, E. E. and J. C. Walter (2007). "Strength in numbers: preventing rereplication via multiple mechanisms in eukaryotic cells." Genes Dev **21**(5): 497-518.

Atienza, J. M., R. B. Roth, et al. (2005). "Suppression of RAD21 gene expression decreases cell growth and enhances cytotoxicity of etoposide and bleomycin in human breast cancer cells." Mol Cancer Ther **4**(3): 361-8.

Balajee, A. S. and C. R. Geard (2001). "Chromatin-bound PCNA complex formation triggered by DNA damage occurs independent of the ATM gene product in human cells." Nucleic Acids Res **29**(6): 1341-51.

Barkley, L. R., H. Ohmori, et al. (2007). "Integrating S-phase checkpoint signaling with trans-lesion synthesis of bulky DNA adducts." Cell Biochem Biophys **47**(3): 392-408.

Bartek, J. and J. Lukas (2001). "Mammalian G1- and S-phase checkpoints in response to DNA damage." Curr Opin Cell Biol **13**(6): 738-47.

Bartek, J. and J. Lukas (2003). "Chk1 and Chk2 kinases in checkpoint control and cancer." Cancer Cell **3**(5): 421-9.

Bartkova, J., Z. Hořejši, et al. (2005). "DNA damage response as a candidate anti-cancer barrier in early human tumorigenesis." Nature **434**: 864-870.

Bekker-Jensen, S., C. Lukas, et al. (2006). "Spatial organization of the mammalian genome surveillance machinery in response to DNA strand breaks." J Cell Biol **173**(2): 195-206.

Bell, S. P. and B. Stillman (1992). "ATP-dependent recognition of eukaryotic origins of DNA replication by a multiprotein complex." Nature **357**(6374): 128-34.

Belyaev, I. Y. (2010). "Radiation-induced DNA repair foci: spatio-temporal aspects of formation, application for assessment of radiosensitivity and biological dosimetry." Mutat Res **704**(1-3): 132-41.

Berkovich, E., R. J. Monnat, Jr., et al. (2007). "Roles of ATM and NBS1 in chromatin structure modulation and DNA double-strand break repair." Nat Cell Biol **9**(6): 683-90.

Bjursell, G. and P. Reichard (1973). "Effects of thymidine on deoxyribonucleoside triphosphate pools and deoxyribonucleic acid synthesis in Chinese hamster ovary cells." J Biol Chem **248**(11): 3904-9.

Bladen, C. L., D. Udayakumar, et al. (2005). "Identification of the polypyrimidine tract binding protein-associated splicing factor.p54(nrb) complex as a candidate DNA double-strand break rejoining factor." J Biol Chem **280**(7): 5205-10.

Blow, J. J. and B. Hodgson (2002). "Replication licensing--defining the proliferative state?" Trends Cell Biol **12**(2): 72-8.

Boiteux, S. and M. Guillet (2004). "Abasic sites in DNA: repair and biological consequences in Saccharomyces cerevisiae." DNA Repair (Amst) **3**(1): 1-12.

Bolderson, E., J. Scorah, et al. (2004). "ATM is required for the cellular response to thymidine induced replication fork stress." Human Molecular Genetics **13**(23): 2937-2945.

Branzei, D. and M. Foiani (2008). "Regulation of DNA repair throughout the cell cycle." Nat Rev Mol Cell Biol **9**(4): 297-308.

Bravo, R., R. Frank, et al. (1987). "Cyclin/PCNA is the auxiliary protein of DNA polymerase-delta." Nature **326**(6112): 515-7.

Brown, R. S. (2005). "Zinc finger proteins: getting a grip on RNA." Curr Opin Struct Biol **15**(1): 94-8.

Burdak-Rothkamm, S., K. Rothkamm, et al. (2008). "ATM acts downstream of ATR in the DNA damage response signaling of bystander cells." Cancer Res **68**(17): 7059-65.

Burgers, P. M. (1991). "Saccharomyces cerevisiae replication factor C. II. Formation and activity of complexes with the proliferating cell nuclear antigen and with DNA polymerases delta and epsilon." J Biol Chem **266**(33): 22698-706.

Carcagno, A. L., M. F. Ogara, et al. (2009). "E2F1 transcription is induced by genotoxic stress through ATM/ATR activation." IUBMB Life **61**(5): 537-43.

Carney, J. P., R. S. Maser, et al. (1998). "The hMre11/hRad50 protein complex and Nijmegen breakage syndrome: linkage of double-strand break repair to the cellular DNA damage response." Cell **93**(3): 477-86.

Celeste, A., O. Fernandez-Capetillo, et al. (2003). "Histone H2AX phosphorylation is dispensable for the initial recognition of DNA breaks." Nat Cell Biol **5**(7): 675-9.

Chan, D. W., B. P. Chen, et al. (2002). "Autophosphorylation of the DNA-dependent protein kinase catalytic subunit is required for rejoining of DNA double-strand breaks." Genes Dev **16**(18): 2333-8.

Cheatham, B., C. J. Vlahos, et al. (1994). "Phosphatidylinositol 3-kinase activation is required for insulin stimulation of pp70 S6 kinase, DNA synthesis, and glucose transporter translocation." Mol Cell Biol **14**(7): 4902-11.

Chen, A. Y. and L. F. Liu (1994). "DNA topoisomerases: essential enzymes and lethal targets." Annu Rev Pharmacol Toxicol **34**: 191-218.

Chen, B. P., D. W. Chan, et al. (2005). "Cell cycle dependence of DNA-dependent protein kinase phosphorylation in response to DNA double strand breaks." J Biol Chem **280**(15): 14709-15.

Choi, W. I., Y. Kim, et al. (2009). "Eukaryotic translation initiator protein 1A isoform, CCS-3, enhances the transcriptional repression of p21CIP1 by proto-oncogene FBI-1 (Pokemon/ZBTB7A)." Cell Physiol Biochem **23**(4-6): 359-70.

Chuang, L. C., L. K. Teixeira, et al. (2009). "Phosphorylation of Mcm2 by Cdc7 promotes pre-replication complex assembly during cell-cycle re-entry." Mol Cell **35**(2): 206-16.

Clay-Farrace, L., C. Pelizon, et al. (2003). "Human replication protein Cdc6 prevents mitosis through a checkpoint mechanism that implicates Chk1." Embo J **22**(3): 704-12.

Coller, H. A., L. Sang, et al. (2006). "A new description of cellular quiescence." PLoS Biol **4**(3): e83.

Collins, F. S. and A. D. Barker (2007). "Mapping the cancer genome. Pinpointing the genes involved in cancer will help chart a new course across the complex landscape of human malignancies." Sci Am **296**(3): 50-7.

Copeland, N. A., H. E. Sercombe, et al. (2010). "Ciz1 cooperates with cyclin-A-CDK2 to activate mammalian DNA replication in vitro." J Cell Sci **123**(Pt 7): 1108-15.

Cortez, D., S. Guntuku, et al. (2001). "ATR and ATRIP: partners in checkpoint signaling." Science **294**(5547): 1713-6.

Cortez, D., Y. Wang, et al. (1999). "Requirement of ATM-dependent phosphorylation of Brca1 in the DNA damage response to double-strand breaks." Science **286**(5442): 1162-1166.

Costes, S. V., I. Chiolo, et al. (2010). "Spatiotemporal characterization of ionizing radiation induced DNA damage foci and their relation to chromatin organization." Mutat Res **704**(1-3): 78-87.

Coverley, D., H. Laman, et al. (2002). "Distinct roles for cyclins E and A during DNA replication complex assembly and activation." Nature Cell Biology **4**: 523-528.

Coverley, D., J. Marr, et al. (2005). "Ciz1 promotes mammalian DNA replication." Journal of Cell Science **118**(1): 101-112.

Dahmcke, C. M., S. Buchmann-Moller, et al. (2008). "Altered splicing in exon 8 of the DNA replication factor CIZ1 affects subnuclear distribution and is associated with Alzheimer's disease." Mol Cell Neurosci **38**(4): 589-94.

De Falco, M., E. Ferrari, et al. (2007). "The human GINS complex binds to and specifically stimulates human DNA polymerase alpha-primase." EMBO Rep **8**(1): 99-103.

den Hollander, P. and R. Kumar (2006). "Dynein light chain 1 contributes to cell cycle progression by increasing cycling-dependent kinase 2 activity in estrogen-stimulated cells." Cancer Research **66**(11): 5941-5949.

den Hollander, P., S. K. Rayala, et al. (2006). "Ciz1, a novel DNA-binding coactivator of the estrogen receptor α, confers hypersensitivity to estrogen action." Cancer Research **66**(22): 11021-11030.

DiFeo, A., J. A. Martignetti, et al. (2009). "The role of KLF6 and its splice variants in cancer therapy." Drug Resist Updat **12**(1-2): 1-7.

Dimitrova, D. S. and D. M. Gilbert (1999). "The spatial position and replication timing of chromosomal domains are both established in early G1 phase." Mol Cell **4**(6): 983-93.

Dimitrova, N. and T. de Lange (2006). "MDC1 accelerates nonhomologous end-joining of dysfunctional telomeres." Genes Dev **20**(23): 3238-43.

Djeliova, V., G. Russev, et al. (2001). "Dynamics of association of origins of DNA replication with the nuclear matrix during the cell cycle." Nucleic Acids Res **29**(15): 3181-7.

Dobbs, T. A., J. A. Tainer, et al. (2010). "A structural model for regulation of NHEJ by DNA-PKcs autophosphorylation." DNA Repair (Amst) **9**(12): 1307-14.

Downs, J. A. and S. P. Jackson (2004). "A means to a DNA end: the many roles of Ku." Nat Rev Mol Cell Biol **5**(5): 367-78.

Dvir, A., S. R. Peterson, et al. (1992). "Ku autoantigen is the regulatory component of a template-associated protein kinase that phosphorylates RNA polymerase II." Proc Natl Acad Sci U S A **89**(24): 11920-4.

Eglen, R. M. and T. Reisine (2009). "The current status of drug discovery against the human kinome." Assay Drug Dev Technol **7**(1): 22-43.

Eker, A. P., C. Quayle, et al. (2009). "DNA repair in mammalian cells: Direct DNA damage reversal: elegant solutions for nasty problems." Cell Mol Life Sci **66**(6): 968-80.

Ellison, V. and B. Stillman (2003). "Biochemical characterization of DNA damage checkpoint complexes: clamp loader and clamp complexes with specificity for 5' recessed DNA." PLoS Biol **1**(2): E33.

Endicott, J. A., M. E. Noble, et al. (1999). "Cyclin-dependent kinases: inhibition and substrate recognition." Curr Opin Struct Biol **9**(6): 738-44.

Essers, J., A. F. Theil, et al. (2005). "Nuclear dynamics of PCNA in DNA replication and repair." Mol Cell Biol **25**(21): 9350-9.

Evans, T. A., A. K. Raina, et al. (2007). "BRCA1 may modulate neuronal cell cycle re-entry in Alzheimer disease." Int J Med Sci **4**(3): 140-5.

Fragkos, M., J. Jurvansuu, et al. (2009). "H2AX is required for cell cycle arrest via the p53/p21 pathway." Mol Cell Biol **29**(10): 2828-40.

Fu, X., S. Wan, et al. (2008). "Etoposide induces ATM-dependent mitochondrial biogenesis through AMPK activation." PLoS One **3**(4): e2009.

Furnari, B., A. Blasina, et al. (1999). "Cdc25 inhibited in vivo and in vitro by checkpoint kinases Cds1 and Chk1." Mol Biol Cell **10**(4): 833-45.

Furstenthal, L., B. K. Kaiser, et al. (2001). "Cyclin E uses Cdc6 as a chromatin-associated receptor required for DNA replication." J Cell Biol **152**(6): 1267-78.

Furuya, K., M. Poitelea, et al. (2004). "Chk1 activation requires Rad9 S/TQ-site phosphorylation to promote association with C-terminal BRCT domains of Rad4TOPBP1." Genes Dev **18**(10): 1154-64.

Gamsjaeger, R., C. K. Liew, et al. (2007). "Sticky fingers: zinc-fingers as protein-recognition motifs." Trends Biochem Sci **32**(2): 63-70.

Gatei, M., B. B. Zhou, et al. (2001). "Ataxia telangiectasia mutated (ATM) kinase and ATM and Rad3 related kinase mediate phosphorylation of Brca1 at distinct and overlapping sites. In vivo assessment using phospho-specific antibodies." J Biol Chem **276**(20): 17276-80.

Gelsthorpe, M., M. Pulumati, et al. (1997). "The putative cell cycle gene, enhancer of rudimentary, encodes a highly conserved protein found in plants and animals." Gene **186**(2): 189-195.

Geng, Y., Y. M. Lee, et al. (2007). "Kinase-independent function of cyclin E." Mol Cell **25**(1): 127-39.

Geng, Y., Q. Yu, et al. (2003). "Cyclin E ablation in the mouse." Cell **114**(4): 431-43.

Gorgoulis, V. G., L.-V. F. Vassiliou, et al. (2005). "Activation of the DNA damage checkpoint and genomic instability in human precancerous lesions." Nature **434**: 907-913.

Gregan, J., K. Lindner, et al. (2003). "Fission yeast Cdc23/Mcm10 functions after pre-replicative complex formation to promote Cdc45 chromatin binding." Mol Biol Cell **14**(9): 3876-87.

Groth, A., J. Lukas, et al. (2003). "Human Tousled like kinases are targeted by an ATM- and Chk1-dependent DNA damage checkpoint." Embo J **22**(7): 1676-87.

Hall-Jackson, C. A., D. A. Cross, et al. (1999). "ATR is a caffeine-sensitive, DNA-activated protein kinase with a substrate specificity distinct from DNA-PK." Oncogene **18**(48): 6707-13.

Hanahan, D. and R. A. Weinberg (2000). "The hallmarks of cancer." Cell **100**(1): 57-70.

Hanahan, D. and R. A. Weinberg (2011). "Hallmarks of cancer: the next generation." Cell **144**(5): 646-74.

Harper, J. W. and S. J. Elledge (2007). "The DNA damage response: ten years after." Mol Cell **28**(5): 739-45.

Hartwell, L. H. and T. A. Weinert (1989). "Checkpoints: controls that ensure the order of cell cycle events." Science **246**(4930): 629-34.

Hidalgo, M., L. L. Siu, et al. (2001). "Phase I and pharmacologic study of OSI-774, an epidermal growth factor receptor tyrosine kinase inhibitor, in patients with advanced solid malignancies." J Clin Oncol **19**(13): 3267-79.

Hirokawa, N., Y. Noda, et al. (1998). "Kinesin and dynein superfamily proteins in organelle transport and cell division." Current Opinion in Cell Biology **10**(1): 60-73.

Hollstein, M., K. Rice, et al. (1994). "Database of p53 gene somatic mutations in human tumors and cell lines." Nucleic Acids Res **22**(17): 3551-5.

Huberman, J. A. and A. D. Riggs (1966). "Autoradiography of chromosomal DNA fibers from Chinese hamster cells." Proc Natl Acad Sci U S A **55**(3): 599-606.

Hubscher, U., G. Maga, et al. (2002). "Eukaryotic DNA polymerases." Annu Rev Biochem **71**: 133-63.

Huyton, T., P. A. Bates, et al. (2000). "The BRCA1 C-terminal domain: structure and function." Mutat Res **460**(3-4): 319-32.

Inoue, Y., M. Kitagawa, et al. (2007). "Phosphorylation of pRB at Ser612 by Chk1/2 leads to a complex between pRB and E2F-1 after DNA damage." Embo J **26**(8): 2083-93.

Iuchi, S. (2001). "Three classes of C2H2 zinc finger proteins." Cell Mol Life Sci **58**(4): 625-35.

Jackson, P. K., S. Chevalier, et al. (1995). "Early events in DNA replication require cyclin E and are blocked by p21CIP1." J Cell Biol **130**(4): 755-69.

Jamil, S., S. Mojtabavi, et al. (2008). "An essential role for MCL-1 in ATR-mediated CHK1 phosphorylation." Mol Biol Cell **19**(8): 3212-20.

Jia, L. Q., M. Osada, et al. (1997). "Screening the p53 status of human cell lines using a yeast functional assay." Mol Carcinog **19**(4): 243-53.

Karlsson-Rosenthal, C. and J. B. Millar (2006). "Cdc25: mechanisms of checkpoint inhibition and recovery." Trends Cell Biol **16**(6): 285-92.

Kastan, M. B. and J. Bartek (2004). "Cell-cycle checkpoints and cancer." Nature **432**: 316-323.

Katsuno, Y., A. Suzuki, et al. (2009). "Cyclin A-Cdk1 regulates the origin firing program in mammalian cells." Proc Natl Acad Sci U S A **106**(9): 3184-9.

Kim, S.-T., D.-S. Lim, et al. (1999). "Substrate specificities and identification of putative substrates of ATM kinase family members." Journal of Biological Chemistry **274**(53): 37538-37543.

Kim, S. T., B. Xu, et al. (2002). "Involvement of the cohesin protein, Smc1, in Atm-dependent and independent responses to DNA damage." Genes Dev **16**(5): 560-70.

Kitagawa, R., C. J. Bakkenist, et al. (2004). "Phosphorylation of SMC1 is a critical downstream event in the ATM-NBS1-BRCA1 pathway." Genes Dev **18**(12): 1423-38.

Klaunig, J. E., Y. Xu, et al. (1998). "The role of oxidative stress in chemical carcinogenesis." Environ Health Perspect **106 Suppl 1**: 289-95.

Krishna, T. S., X. P. Kong, et al. (1994). "Crystal structure of the eukaryotic DNA polymerase processivity factor PCNA." Cell **79**(7): 1233-43.

Krude, T., M. Jackman, et al. (1997). "Cyclin/Cdk-dependent initiation of DNA replication in a human cell-free system." Cell **88**(1): 109-19.

Kryston, T. B., A. B. Georgiev, et al. "Role of oxidative stress and DNA damage in human carcinogenesis." Mutat Res **711**(1-2): 193-201.

Larner, J. M., H. Lee, et al. (1999). "Radiation down-regulates replication origin activity throughout the S phase in mammalian cells." Nucleic Acids Res **27**(3): 803-9.

Lee, J. H. and T. T. Paull (2005). "ATM activation by DNA double-strand breaks through the Mre11-Rad50-Nbs1 complex." Science **308**(5721): 551-4.

Lee, S. J., M. F. Schwartz, et al. (2003). "Rad53 phosphorylation site clusters are important for Rad53 regulation and signaling." Mol Cell Biol **23**(17): 6300-14.

Li, C. J., J. A. Bogan, et al. (2000). "Selective activation of pre-replication complexes in vitro at specific sites in mammalian nuclei." J Cell Sci **113 (Pt 5)**: 887-98.

Li, F., J. Chen, et al. (2001). "The replication timing program of the Chinese hamster beta-globin locus is established coincident with its repositioning near peripheral heterochromatin in early G1 phase." J Cell Biol **154**(2): 283-92.

Li, S., N. S. Ting, et al. (2000). "Functional link of BRCA1 and ataxia telangiectasia gene product in DNA damage response." Nature **406**(6792): 210-5.

Li, T. K. and L. F. Liu (2001). "Tumor cell death induced by topoisomerase-targeting drugs." Annu Rev Pharmacol Toxicol **41**: 53-77.

Lin, S. Y., Y. Liang, et al. (2010). "Multiple roles of BRIT1/MCPH1 in DNA damage response, DNA repair, and cancer suppression." Yonsei Med J **51**(3): 295-301.

Lopez-Girona, A., B. Furnari, et al. (1999). "Nuclear localization of Cdc25 is regulated by DNA damage and a 14-3-3 protein." Nature **397**(6715): 172-5.

Lou, Z., B. P. Chen, et al. (2004). "MDC1 regulates DNA-PK autophosphorylation in response to DNA damage." J Biol Chem **279**(45): 46359-62.

Lou, Z., C. C. S. Chini, et al. (2003). "Mediator of DNA damage checkpoint protein 1 regulates BRCA1 localization and phosphorylation in DNA damage checkpoint control." Journal of Biological Chemistry **278**(16): 13599-13602.

Lou, Z., K. Minter-Dykhouse, et al. (2006). "MDC1 maintains genomic stability by participating in the amplification of ATM-dependent DNA damage signals." Mol Cell **21**(2): 187-200.

Lou, Z., K. Minter-Dykhouse, et al. (2003). "MDC1 is coupled to activated CHK2 in mammalian DNA damage response pathways." Nature **421**(6926): 957-61.

Lowndes, N. F. (2010). "The interplay between BRCA1 and 53BP1 influences death, aging, senescence and cancer." DNA Repair (Amst) **9**(10): 1112-6.

Lu, X., J. Liu, et al. (2009). "Cyclin E is stabilized in response to replication fork barriers leading to prolonged S phase arrest." J Biol Chem **284**(51): 35325-37.

Lukas, C., J. Falck, et al. (2003). "Distinct spatiotemporal dynamics of mammalian checkpoint regulators induced by DNA damage." Nature Cell Biology **5**: 255-265.

Lukas, C., F. Melander, et al. (2004). "Mdc1 couples DNA double-strand break recognition by Nbs1 with its H2AX-dependent chromatin retention." Embo J **23**(13): 2674-83.

Lukasik, A., K. A. Uniewicz, et al. (2008). "Ciz1, a p21(cip1/waf1)-interacting zinc finger protein and DNA replication factor is a novel molecular partner for human enhancer of rudimentary homolog." FEBS Journal **275**(2): 332-340.

Luo, H., Y. Li, et al. (2008). "Regulation of intra-S phase checkpoint by ionizing radiation (IR)-dependent and IR-independent phosphorylation of SMC3." J Biol Chem **283**(28): 19176-83.

Mailand, N. and J. F. Diffley (2005). "CDKs promote DNA replication origin licensing in human cells by protecting Cdc6 from APC/C-dependent proteolysis." Cell **122**(6): 915-26.

Manke, I. A., D. M. Lowery, et al. (2003). "BRCT repeats as phosphopeptide-binding modules involved in protein targeting." Science **302**(5645): 636-9.

Marheineke, K. and O. Hyrien (2004). "Control of replication origin density and firing time in Xenopus egg extracts: role of a caffeine-sensitive, ATR-dependent checkpoint." J Biol Chem **279**(27): 28071-81.

Matsumoto, Y., K. Kim, et al. (1994). "Proliferating cell nuclear antigen-dependent abasic site repair in Xenopus laevis oocytes: an alternative pathway of base excision DNA repair." Mol Cell Biol **14**(9): 6187-97.

Matsuoka, S., B. A. Ballif, et al. (2007). "ATM and ATR substrate analysis reveals extensive protein networks responsive to DNA damage." Science **316**(5828): 1160-1166.

Matsuoka, S., M. Huang, et al. (1998). "Linkage of ATM to cell cycle regulation by the Chk2 protein kinase." Science **282**(5395): 1893-7.

McCabe, K. M., S. B. Olson, et al. (2009). "DNA interstrand crosslink repair in mammalian cells." J Cell Physiol **220**(3): 569-73.

McKenna, W. G. and R. J. Muschel (2003). "Targeting tumor cells by enhancing radiation sensitivity." Genes Chromosomes Cancer **38**(4): 330-8.

Mechali, M. (2011). "Eukaryotic DNA replication origins: many choices for appropriate answers." Nat Rev Mol Cell Biol **11**(10): 728-38.

Mehta, T. S., H. Lu, et al. (2009). "A unique sequence in the N-terminal regulatory region controls the nuclear localization of KLF8 by cooperating with the C-terminal zinc-fingers." Cell Res **19**(9): 1098-109.

Melchionna, R., X. B. Chen, et al. (2000). "Threonine 68 is required for radiation-induced phosphorylation and activation of Cds1." Nat Cell Biol **2**(10): 762-5.

Mitchell, D. L. and R. S. Nairn (1989). "The biology of the (6-4) photoproduct." Photochem Photobiol **49**(6): 805-19.

Mitsui, K., A. Matsumoto, et al. (1999). "Cloning and characterization of a novel $P21^{Cip1/Waf1}$– interacting zinc finger protein, Ciz1." Biochemical and Biophysical Research Communications **264**(2): 457-464.

Mladenov, E., B. Anachkova, et al. (2006). "Sub-nuclear localization of Rad51 in response to DNA damage." Genes Cells **11**(5): 513-24.

Moldovan, G.-L., B. Pfander, et al. (2007). "PCNA, the maestro of the replication fork." Cell **129**(4): 665-679.

Moll, D., A. Prinz, et al. (2006). "Biomolecular interaction analysis in functional proteomics." J Neural Transm **113**(8): 1015-32.

Munkley, J., N. A. Copeland, et al. (2010). "Cyclin E is recruited to the nuclear matrix during differentiation, but is not recruited in cancer cells." Nucleic Acids Res.

Murray, A. W. (2004). "Recycling the cell cycle: cyclins revisited." Cell **116**(2): 221-34.

Murray, A. W. and M. W. Kirschner (1989). "Cyclin synthesis drives the early embryonic cell cycle." Nature **339**(6222): 275-80.

Musacchio, A. and K. G. Hardwick (2002). "The spindle checkpoint: structural insights into dynamic signalling." Nat Rev Mol Cell Biol **3**(10): 731-41.

Musacchio, A. and E. D. Salmon (2007). "The spindle-assembly checkpoint in space and time." Nat Rev Mol Cell Biol **8**(5): 379-93.

Nakanishi, M., Y. Katsuno, et al. (2010). "Chk1-cyclin A/Cdk1 axis regulates origin firing programs in mammals." Chromosome Res **18**(1): 103-13.

Nam, C., K. Doi, et al. (2010). "Etoposide induces G2/M arrest and apoptosis in neural progenitor cells via DNA damage and an ATM/p53-related pathway." Histol Histopathol **25**(4): 485-93.

Nichols, A. F. and A. Sancar (1992). "Purification of PCNA as a nucleotide excision repair protein." Nucleic Acids Res **20**(13): 2441-6.

Norman, B. H., C. Shih, et al. (1996). "Studies on the mechanism of phosphatidylinositol 3-kinase inhibition by wortmannin and related analogs." J Med Chem **39**(5): 1106-11.

Nyberg, K. A., R. J. Michelson, et al. (2002). "Toward maintaining the genome: DNA damage and replication checkpoints." Annu Rev Genet **36**: 617-56.

O'Neill, T., A. J. Dwyer, et al. (2000). "Utilization of oriented peptide libraries to identify substrate motifs selected by ATM." Journal of Biological Chemistry **275**(30): 22719-22727.

Obenauer, J. C., L. C. Cantley, et al. (2003). "Scansite 2.0: proteome-wide prediction of cell signaling interactions using short sequence motifs." Nucleic Acids Research **31**(13): 3635-3641.

Oehlmann, M., A. J. Score, et al. (2004). "The role of Cdc6 in ensuring complete genome licensing and S phase checkpoint activation." J Cell Biol **165**(2): 181-90.

Okumara, K., M. Nogami, et al. (1998). "Mapping of human DNA-binding nuclear protein (NP220) to chromosome band 2p13.1-p13.2 and its relation to matrin 3." Biosci Biotechnol Biochem **62**(8): 1640-2.

Paull, T. T. and J. H. Lee (2005). "The Mre11/Rad50/Nbs1 complex and its role as a DNA double-strand break sensor for ATM." Cell Cycle **4**(6): 737-40.

Peng, A. and P.-L. Chen (2005). "NFBD1/Mdc1 mediates ATR-dependent DNA damage response." Cancer Research **65**(4): 1158-1163.

Petersen, B. O., J. Lukas, et al. (1999). "Phosphorylation of mammalian CDC6 by cyclin A/CDK2 regulates its subcellular localization." Embo J **18**(2): 396-410.

Pieler, T. and E. Bellefroid (1994). "Perspectives on zinc finger protein function and evolution--an update." Mol Biol Rep **20**(1): 1-8.

Polager, S., Y. Kalma, et al. (2002). "E2Fs up-regulate expression of genes involved in DNA replication, DNA repair and mitosis." Oncogene **21**(3): 437-46.

Prinz, A., M. Diskar, et al. (2006). "Application of bioluminescence resonance energy transfer (BRET) for biomolecular interaction studies." Chembiochem **7**(7): 1007-12.

Rahman, F. A., J. F.-X. Ainscough, et al. (2007). "Cancer-associated missplicing of exon 4 influences the subnuclear distribution of the DNA replication factor Ciz1." Human Mutation **28**(10): 993-1004.

Rhind, N. and P. Russell (2000). "Checkpoints: it takes more than time to heal some wounds." Curr Biol **10**(24): R908-11.

Rodriguez-Bravo, V., S. Guaita-Esteruelas, et al. (2006). "Chk1- and claspin-dependent but ATR/ATM- and Rad17-independent DNA replication checkpoint response in HeLa cells." Cancer Res **66**(17): 8672-9.

Roninson, I. B. (2002). "Oncogenic functions of tumour suppressor p21/Waf1/Cip1/Sdi1: association with cell senescence and tumour-promoting activities of stromal fibroblasts." Cancer Letters **179**(1): 1-14.

Rowland, B. D. and D. S. Peeper (2006). "KLF4, p21 and context-dependent opposing forces in cancer." Nat Rev Cancer **6**(1): 11-23.

Rudolf, K., M. Cervinka, et al. (2009). "Cytotoxicity and mitochondrial apoptosis induced by etoposide in melanoma cells." Cancer Invest **27**(7): 704-17.

Salton, M., Y. Lerenthal, et al. (2010). "Involvement of matrin 3 and SFPQ/NONO in the DNA damage response." Cell Cycle **9**(8).

Sarkaria, J. N., R. S. Tibbetts, et al. (1998). "Inhibition of phosphoinositide 3-kinase related kinases by the radiosensitizing agent wortmannin." Cancer Res **58**(19): 4375-82.

Schwartz, M. F., J. K. Duong, et al. (2002). "Rad9 phosphorylation sites couple Rad53 to the Saccharomyces cerevisiae DNA damage checkpoint." Mol Cell **9**(5): 1055-65.

Sedelnikova, O. A., E. P. Rogakou, et al. (2002). "Quantitative detection of (125)IdU-induced DNA double-strand breaks with gamma-H2AX antibody." Radiat Res **158**(4): 486-92.

Shang, Y. L., A. J. Bodero, et al. (2003). "NFBD1, a novel nuclear protein with signature motifs of FHA and BRCT, and an internal 41-amino acid repeat sequence, is an early participant in DNA damage response." J Biol Chem **278**(8): 6323-9.

Shapiro, G. I. (2006). "Cyclin-dependent kinase pathways as targets for cancer treatment." J Clin Oncol **24**(11): 1770-83.

Shechter, D., V. Costanzo, et al. (2004). "ATR and ATM regulate the timing of DNA replication origin firing." Nat Cell Biol **6**(7): 648-55.

Sherr, C. J. (1995). "Mammalian G1 cyclins and cell cycle progression." Proc Assoc Am Physicians **107**(2): 181-6.

Sheu, Y. J. and B. Stillman (2006). "Cdc7-Dbf4 phosphorylates MCM proteins via a docking site-mediated mechanism to promote S phase progression." Mol Cell **24**(1): 101-13.

Shieh, S.-Y., J. Ahn, et al. (2000). "The human homologs of checkpoint kinases Chk1 and Cds1 (Chk2) phosphorylate p53 at multiple DNA damage-inducible sites." Genes & Development **14**(3): 289-300.

Shimada, M. and M. Nakanishi (2008). "Checkpoints meet the transcription at a novel histone milestone (H3-T11)." Cell Cycle **7**(11): 1555-9.

Shimada, M., H. Niida, et al. (2008). "Chk1 is a histone H3 threonine 11 kinase that regulates DNA damage-induced transcriptional repression." Cell **132**(2): 221-32.

Shrivastav, M., L. P. De Haro, et al. (2008). "Regulation of DNA double-strand break repair pathway choice." Cell Res **18**(1): 134-47.

Siatecka, M., F. Lohmann, et al. (2010). "EKLF directly activates the p21WAF1/CIP1 gene by proximal promoter and novel intronic regulatory regions during erythroid differentiation." Mol Cell Biol **30**(11): 2811-22.

Simmen, R. C., J. M. Pabona, et al. (2010). "The emerging role of Kruppel-like factors in endocrine-responsive cancers of female reproductive tissues." J Endocrinol **204**(3): 223-31.

Sopasakis, V. R., P. Liu, et al. (2010). "Specific roles of the p110alpha isoform of phosphatidylinsositol 3-kinase in hepatic insulin signaling and metabolic regulation." Cell Metab **11**(3): 220-30.

Soutoglou, E. and T. Misteli (2008). "Activation of the cellular DNA damage response in the absence of DNA lesions." Science **320**(5882): 1507-10.

Srivastava, N., S. Gochhait, et al. (2008). "Role of H2AX in DNA damage response and human cancers." Mutat Res.

Staropoli, J. F. (2008). "Tumorigenesis and neurodegeneration: two sides of the same coin?" Bioessays **30**(8): 719-27.

Stefan, E., S. Aquin, et al. (2007). "Quantification of dynamic protein complexes using Renilla luciferase fragment complementation applied to protein kinase A activities in vivo." Proc Natl Acad Sci U S A **104**(43): 16916-21.

Stevens, C. and N. B. La Thangue (2004). "The emerging role of E2F-1 in the DNA damage response and checkpoint control." DNA Repair (Amst) **3**(8-9): 1071-9.

Stevens, C., L. Smith, et al. (2003). "Chk2 activates E2F-1 in response to DNA damage." Nat Cell Biol **5**(5): 401-9.

Stewart, G. S., B. Wang, et al. (2003). "MDC1 is a mediator of the mammalian DNA damage checkpoint." Nature **421**(6926): 961-6.

Stiff, T., M. O'Driscoll, et al. (2004). "ATM and DNA-PK function redundantly to phosphorylate H2AX after exposure to ionizing radiation." Cancer Res **64**(7): 2390-6.

Stillman, B. (1989). "Initiation of eukaryotic DNA replication in vitro." Annu Rev Cell Biol **5**: 197-245.

Stokes, M. P., J. Rush, et al. (2007). "Profiling of UV-induced ATM/ATR signaling pathways." Proc Natl Acad Sci U S A **104**(50): 19855-60.

Stracker, T. H., T. Usui, et al. (2009). "Taking the time to make important decisions: the checkpoint effector kinases Chk1 and Chk2 and the DNA damage response." DNA Repair (Amst) **8**(9): 1047-54.

Stucki, M., J. A. Clapperton, et al. (2005). "MDC1 directly binds phosphorylated histone H2AX to regulate cellular responses to DNA double-strand breaks." Cell **123**(7): 1213-26.

Takeda, D. Y. and A. Dutta (2005). "DNA replication and progression through S phase." Oncogene **24**(17): 2827-43.

Tian, X., G. Chen, et al. (2007). "The relationship between the down-regulation of DNA-PKcs or Ku70 and the chemosensitization in human cervical carcinoma cell line HeLa." Oncol Rep **18**(4): 927-32.

Traven, A. and J. Heierhorst (2005). "SQ/TQ cluster domains: concentrated ATM/ATR kinase phosphorylation site regions in DNA-damage-response proteins." Bioessays **27**(4): 397-407.

Tsakraklides, V. and S. P. Bell (2010). "Dynamics of pre-replicative complex assembly." J Biol Chem **285**(13): 9437-43.

Umar, A., A. B. Buermeyer, et al. (1996). "Requirement for PCNA in DNA mismatch repair at a step preceding DNA resynthesis." Cell **87**(1): 65-73.

Ura, K. and J. J. Hayes (2002). "Nucleotide excision repair and chromatin remodeling." Eur J Biochem **269**(9): 2288-93.

Urist, M., T. Tanaka, et al. (2004). "p73 induction after DNA damage is regulated by checkpoint kinases Chk1 and Chk2." Genes Dev **18**(24): 3041-54.

Vadlamudi, R. K., R. Bagheri-Yarmand, et al. (2004). "Dynein light chain 1, a p21-activated kinase 1-interacting substrate, promotes cancerous phenotypes." Cancer Cell **5**(6): 575-585.

Vlahos, C. J., W. F. Matter, et al. (1994). "A specific inhibitor of phosphatidylinositol 3-kinase, 2-(4-morpholinyl)-8-phenyl-4H-1-benzopyran-4-one (LY294002)." J Biol Chem **269**(7): 5241-8.

Vousden, K. H. and X. Lu (2002). "Live or let die: the cell's response to p53." Nat Rev Cancer **2**(8): 594-604.

Wakeling, A. E., S. P. Guy, et al. (2002). "ZD1839 (Iressa): an orally active inhibitor of epidermal growth factor signaling with potential for cancer therapy." Cancer Res **62**(20): 5749-54.

Wang, H., X. Zhang, et al. (2009). "Artemis regulates cell cycle recovery from the S phase checkpoint by promoting degradation of cyclin E." J Biol Chem **284**(27): 18236-43.

Warder, D. E. and M. J. Keherly (2003). "Ciz1, Cip1 interacting zinc finger protein 1 binds the consensus DNA sequence ARYSR(0-2)YYAC." Journal of Biomedical Science **10**(4): 406-417.

Watanabe, F., K. Shinohara, et al. (2003). "Involvement of DNA-dependent protein kinase in down-regulation of cell cycle progression." Int J Biochem Cell Biol **35**(4): 432-40.

Watts, F. Z. and N. C. Brissett (2010). "Linking up and interacting with BRCT domains." DNA Repair (Amst) **9**(2): 103-8.

Willis, N. and N. Rhind (2009). "Regulation of DNA replication by the S-phase DNA damage checkpoint." Cell Div **4**: 13.

Witkiewicz-Kucharczyk, A. and W. Bal (2006). "Damage of zinc fingers in DNA repair proteins, a novel molecular mechanism in carcinogenesis." Toxicol Lett **162**(1): 29-42.

Wohlschlegel, J. A., B. T. Dwyer, et al. (2001). "Mutational analysis of the Cy motif from p21 reveals sequence degeneracy and specificity for different cyclin-dependent kinases." Mol Cell Biol **21**(15): 4868-74.

Woo, R. A. and R. Y. Poon (2003). "Cyclin-dependent kinases and S phase control in mammalian cells." Cell Cycle **2**(4): 316-24.

Workman, P., P. A. Clarke, et al. (2010). "Drugging the PI3 kinome: from chemical tools to drugs in the clinic." Cancer Res **70**(6): 2146-57.

Wu, J. R. and D. M. Gilbert (1997). "The replication origin decision point is a mitogen-independent, 2-aminopurine-sensitive, G1-phase event that precedes restriction point control." Mol Cell Biol **17**(8): 4312-21.

Xiao, Z., Z. Chen, et al. (2003). "Chk1 mediates S and G2 arrests through Cdc25A degradation in response to DNA-damaging agents." J Biol Chem **278**(24): 21767-73.

Xu, B., A. H. O'Donnell, et al. (2002). "Phosphorylation of serine 1387 in Brca1 is specifically required for the Atm-mediated S-phase checkpoint after ionizing irradiation." Cancer Res **62**(16): 4588-91.

Xu, X., L. M. Tsvetkov, et al. (2002). "Chk2 activation and phosphorylation-dependent oligomerization." Mol Cell Biol **22**(12): 4419-32.

Yam, C. H., T. K. Fung, et al. (2002). "Cyclin A in cell cycle control and cancer." Cell Mol Life Sci **59**(8): 1317-26.

Yang, S., C. Kuo, et al. (2002). "PML-dependent apoptosis after DNA damage is regulated by the checkpoint kinase hCds1/Chk2." Nat Cell Biol **4**(11): 865-70.

Yazdi, P. T., Y. Wang, et al. (2002). "SMC1 is a downstream effector in the ATM/NBS1 branch of the human S-phase checkpoint." Genes Dev **16**(5): 571-82.

You, Z. and J. M. Bailis (2010). "DNA damage and decisions: CtIP coordinates DNA repair and cell cycle checkpoints." Trends Cell Biol.

You, Z., L. Z. Shi, et al. (2009). "CtIP links DNA double-strand break sensing to resection." Mol Cell **36**(6): 954-69.

Yu, X., C. C. Chini, et al. (2003). "The BRCT domain is a phospho-protein binding domain." Science **302**(5645): 639-42.

Yun, M. H. and K. Hiom (2009). "CtIP-BRCA1 modulates the choice of DNA double-strand-break repair pathway throughout the cell cycle." Nature **459**(7245): 460-3.

Zeitz, M. J., K. S. Malyavantham, et al. (2009). "Matrin 3: chromosomal distribution and protein interactions." J Cell Biochem **108**(1): 125-33.

Zhang, J., J. C. Grindley, et al. (2006). "PTEN maintains haematopoietic stem cells and acts in lineage choice and leukaemia prevention." Nature **441**(7092): 518-22.

Zhou, B. B. and S. J. Elledge (2000). "The DNA damage response: putting checkpoints in perspective." Nature **408**(6811): 433-9.

Zhuang, J., J. Zhang, et al. (2006). "Checkpoint kinase 2-mediated phosphorylation of BRCA1 regulates the fidelity of nonhomologous end-joining." Cancer Res **66**(3): 1401-8.

Zou, L. and S. J. Elledge (2003). "Sensing DNA damage through ATRIP recognition of RPA-ssDNA complexes." Science **300**(5625): 1542-8.